P B G U N S ©

AN INTERACTIVE PROGRAM
FOR THE SIMULATION OF ELECTRON AND ION BEAMS AND GUNS

PBGUNS Version 5.2

Copyright 1994-2016

by

FAR-TECH, Inc.

10350 Science Center Drive, Suite 150

San Diego CA 92121

Phone: 858-455-6655

Email support@far-tech.com

URL http://www.far-tech.com/pbguns

For assistance, please contact FAR-TECH, Inc. at support@far-tech.com.

Abstract

PBGUNS is an interactive computer program for the Poisson simulation of virtually any type of axially symmetric or two-dimensional electron or ion beam extraction or transport system. The program can be run fully relativistic or completely non-relativistic. Electron beam sources can be thermionic, field emission or forced emission. Positive and negative ion beam sources can be plasma (including multiple ion types), thermionic and sputter ion. Thermal angular spreads can be added to the injected particles. Applied axisymmetric magnetic fields can be included, either as axis values or full axisymmetric matrices specifying the axial components, in addition to the relativistic beam induced magnetic fields. Magnetic fields perpendicular to the plane of simulation can be used with rectangular configurations, still including self-induced magnetic effects in relativistic problems. Transverse magnetic fields for separation of electrons from negative ion beams may also be approximated. Trajectories are computed independently so that crossing trajectories do not invalidate the results. The particle beam is simulated by computing up to 30,000 representative trajectories through the problem from any type of source. For low voltage, thermionic, electron guns the program is sensitive to the position of the potential minimum that occurs in front of the emission area, as well as, the angular spread. The potentials are simulated on a large rectangular matrix array and a fine matrix covering the cathode or plasma region to improve accuracy and stability, both of which are solved by basic, iterative, relaxation techniques. Poisson's Equation is solved at each point within the configuration using space-charge densities computed from the trajectories. Five to thirty cycles through the trajectory-voltage calculations are usually sufficient to solve a typical problem. The beam can be restarted (on a new mesh or the same mesh) for extended drift, lens or acceleration regions. Results within a few percent of experiment are easily obtainable. Runs can take from a few minutes to hours, depending on the problem resolution and complexity. The program runs on the laptops with at least 1024 by 768 pixel screens and Macintoshes with the Windows emulator.

The program is fully interactive. The configuration can be changed interactively by interrupting the execution, without stopping the run. Parameters and electrode shapes can be changed interactively, then the program run continued. Results are continuously displayed on the screen as the program executes.

Contents

7   Appendix A: Trouble-Shooting PBGUNS   **154**

8   Appendix B: Theoretical Development of PBGUNS   **157**

References   **171**

1 Getting Started

1.1 Windows Installation

To install **PBGUNS**, simply insert the installation disk and double-click on "PBGUNS_Setup.exe". The program will install in the directory C:\PBGUNS. It is important that the program is located in the C:\ directory, as problems may occur if it is installed elsewhere. Then insert the USB security device. The security device must be plugged in every time you run the program. If it is not, you will get the error message "HASP key not found" and the program will terminate.

1.2 Program Execution

The PBGUNS executable PBGUNS.exe, accomodates the largest matrix the program can currently handle. A detailed description of the matrix-size parameters in this executable is given at the beginning of Section 4. Execution can be initiated by double-clicking the PBGUNS icon in the C:\PBGUNS directory. All results produced by the program will appear in the same directory where the program execution was initiated. Note that any PBGI.LOG, PBGDD.BIN, PBBMSV.BIN and *.PLT files present in the directory will be over-written by the program.

1.3 Program Output

A log file called PBGI.LOG is generated as the program runs. Although PBGI.LOG contains a great deal of information generated by the program, it is usually not necessary to look at this file.

The most useful output from the program is the plots. Hard copy plots can be obtained on most printers or plotters using the INTPRINT program. If you have a postscript printer, try both the color and black/white drivers even if it is a B-W printer. Sometimes problems occur when printing directly to a postscript printer, as this can hang the computer. Try printing to a file and copying the file to the plotter. The plots can be viewed on-screen after program execution using the INTVIEW program. Both these programs are self explanatory (and have useful help files) after they are started. It is usually best to start INTPRINT or INTVIEW from a DOS command line in the directory where the plot files reside. Starting from Windows does not put you in the right directory, so you have to supply a path for each plot file. All plots are in HP-GL/2 (Hewlett-Packard plotter format) and have the extension .PLT. A list of these plot files and their contents are shown below in Table 1:

PBGI.PLT	Trajectories or trajectories and equipotentials
EQPLT.PLT	Equipotentials
EQFINE.PLT	Fine matrix equipotentials
CURSO.PLT	Distribution of current at source
EMIT1-4.PLT	Emittance plots (maximum of 4)
DISTOR.PLT	Radius at source vs. radius at target
CUREXP.PLT	Current density at exit plane or target
CURD1-4.PLT	Current density distribution at emittance plot plane (maximum of 4)

Table 1: Standard PBGUNS output plots

Note that it is essential that the ratio of image width to height always be 4 to 3 or the plot will be distorted. Frequently used values are 8.0 to 6.0, 10.0 to 7.5 and even 11.0 to 8.25 (in landscape mode) on a laser printer; values as high as 20.0 to 15.0 will work on a wide carriage dot matrix printer. The plotter routines have not been tested, so the colors may not be optimal (in particular, yellow usually does not work well). Plots can be made as large or as small as you want, but be sure to maintain the 4 to 3, width to height, ratio.

1.4   Examples

PBGUNS comes with a variety of example problems. Running these can be a good way to familiarize yourself with the program. Table 2 summarizes the type of simulations found in each of the example files, as well as the Section in this manual where you can find information on that particular simulation (also see Section 6 Simulation Examples). Note that there is an additional .dat file in the program directory: PBGI.dat. This is not an example file; this file is generated/over-written by the program as it executes. PBGI.dat is useful for restarting the program.

This directory also contains files that help initialize the interactive data (Ebeam.DTA, Rebeam.DTA, ibeam.dta, etc). These files supply initial defaults for many parameters. These can be edited if you want to change the parameters or they can easily be changed interactively at the startup of the program.

Section	Simulation	ICT	Filename
6.1	Electron Field Emitters	1	mfe.dat
6.2.1	2.2 Micro-Perveance Electron Gun	2	neg.dat
6.2.2	1.9 Micro-Perveance, Low Energy Electron Gun	2	leeg.dat
6.3	Relativistic Electron Gun	2	reg.dat
6.4.1	Relativistic Slit Electron Beam Gun	2	rsb.dat
6.4.2	Non-Relativistic Hollow Beam Electron Gun	2	hbeg.dat
6.5	Magnetron Injection Electron Gun	2	mig.dat
6.6.1	Negative Ion Sputter Source	14	iss.dat
6.6.2	Primary Beam Sputter Ion Source	5	pbbs.dat
6.6.3	Secondary Sputtered Ion Beam from Target	5	sbt.dat
6.7	CRT Guns	11	crt.dat
6.8.1	Negative Ion Beam Extraction From a Plasma	11	nib.dat
6.8.2	Positive Ion Beam Extraction From a Plasma	12	pib.dat
6.8.5	Emittance Plots for Multi Ion Beams	11	ecris.dat
6.9.1	Injected Beam Through a Lens	18	lens.dat
6.9.2	Low Energy Ion Beam Neutralization	18	leb.dat

Table 2: Available Example Data Sets

1.5   Graphics Customization

PBGUNS contains the configuration settings file "Interact", which is used to specify various quantities required by Interacter to indicate your screen resolution, etc. By editing this file, the default settings can be customized for your machine and printer.

A sample "Interact" file is given in Fig. 1. It sets the PBGUNS resolution (PIXELH, PIXELV) to 1280 by 1024. The PBGUNS window can be set at or less than the Windows resolution; for instance it is okay to run Windows at 1600 by 1200 and PBGUNS at 1280 by 1024.

The PBGUNS window described in the sample "Interact" file will be centered on the screen (WINPOS 0 0). It will use a 10x18 font (TEXTFONT). Textfont defines the font for (non graphic) text on the screen. The 10x18 font works well for the two higher resolutions, but the 12x16 font looks better (you can read it) at the lowest resolution on both laptops and standard PC screens. At the lower resolution the mouse does not always come up at the intended position on the screen; unfortunately, a solution for this problem has not been

```
REM SET YOUR DISK ON LINE BELOW
CHARSET = c:\PBG501\DUPLEXR.chr
MOUSE = 2
REM WINDOW POSITION 0,0 CENTERS THE SCREEN WINDOW
WINPOS = 0 0
TEXTFONT = 10 18
REM SET EITHER YOUR SCREEN RESOLUTION OR THE EXECUTABLE
REM WINDOW SIZE BELOW
PIXELH = 1280
PIXELV = 1024
REM
REM PIXELH = 1024
REM PIXELV = 768
REM TEXTFONT = 12 16
REM
REM PIXELH = 1600
REM PIXELV = 1200
REM
PLNAME = PRN
PLOTTER = 6
PRINTER = 29
PRNAME = PRN
MOUSE = 2
```

Figure 1: Interact file

found.

Additionally, there is a graphics character file (DUPLEXR.CHR) which is called by the program.

2   Introduction to the Program

2.1   Program Overview

The code produces excellent agreement with experimental results for both relativistic and non-relativistic problems, and thermionic as well as field emission cathodes. It is written in largely generic FORTRAN 77 or 90 and should run on virtually any machine from a PC to a CRAY. The Windows PC version is compiled with LF95 FORTRAN (from Lahey) with the Interacter plotting package (producing gorgeous Postscript plots), which is distributed in the U.S. by Lahey.

The simulation is carried out on a large regular grid/mesh (an array of squares), with a finer grid/mesh (also an array of squares) covering the cathode emission region. Problems as small as 100 by 50 often run in minutes on a PC, and 400 by 200 problems may require between minutes to a few hours depending on the problem complexity.

All floating point calculations are done in double precision (8 Byte, 64 bit) arithmetic. Interactive changes may increase the total run time to several hours. Configurations with many electrodes tend to converge faster, while configurations with large regions with no electrodes tend to converge slower.

2.2   Simulation Approach

PBGUNS employs relaxation techniques while alternately computing trajectories and voltages. The voltages in the configuration are simulated on a rectangular array of squares. The voltages are iteratively relaxed (by passing back and forth through the matrices) using Poisson's equation in difference form at each point on the voltage arrays. The space-charge densities used are computed from the macro-particle trajectories and are stored at adjacent points along the path on arrays identical to the voltage arrays. The electrodes in the configuration are defined by quadratic line segments.

The accuracy of the program is derived directly from the resolution of the fine matrix that covers the particle emission surface for both electron and ion beams, and indirectly by the resolution of the regular mesh. Accuracy is also enhanced by the rather simple mesh of squares which makes the calculations easier and more accurate.

The trajectories are computed by solving either the relativistic or non-relativistic Lagrangian equation or the Lorentz force equation in axisymmetric cylindrical coordinates or in rectangular coordinates. Each trajectory carries a current fixed at the source and stores the space-charge at adjacent matrix points along its path. The space-charge densities and current distribution are computed from the trajectories by requiring zero divergence of the

current density. The z-directed current distribution is computed and used to compute the induced magnetic field for the relativistic calculations. Since each trajectory is computed independent of all the others, crossing is not a problem in relativistic beams. The smoothness of the space-charge distribution is a function of the number of trajectories that are computed. One trajectory per fine matrix square along the cathode is the minimum requirement, while 2 to 4 (for thermionic emitters) and 100 to 200 (for field emitters) per fine matrix square will produce the best results.

Current densities from the cathode can be computed using either Child's Law (with Langmuir-Blodgett corrections for curved surfaces[8][9]) for space-charge limited emission or the Fowler-Nordheim equation for field emission (see Appendix B: Theoretical Development of PBGUNS). For space-charge limited emission the voltage employed in the calculation is at a matrix position of two fine mesh increments in front of the cathode. It is important that this calculation be made as close to the cathode surface as possible as the variations in current density along the cathode can be masked by using a larger spacing. In the actual device the current density at a given point along the cathode is determined a differential distance off the cathode surface (actually at a virtual cathode caused by the electrons finite emission energy), only the total current is determined by the anode voltages. Going ten to twenty percent of the distance to the anode, as seems to be popular with finite element codes, will almost certainly mask a sharp rise (or fall) in current density frequently found at the edge of a cathode. The electric field required at the electrode surface for field emission is computed at the electrode surface from a cubic fit to the potentials just in front of the emitting surface.

Applied magnetic fields are introduced through the trajectory equations. In axisymmetric configurations only axisymmetric magnetic fields may be employed, with one exception; electrons can be separated from a negative ion beam with a transverse magnetic field using an approximate calculation. The magnetic field may be uniform, may vary slowly with axial position (field defined on the axis), or may be supplied from a magnetic field generating program (field defined on a mesh identical to the voltage mesh). Unless the magnetic field is extremely complicated, values on the axis of the beam are usually sufficient. The two dimensional configurations can use a uniform field normal to the plane of simulation or the field may vary in the z-direction. In either case, the self-induced magnetic fields are automatically included when relativistic, electron beam solutions are obtained.

For many problems it is necessary to use double precision (8 byte, 64 bit) arithmetic. The most significant problem occurs when the particle accelerations are so small that the acceleration increment differs from the numerical trajectory location numbers by more than the precision of the machine. Several problems were observed with 32 bits, no problems have

been observed at 64 bits. The program also appears somewhat more stable on problems that do not necessarily require double precision. The program is supplied using double precision arithmetic.

The program permits the computation of either a positive or negative ion beam onto a target and then the computation of an opposite sign ion beam with the same current distribution from this target. This is accomplished by saving the space charge from the primary beam and restoring it to the REVERSED problem on the same size matrix. The fine meshes are restricted to INF = 1, 2 or 4 and are handled automatically as usual. Current densities injected from the cathode of the second run are proportional to the space charge densities at the target of the first run. This could also be used to determine secondary electron trajectories for a positive ion beam device.

Another capability of the program allows the computation of an x - x' emittance plot derived from the standard r - r' emittance plot. Chan, et al's technique[6] for adding azimuthal particles is used in the angular spread routines to generate the necessary information. An x - x' emittance plot can be strikingly different from the r - r' plot. Comparison with experimental data, which is usually obtained in the x - x' format is greatly enhanced. The utility XXP is supplied with the program for this calculation.

Files used by the program include the input data file, PBGI.DAT (or PBGA.DAT), and the output data file, PBGI.LOG. Be aware that the program will delete any file by the name PBGI.LOG before starting execution. For complete magnetic field problems a file MAGB.DAT, containing the Z component of the normalized field, is read. The program will save binary data for restarts in a file called PBGDD.BIN and then rename it to match the input data file name. Note that this file may be up to 5 Mbytes long (typically 1 Mbyte for relativistic problems). On restarts, the program will tolerate significant changes in the input data, including the anodes, however care must be taken when the cathode is changed. The last data and binary files must be renamed at the end of the run to save them.

The beam data can be saved in a file PBBMSV.BIN. Files with various names (PBGI.PLT, EMIT1.PLT - EMIT4.PLT, CURD1 - CURD4.PLT, EQFINE.PLT, EQPLOT.PLT, CUREXP.PLT and DISTOR.PLT) are generated by the plotting routines and contain the information required to generate hard copies of the results or to review on the screen; again, previous files with these names will be deleted. The reversed sign space-charge density (used for positive-negative sputter sources) is stored in a file RHOS.DAT (or RHOP.DAT) and does not need to be renamed when used.

When an x - x' emittance plot is needed, a file called NEP1.DAT is generated. This plot can be used directly by the XXP program, or renamed NEP2.DAT, to generate the plot.

2.3   Checking for Validity of Results

This program now contains over 58,000 lines of code and an enormous number of options. **PBGUNS** has been extensively tested, however not every combination of parameters have been tried. In addition, the user needs to be on the alert for details that can reduce the validity of the results.

Some things are easily observed; such as a beam with a significant, non-zero current, crossing the axis at a single point so that the space charge density becomes excessive and the resolution of the matrix inadequate (a finer mesh is probably needed). More subtle problems can occur in an ion beam source plasma. If a converging plasma is injected [DO NOT READ THIS AS BEAM] (particles in a PLASMA are started at an angle toward the axis), the ion space charge density may attempt to force the plasma potential to negative values. The program will tolerate this effect (by limiting the voltage at zero) and the results can be invalid (or compromised) with nothing to suggest that there was a problem. That is the reason the potentials on the beam axis are printed out at the end of the PBGI.LOG file. Anytime a converging flow is started in the plasma (as in plasma sputter sources), an angular thermal spread should be used. Any angular distribution in the plasma should include skew energy to help keep particles off the axis, and to produce the best results for x - x' plots.

2.4   Running Without Invoking PBGUNS Internal GUI Interactions

A command line feature which allow **PBGUNS** runs without invoking the standard **PBGUNS** GUI interface dialogue is available (i.e., avoiding the prompts typically encountered in starting up a run). This allows both:

1. Running multiple **PBGUNS** problems in batch mode without any user intervention.

2. Re-running a **PBGUNS** problem using a different the major cycle parameter MM without modifying the original problem input file (effectively, replacing the value read in from the input file with the command line argument MM as shown below). Note, a major cycle consisting of one complete voltage relaxation and trajectory computation.

The required command format is

   PBGUNS_ PBGI.exe Input_ File.dat MM,

where the command line is executed within the directory in which the input problem file Input_ File.dat is located, and MM is the replacement major cycle parameter. When there is no MM argument, **PBGUNS** will run in regular GUI mode.

3   Interactive Input

The program can and should be run entirely interactively. There is no reason (except for old data sets that you might want to salvage) to ever make up an input data set using an editor. It is often easier to enter a data set interactively than to fix an old version. All of the input data can be entered interactively using either the keyboard or the mouse; you should be prompted for all necessary input data as it is needed (and many parameters will be set to default values without your knowledge). The electrode configuration can be entered only on the graphics screen. It is a good idea to read Section 4, paying particular attention to the parameters that affect the specific types of problems that you intend to run. Inexperienced users will find the program's prompting for information is extremely helpful in generating a complete input data set. Remember that incorrectly formatted data sets cannot be read by the program.

When starting the program you will be asked a series of questions about the type of simulation desired and some of the parameters needed to run the problem. It would be a good idea to make a sketch of the problem and determine scaling parameters before starting (the size of the mesh, the matrix increment and the length of a scaled unit). It is highly desirable to have the scaled unit length of the mesh to be the order of 5 to 50. An example would be a problem with a real world length the order of one inch, a scaled unit (ZSCALE) of a tenth of an inch (0.00254 meters) would make the mesh 10 units long. Scaled unit lengths between 5 and 50 will generally produce a grid on the screen that will be the most useful when drawing electrodes. Many other parameters will be set in this initial setup. Once all these parameters are established, the electrodes can be drawn.

The problem matrix size can also be expanded interactively, so that as one portion of an extraction system approaches the desired solution, the matrix can be extended, either radially or axially, and the beam traced through a greater distance. The beam can also be saved near the exit plane and restarted on a new mesh (downstream) for very long beam lines. The matrix can be made finer or coarser by changing the value of DR in the Parameters Menu.

The scaling voltage (VSCALE) and the length scaling (ZSCALE) should only be changed in the Parameters Menu. Changing either parameter can cause significant transients, but changes in the Parameters Menu will minimize the transient effects, as other parameters impacted by the changes will be automatically modified by the program.

The regular matrix should be kept as small as possible for speed in execution, and made larger as greater accuracy is needed (on very fast computers larger matrices may be desirable to slow down the progress of the calculations). Electrodes must be at least one matrix square

thick (DZ), which in some cases will determine the minimum matrix size. Sharp points may also require larger (finer resolution) matrices. Most of the accuracy of the program is determined by the resolution of the fine mesh covering the emitting surface or plasma region.

The size of the regular mesh can be changed interactively (the width NR and length NZ), without exiting the program. Electrodes that reach a boundary will be shortened or extended as the boundary is moved. Electrodes that exist only in a region that is being cut off should be deleted before reducing the matrix size. The matrix size change must be carried out in the Parameters Menu, and can be viewed on the graphics screen immediately after the change.

The mouse cursor is an arrow or a poor cross, as the Interacter routines cannot use the more precise "+" cursor due to some disagreement with Windows, and their substitute cursor is not very precise. The arrow cursor is not as exact in its point as the cross cursor, but the numbers in the box on the screen are accurate.

When working with menus, the mouse will drag the highlighted choice or you can click it directly on the choice you want to make. The actual choice is made when you release the button. If you drag the cursor off the menu before you release the button, no choice will be made.

There are rules that must be followed when drawing electrodes. Perimeters of electrodes must be defined in a counterclockwise (ccw) manner. Any electrode that appears on the fine mesh (which covers the plasma or emission surface region) must be defined as a cathode electrode. **PBGUNS** by itself cannot tell if an electrode is or is not on the fine mesh.

Remember that every electrode that starts at a boundary must end at a boundary, and an electrode that does not start at a boundary must close on itself.

Each line on the electrode is drawn in two stages. The first point is defined using the mouse cursor, and then the arrow keys if more precision is needed. The Mouse cursor is limited in position accuracy by the steadiness of the hand, quality of the mouse and by the pixel size on the screen. These errors may be significant in some cases. Each point should be determined by the mouse cursor, as close as possible to the desired point, followed by clicking the left mouse button once. *If making a small, precise change, clicking the right mouse button will put you in the arrow key mode immediately without changing the starting point.*The cursor can only be moved with the arrow keys once either button is pushed. After the first left mouse click, the exact point, as determined by the mouse cursor, is rounded to the nearest hundredth of the scaled units of the screen and is displayed on the screen. If this is good enough, a second click of the left mouse button or <ESC> (the Escape key) accepts this value.

If this is not accurate enough, the arrow keys can be used to increase the number of digits

out to a maximum of 4 decimal points (only 4 digits after the decimal point are generally used by the program). The arrow keys increment is initially set at 0.01 (0.1 for a right mouse click) so that they will first adjust the second decimal point of the x and/or y position using a this increment. A <CR> (Carriage Return or Enter key) will reduce the increment by factor of 10, to adjust the third and succeeding decimal point. Pressing <CTRL-CR> (Control and Carriage Return keys, simultaneously) will increase the decrement by a factor of 10. This process can be extended to the 4th decimal point which is the precision limit for the end point of a line, The location of the center of a circle can be determined out to 6 decimal digits. A second left mouse click or <ESC> (the Escape key) will fix the value to what is displayed on the screen and end the routine.

Once the first point of a line is defined, the end point is determined in the same manner except that a rubber band line will follow the cursor. The line can then be redefined to be a circle, parabola or ellipse if desired after the endpoints are defined. All circles must have a radius greater than a matrix increment. As each segment is completed it will remain on the screen.

Other ways of drawing line segments are also possible. If a line is perpendicular to the preceding line, parallel to some other line, or is the extension of a previous line this fact can be used to draw the line in a most simple manner. A menu will present these options for each line segment.

The area that the fine mesh covers is automatically determined by the program for problems with emitting surfaces (electrons and thermally emitted or sputtered ions). For ion sources that involve plasmas the front (right edge) of the plasma region must be specified by the user and the program will prompt you for this value. This should be defined so that several regular matrix points will be to the right of the actual plasma surface. For plasma sputter sources the radial width of the fine mesh will probably need to be specified because the plasma is generally significantly larger than the emitting surface. Again the program will prompt you for this value.

PBGUNS assumes the beam is going from left to right with one exception. A secondary beam sputtered from a target can be computed from left to right.

The active fine mesh can be modified in length interactively as long as only the front or the back limit is changed. If both front and back need to be changed, modify one, restart the execution, interrupt the program a second time and modify the other limit. This is used mostly to change the end of the plasma region for ion extraction problems when the plasma surface moves significantly forward or back. Remember the smaller the fine mesh (especially for plasma calculations) the faster the program will run. Extending a thermionic emission region may give the program a bit of a shock, but it will probably recover.

The ratio of the fine mesh to that of regular mesh (INF) must be specified, and is always requested when a new problem is being started. Defaults are offered by the program that will work in many cases (but not all). Plasmas (especially those with low thermal temperatures) and field emitters tend to require finer meshes than thermionic emission surfaces. Greater accuracy and stability are obtained with finer meshes, at the expense of increased execution time.

Circles can be determined in several ways. The program previously had a problem with circles that extended radially above and below its center, as a result the circle had be defined as two or more segments that exist only above or below it's radial center line. This problem has been largely cured in this version of PBGUNS, although for very small radii (one or two matrix squares) it may still be necessary to use two lines, one above the center and one below it.

Complete circles are defined in the following manner. The bottom half of the circle is always defined first. A horizontal line is drawn the diameter of the circle from left to right and the circle is declared to be below the line. The top half is then determined by drawing the reverse line and declaring it to be a circle.

Many circles are used to round off corners of electrodes. These can be defined by drawing a 45 degree line across the corner, declaring it a circle and answering the questions on the screen.

Circles on the axis are handled in a slightly different manner because the end points of the circle may not be easily defined and a fixed radius may need to be specified. Draw the straight line that best approximates the circle (one of these end points must be usable as the circle end or start point and the other must be the exact radial end or start point) and answer the questions on the screen and the problem becomes quite simple.

To change a circle already defined on the screen it should first be reduced to a straight line, modified, and then reset as a circle. This must also be done if an end point is changed because an adjacent line is being modified.

General circles (those not determined above) can be determined by moving the center of the circle on a line normal to the two endpoints and midway between them. This is automated in the program. Again the mouse and then the arrow keys are used to determine the exact center.

PBGUNS can handle (horizontal axis) parabolas in a similar manner to the circles.

You can move around MENU's either with the mouse or using the up and down arrow keys. An option is selected either by clicking the left mouse button on the line or by <CR> with the line highlighted by using the arrow keys.

Numbers that appear in menus in black on a white background can be changed by the

user. You can move from line to line with the <TAB> key (and backwards using <SHIFT-TAB>) or by clicking the left mouse button with the cursor on the number you wish to change. A <CR> terminates a menu that allows the setting of parameters.

Many of the questions asked by the program will depend on the exact type of problem you are solving. Plasma source problems will ask for plasma parameters, field emission problems will ask for work functions and fudge factors, etc. Again, if a number appears in a box, in black with a white background it can be changed as desired by editing the screen value. The value displayed will usually be the default or the current value.

Sometimes changing one parameter effects other parameters and the program will prompt for new values. These can sometimes be ignored if they are not effected, a <CR> accepts the current value.

Once the scaling parameters are defined, the graphics grid is established and graphical input of the configuration can be started. Unless there is a previously saved beam that is being injected, or an arbitrary beam is being injected, the first electrode defined must be the cathode electrode and must have the emission or plasma injection surface on it. The order of the entering of the remaining electrode descriptions does not matter as long as electrodes that appear on the fine matrix are defined as cathode electrodes. In the case of a beam sputter source the first electrode must be the cathode, and if the second electrode is the target, the program can set up the secondary beam interactively.

If the first cathode electrode is deleted, ALL the cathode electrodes must be deleted, if a new emission or injection surface is to be added.

If the program stops and says NTT is too small, anode electrodes can be renamed as cathode electrodes (or vice versa), although you must do this manually or by deleting the electrode and then re-entering it. The NTT=60,000 point limit of the current version of **PBGUNS** handles all the current test problems.

A plasma sputter source may restart the beam in the plasma region and will require a plasma (cathode) electrode to cover this region; an emission or injection region is not required.

When running **PBGUNS** interactively, one must choose the input data file, either PBGI.DAT or an alternative input file named filename.DAT, where "filename" was the user assigned problem input file name. If the alternative input file filename.DAT is chosen, the file contents are copied to the file PBGI.DAT (overwriting any previous PBGI.DAT), which is then treated as the PBGUNS working input file.

PBGUNS can be interrupted at any time while the potential relaxation is proceeding by using the F1 function key or clicking the left mouse button key on the F1 box location on the screen. It will then ask if you want to modify the input data file PBGI.DAT, the

already modified file version, PBGA.DAT, or if you would just like to pause before you continue execution. Runtime changes to the initial simulation settings in PBGI.DAT are written PBGA.DAT, preserving the original input file. At the end of the run it is a good idea renaming the PBGA.DAT file, to save the changes, as this file can be overwritten when running **PBGUNS** again.

Note that if you chose PBGI.DAT, the file PBGA.DAT will be created from PBGI.DAT, and your modifications will be to PBGA.DAT, preserving the original PBGI.DAT. The pause was added because for some problems the computer is so fast that it makes it difficult to digest the results on the screen. The desired data file can then be read into the interactive routines and a series of options will be presented allowing modification.

The program can also be interrupted at the completion of the trajectory calculation by pressing F2 to modify PBGI.DAT or F3 to modify PBGA.DAT or clicking the left mouse button on the screen locations where the option is shown. F2 or F3 can be activated while the trajectories are being calculated, but will not cause the interruption until they are complete. Eventually the cursor will appear on the default option for any case.

There is no CAD input program connection, because it is not the purpose of the program to analyze a configuration, but to develop it. The finalized input file (usually PBGA.DAT), will consist largely of a list of line endpoints for each electrode which can easily be used as input data to a CAD program. The Intprint program allows the generation of an Autocad formatted plot.

For a new user it is recommended that all the menus be explored to familiarize one with where and what changes can be made. Changes in ordinary parameters can be done most easily in the Parameter Menus. Changes in the magnetic field and other configuration related parameters are generally under the Geometric Routines.

Restarting **PBGUNS** is nearly automatic. If the program is interrupted to change the configuration or some parameters, the voltage matrices (regular and fine) are written to the disk and are restored when the program restarts. If the program runs to conclusion and generates output plots, a much more inclusive file (PBGDD.BIN) is created and stored on the disk for future restarts. When **PBGUNS** is restarted either from the original file (PBGI.DAT) or the modified file (PBGA.DAT) it will search for the PBGDD.BIN file.

The data files generated can be saved with unique names, and will be available and selectable from a menu when the program is started. The PBGDD.BIN file will have the same name as the input data file. When starting, the program will make copies of the .dat and .bin files so that the original input file information is not lost if the program does not complete normally. However, the original files will be overwritten if no action is taken to rename them at the end of the program execution.

PBGUNS is quite flexible and tolerant of changes in the configuration in either case - almost anything can be changed, including the sizes of matrices. It may be desirable to start with a relatively short matrix and extend it as the desired beam is obtained. **PBGUNS** extends (or shortens) lines that reach the borders of the mesh when the mesh is made larger (or smaller). There may be problems if circles on the electrodes reach the boundary but the program will usually tell you what may need to be fixed. The best thing to do is view the electrodes on the screen to be sure they are complete, i.e., they reach the boundaries or close on themselves.

One of the most difficult problems occurs when a thermionic cathode is moved a small distance backwards. The space charge densities from the preceding results immediately in front of a cathode are extremely large and may cause significant transients in the relaxation. However the program will now usually recover.

4   Input Data

This section describes the two sets of data required to run PBGUNS; the problem size related Fortran parameters, either hard-coded or dynamically assigned at runtime, and the problem input file format.

4.1   Maximum Problem Size Related Parameters

The program must be given the maximum size of several of the matrices employed in the simulation and data describing the configuration to be simulated (included in the configuration data is the logical information describing the electrode configuration). Most of the matrix-size parameters are hard-coded and set a limit related to some aspects of problem size and evaluation, while a few are allocated dynamically allowing sizing up to the available 32-bit addressable memory. The critical matrices are described below, indicating the ones which are dynamically allocated:

NZZ - the maximum axial length of the problem coarse grid, defining among other matrices, the axial extent of the coarse voltage matrix. Sized to be n+1, where n is the maximum number of axial grid cells. (*dynamically allocated*)

NRR - the maximum radial extent of the problem coarse grid, defining among other matrices, the radial extent of the coarse voltage matrix. Sized to be n+1, where n is the maximum number of radial grid cells. (*dynamically allocated*)

NZF - the maximum axial length of the problem fine grid, defining among other matrices, the axial extent of the fine voltage matrix. The fine grid size used in a problem is determined by PBGUNS based on the input data describing the electron/ion beam source configuration. (*dynamically allocated*)

NRF - the maximum radial extent of the problem fine grid, defining among other matrices, the radial extent of the fine voltage matrix. The fine grid size used in a problem is determined by PBGUNS based on the input data describing the electron/ion beam source configuration. (*dynamically allocated*)

NTP - the maximum number of trajectories to be traced. (*NTP = 30000*)

NMAT - the maximum number of matrices needed to describe the configuration. (*NMAT = 24*)

NMATF - the maximum number of fine matrices needed to describe electrodes on the fine mesh. (*NMATF = 24*)

MREG - The maximum number of logical axial divisions allowed to describe the configuration. (*MREG = 250*)

NTS - The maximum number of equations allowed to describe the electrodes. (*NTS = 300*)

NTT - The length of the arrays describing the configuration, obtained from the electrode equations. (*NTT = 60000*)

NIP - the maximum number of beams injected into problem. (*NIP = 100*)

IIPB - the number of breakpoints allowed in plasma distribution for ion beams. (*IIPB = 200*)

NEQ - the maximum number of equipotentials that can be plotted. (*NEQ = 40*)

NLINS - the maximum number of straight lines in a column of the matrix. (*NLINS = 24*)

NCIR - the maximum number of circles in a column of the matrix. (*NCIR = 10*)

NPLNS - the maximum number of lines in the datafile. (*NPLNS = 300*)

The relation of these parameters to problem setup will become more evident as the input data for a PBGUNS simulation is described in Section 4.3. If you find that the default hard-coded parameters are inadequate, For assistance, please contact FAR-TECH, Inc. at support@far-tech.com, about the possibility of providing a version of PBGUNS with appropriately modified matrix-size limit parameters for your problem.

4.2   The Logical Description of the Configuration

The newly updated **PBGUNS** has implemented the Ray-Casting algorithm to calculate the logic of region configurations. It covers any region with line segments that can be described by quadratic equations.

The number of regions can become quite large when complex electrode shapes become involved. The current limit is 250 regions (defined by MREG) and 300 line segments (defined by NTS). The number of regions start to increase significantly when one begins rounding sharp corners and expanding the simulation into regions adjacent to the main part of the simulation.

4.3   The Input Data File PBGI.DAT

The default input file that PBGUNS actually runs is PBGI.DAT. Alternatively, the user can provide an input file named filename.DAT, that is then used to create PBGI.DAT. The naming convention for filename.DAT is that filename can be any text string not containing spaces.

The input data file can be as short as 10 to 15 lines for simple configurations or as long as 40 to 60 lines for complex, multi-electrode configurations. The exact form of this file will be described here. Some numerical examples are shown in the following chapters. All of this file can and should be generated interactively.

The format of the input file is critical; the program cannot read the data if it is not in the correct format. Each variable is allotted a fixed number of characters and is expected to be of a certain type. For instance, if the format description says "I4", there must be an integer (I) which is 4 or fewer digits long at that point in the input file. If the integer is fewer than 4 digits, it must be right-justified within those 4 spaces. If the format description is preceded by another number, the format is repeated that many times. (Example: "20 I4" means that 20 integers with 4 digits each are expected.) "F" signifies a floating point number; for instance, "F8" means that there are 8 digits reserved in the file for the floating point number.

Table 3 below lists the input variable names and expected format for each line of the input file. It is okay to skip some variables as long as you leave the appropriate amount of blank space for them. Required lines are marked by an *.

Line #	Variables	Format
1*	MM, KKM, NZ, NR, NR0, ICAT, NAN, INF, IBMAG, IDG, NFZ, NFR, NZOF, NROF, IDIS, IOVL, IGRF, I9, ITP, IPD	20 I4
2*	MU, ITD, INEG, IXP, ISP, NOREL, ISCS, IENJ, IRST, IPRV, NION, IEQ, INCR, IRF, NRLO, NRHI, NZLO, NZHI, IRTD, RATD	19 I4, F4
3*	SZERO, VSCALE, ZSCALE, DZ, EPSV, BMAG, AMASS, E0	8 F10
4*	BETA, DTGT, STLIM, ZINE, ZITC, BENU, CEN, ECAT, EEL, EINT	10 F8
5*	ZEP(1), ZEP(2), ZEP(3), ZEP(4), ZSAV, ZSKP(1), ZSKP(2), ZSKP(3), ZSKP(4), ZTARG	10 F8
6	EINJ, PPINJ, ZLENJ, ZHENJ, RBBOT, RBTOP	6 F8
7*	NK, VLT, NEX(1), ICT, RSTRT, ZSTRT, REND, ZEND, SLITLN, ZNEP, NROFF, NZOFF, NMAX	I4, F8, 2 I4, 6 F8, 3 I4
8a	WORK, GAMMA, ESTRT, DTGTA, VTGTA	5 F8
8b	ISPRD, AINC, SKEW	I4, 2 F8
9a	PCRNT, ISPRD, NBSP, ISPN, ITBP, IPLBL, IPLBH, AINC, SKEW, ITBPS, VBIASC, VBIASE	F8, 6 I4, 2 F8, I4, 2 F8
9b	ZDIV, ZSURF, TE, TPI, PIR, TNI, RHIN, RHEND	8 F8
10	PP(I), I=1,NION	10 F8
11	RCUR(I), I=1,NION	10 F8
12	EPP(I), I=1,NION	10 F8
13	XS(KK), KK=1,ITBP	10 F8
14	SC(KK), KK=1,ITBP	10 F8
15	ANG(KK), KK=1,ITBP	10 F8
16	PIRZ(I), I=1,ITBPS	10 F8
16a	PIRP(I), I=1,ITBPS	10 F8
17 (&20)*	SYMB, ZB, RB, ZZ2, RR2, ZC(K+1), RC(K+1), RO(K+1), ZO(K+1), CX	A3, 9 F8
18 (&21)*	SYMB, ZB, RB, ZZ2, RR2, SP(1,K+1), SP(2,K+1), SP(3,K+1), SP(4,K+1), SP(5,K+1), SP(6,K+1), CX	A3, 11 F7
19*	NK, VLT, NEX(L)	I4, F8, I4
22*	FMT(1:80)	A80
23	BM(I), I=1,NZ	10 F8
24a	IBB	I4
24b	XS(K), K=1,IBB	10 F8
24c	VY(K), K=1,IBB	10 F8
25	CSV(K), K=IESTRT,NOEL	10 F8
26	VCON(I), I=1,NEQ	10 F8

Table 3: Input File Format. Required lines are marked by an *.

Table 4 gives the conditions for when the optional lines must be present.

Line #	When it is Read
6	Line 2: IENJ > 0
8a	Line 7: ICT = 1
8b	Line 7: ICT = 5 *or* Line 2: ISCS = 2
9a-b	Line 7: 10 < ICT < 17
10-12	Line 7: ICT = 8 *or* = 9 *or* > 10
	AND
	Line 2: NION > 1 *and* Line 2: IRST = 0
13-15	Line 7: 10 < ICT < 17 *and* Line 9a: ITBP > 1
	OR
	Line 7: ICT = 8 *or* = 9 *or* =18 *and* Line 7: NROFF > 1
16, 16a	Line 7: 10 < ICT < 17 *and* Line 9a: ITBPS > 0
23	Line 1: IBMAG = 1 *or* 4
24a-c	Line 1: IBMAG = 6 *or* 7
25	Line 2: IRST <= 0 *and* Line 7: ICT = 4
26	Line 2: IEQ = 2

Table 4: Optional Input Lines

Table 5 gives the conditions for when auxillary input data files must be present.

File Name	When it is Read
MAGB.DAT	Line 1: IBMAG = 2 *or* 5
AXMAG.DAT	Line 1: IBMAG = 8

Table 5: Optional Auxillary Input Data Files

A description of each input line associated variable is given below.

4.3.1 LINE 1. FORMAT (20 I4)

1. **MM** - The number of major cycles to be computed in this run. A major cycle consists of one complete voltage relaxation and trajectory computation. Extreme numbers would be 3, for a low current, low space-charge device, to 40, a high current and space-charge dense device, or even 200 for a magnetron injection electron gun. Most problems will fall between the lower two extremes. Magnetron injection guns are a special case.

2. **KKM** - The number of passes through the voltage matrix on the first cycle through the program, typically 200 to 1500. It is neither necessary nor desirable for the voltage relaxation to converge for several major cycles through the program, especially if there are significant space charge effects. Dense electron beam problems have ran well with KKM at 600 to 900. Generally field emission and very low space charge problems should use larger values of KKM and smaller MM's. KKM is reduced by up to 4 percent of the initial value during the first 10 cycles, down to a minimum of 200. It can vary from 250 to 3000 depending mostly on matrix size and space charge effects. Low space charge and Laplace solutions should use higher values. A wide range of damping can be obtained with the above two parameters combined with variations of BETA, the damping factor defined below. The only problem that could not be stabilized at all was a Magnetron Injection Gun with a cathode that had a 6 degree half angle (current from the back of the cathode can cycloid back near the front of the cathode and cause instability) although a pretty good estimate of the experimental current was still obtained. Sometimes extremely sharp field emitters become unstable, especially when current densities exceed 10^{10} A/m^2 at the tip.

3. **NZ** - The number of axial matrix points (number of coarse grid axial cells plus one). This will typically be a number in the range of 101 to 201. The odd numbers are typical because n matrix squares require n+1 points. This number can be changed interactively in the parameters menu.

4. **NR** - The number of radial matrix points (number of coarse grid radial cells plus one). This will typically be a number in the range of 51 to 101. The odd numbers typical because n matrix squares require n+1 points. This number can be changed interactively in the parameters menu.

The above two parameters are selected by taking several things into account. If the electrodes are thin sheet metal or have sharp points then these numbers should be selected so that every electrode is at least one matrix square thick (two is much better). Any gap between electrodes must be at least 2 or 3 matrix squares across (in the case of the cathode or plasma regions this applies only to the fine mesh). Most of the program's accuracy depends on the fine mesh resolution. One might also start with a coarser fine mesh and progress to finer meshes as the final design is approached. Note that the larger these meshes become the longer the program will require to run, but the greater the accuracy, and usually stability, is obtainable.

5. **NR0** - The offset of the matrix from the axis of symmetry, in units of matrix squares. For rectangular (2-D) configurations NR0 = 9999, for solid axisymmetric beams NR0 = 0. Hollow beams (simulation region not including the axis) can be simulated with values less than 9999.

6. **ICAT** - The total number of plasma, cathode and anode electrodes (to be described below). ICAT should only be changed by the electrode drawing or modifying routines.

7. **NAN** - No longer used

8. **INF** - The ratio of the regular mesh increment to that of a fine mesh increment. This must be an integer, usually between 2 and 20, and INF must be ≥ 1. The default value is INF = 4. The larger this number becomes, the more precision is obtained in the calculations near the emission surface or in the plasma, but the longer it will take the program to execute. Electron beam guns generally run best with a ratio around 8. Negative ion beams generally require higher ratios.

9. **IBMAG** - The type of magnetic field to be employed.

0 - No applied magnetic field

1 - An axisymmetric magnetic field which is slowly varying and is defined by its values on the axis (normalized to BMAG). See 6 below.

2 - An axisymmetric magnetic field generated by magnetic field codes and defined by only the axial components Bz on a matrix identical to the voltage matrix. It must be available in a binary file MAGB.DAT (in double precision), in the same directory as the program is running. The file is read in by the statement:

$$READ\ N\ ((BZ(I, J), I = 1, NZ), J = 1, NR) \tag{1}$$

These numbers are also normalized to BMAG. The magnetic field does not need to cover the entire simulation region. The actual radial extent of the matrix can be less than NR, However, still must cover the beam.

3 - A uniform magnetic field (BMAG) normal to the plane of simulation in two dimensions.

4 - A one-dimensional magnetic field normal to the 2-D plane of simulation but varying in the z (x) direction. The values, normalized to BMAG, are read into each point along the matrix. See 7 below.

6, 7 - Reads in an axial variation along the axis of the beam using the breakpoint method. Then, if IBMAG = 6, it is reset to IBMAG = 1, or if IBMAG = 7, it is reset to IBMAG = 4.

8 - Reads axis magnetic values from a file called AXMAG.DAT in a 10F8 format. These numbers are also normalized to BMAG.

10. **IDG** - Controls print out from the configuration setup routines and subroutine calls. Useful for debugging data. Normally left 0.

   0 - deletes printout - the usual value,

   1 - prints diagnostic output,

   2 - adds more diagnostic printout.

11. **NFZ** - It is recommended that this number be left zero, letting the program compute its value. This specifies the number of axial (z or x) matrix points on the fine matrix. This should be large enough to cover the cathode emission area plus a few (5 to 10) matrix points in front of the cathode (or the plasma region for an ion beam). (NFZ − 1)/INF must exactly equal an integer and will be enforced by the program. If NFZ is zero the fine mesh is determined automatically by the program and will cover the cathode emission region plus a small region around it, or the plasma region for an ion beam (see ZDIV below). NFZ would also be zero in the case of a (restarted) drifting beam. It is essential that all (and only) cathode related electrodes be employed on the fine mesh. If any part of an electrode appears on the fine mesh it must be described as a cathode electrode.

12. **NFR** - It is also recommended that this number be left zero. Only in the case of a plasma sputter ion source, where the plasma region is typically larger than the emission region should this number be specified. This specifies the number of radial (r or y) matrix points on the fine matrix. This too should be large enough to cover the cathode emission area plus a few (5 to 10) matrix points above and below the cathode.

(NFR − 1)/INF) must equal an integer and is enforced by the program. The larger NFZ and NFR become, the slower the program will run, however the more accurate the cathode and plasma emission surface calculations become. When the beam is saved in the plasma, NFR must be the same in both the initial and extended run.

If the data is being restarted (MU > 2), a small change in a thermionic cathode may cause the restart to fail or become unstable because of the extremely high space-charge densities near the cathode. Changes in the plasma injection surface generally do not cause a serious problem, although they will probably cause a transient.

13. **NZOF** - The number of matrix squares, on the coarse matrix, by which the fine matrix is offset from the left boundary. This is calculated by the program and should normally be left zero.

14. **NROF** - The number of matrix squares, on the coarse matrix, by which the fine matrix is offset from the lower boundary. It is recommended (but is not necessary) that if the configuration is symmetric about its center line that the fine matrix be centered about the cathode. This too is calculated by the program and should normally be left zero.

15. **IDIS** - Generates focusing-distortion plot (useful for image intensifiers) if IDIS = 1, IDIS = 0 skips plot.

16. **IOVL** - Controls whether or not the trajectories overlay the equipotential plot.

    0 - will overlay the trajectories,
    1 - will produce separate plots of trajectories and equipotentials, but will not shade electrodes on equipotential plot.
    2 - will shade electrodes on both plots

17. **IGRF** - If IGRF = 0, regular plots are produced, if IGRF = 1, cleaner plots with no grids and some annotation removed; good for viewgraphs. If IGRF = 2, even more annotation is removed. Note that IOVL and IGRF can be employed at the same time to remove extraneous annotation.

18. **I9** - Causes a linear decrease in the current emitted from the cathode from trajectory I9 to NOEL, where NOEL is the total number of electron trajectories. This has been of some use for very high currents emitted by flash x-ray machines, tending to stabilize the results. In general, if the current is this high, one should be wary of the results

(you might want to use a PIC code). Ordinarily this can be left 0, which will default to I9 = NOEL, so there will be no effect.

19. **ITP** - Program prints data from the emittance routines if ITP = 1. Typically not a lot of particularly useful data would be printed out. Normally left 0.

20. **IPD** - Controls printing of voltage and space-charge density matrices. This print output is used mostly for debugging when there is some problem with the results. This could take up a lot of disk space for a large problem. Generally should be 0.

0 - does not print,
1 - prints matrices.

4.3.2   LINE 2. FORMAT (19 I4, F4)

1. **MU** - Generally the program will set this for you. A parameter for saving and restoring data for restarts. If the program has not converged, or if changes are made in the configuration, the program can be restarted with the data saved from a preceding run. The data file consists of about 1.3 Mbytes for a (non-relativistic) 401 x 201 voltage matrix or about 2.5 Mbytes for a relativistic set.

1 - neither saves nor restores data,
2 - saves data, but does not restore old data,
3 - restores old data and saves new data,
4 - restores old data, but does not save new data,
5, 6, 7 - used in the interactive routines.

New data generated by the program is saved in a file called PBGDD.BIN, and old data is restored from the same file. At the beginning and end of a PBGUNS run this data can be restored or saved using any name desired. PBGDD.BIN is usually copied to a file named filename.BIN, such that it matches the original input data file name (i.e. filename.DAT).

On a restart the potentials on electrodes and between them on the boundaries will be reset if ISP = 0 (see ISP below). This permits some changes in electrodes between runs without changing the potentials between electrodes. A change in the cathode emission area (or plasma region) may occasionally require restarting the program from scratch.

2. **ITD** - The default value is ITD = 1, and would plot all the trajectories. As ITD is increased, fewer trajectories should be plotted. A typical value would be ITD = 3 to 6, for a field emitter or, ITD = 20 to 100 for a spread in injection angles. Many plots will be solid black (or red on the screen) if too many trajectories are plotted.

3. **INEG** - INEG = 0 for electron and positive ion beams, and INEG = 1 for negative ion beams (plasma or sputter source). This is not used for electron beams.

4. **IXP** - Controls whether or not the exit plane will be relaxed assuming that the axial field is zero. The exit plane should not be relaxed if there is either an accelerating or decelerating field, or if the beam is significantly converging or diverging.

   0 - does not relax the exit plane at NZ, typical of field emitters,
   1 - causes the exit plane to be relaxed, typical of thermionic and plasma generated beams,
   2 - relaxes both exit planes for a secondary, sputtered beam, see ISCS = 3 below.

5. **ISP** - Controls how the initial potentials are set on the voltage matrices. This parameter is usually handled by the program, but it can be changed by the user.

   -1 - Does not reset any potentials on a restarted run. Use if there are no changes in the configuration on a restarted run.
   0 - All potentials are set automatically by the POTSET subroutine. On a restart only electrode potentials and boundary conditions will be reset. This allows significant changes in electrode voltages and/or shapes between runs.

6. **NOREL** - If NOREL = 0, the electron trajectories computation will be fully relativistic. If NOREL > 0, only non-relativistic computations will be made. This can significantly speed calculations for electron guns below 10 kV. Ion beams are always non-relativistic.

7. **ISCS** - If ISCS = 1, saves the space-charge density matrix (RHO) with voltage normalization removed, sign reversed, and reversed axially in a file RHOSP.BDT (Primary). If ISCS = 3, the same file is saved except it is not reversed axially. If ISCS = 2, adds RHOSP.BDT, the reversed sign space charge, to the regular space charge just before relaxation of potentials begins. If ISCS = 2 there is an option to save the secondary space-charge densities in a file called RHOSS.BDT (Secondary), again with reversed sign so that it can be added to an ISCS = 3 run if desired. In any case the initial

run must be with ISCS = 1 or 3. If ISCS = 0 there is no effect on the calculations. BETA MUST be equal to 1.0 and no stripping or relativistic effects are allowed. This allows the space charge from a beam to be overlaid onto another beam of opposite sign, both configurations must be identical but reversed (1) or the cathode-target must be switched (3). The emitted beam current distribution from the second run (ISCS = 2) is proportional (and it is multiplied by SZERO) to the target current distribution of the primary beam. INF must be 2 or 4 for either run. Different VSCALE values can be used, the problem must be non-relativistic.

8. **IENJ** - Injected electron beam or negative ion beam, typically IENJ = 10 to 20. This is the number of trajectories per coarse matrix square (DR). This number must be positive and parameters on LINE 6 must be set in order to add these particles to the simulation.

9. **IRST** - Beam restore parameter. If IRST = 0, no beam is restored. If IRST = 1, a beam can be restored in a drift region, but no plasma or cathode region may be present. If IRST = 2, the injected particles in a plasma can be restored in the plasma (this is useful in sputter ion sources because of the typically long drift region in the plasma which can require a long time to compute). Saving the particle distribution near the plasma extraction plane can save a great deal of computer time while designing the extraction electrodes using the restored beam. Note that NFR must be the same for both plasmas.

10. **IPRV** - IPRV = 1 generates a preview plot of the electrodes. IPRV = 0 or field left blank will skip this plot. This will put a plot of the electrodes described by the input data on the screen for up to 2 minutes, then the program will continue. A good test for a new or modified data set. There is an option to terminate the run if the preview is not correct. Available only if the execution is started from a complete input data file.

11. **NION** - Number of ion masses to be injected. (up to a maximum of NION = 20)

12. **IEQ** - Controls the equipotentials to be plotted. Note that the actual equipotentials plotted are different for thermionic emitters and plasma sources. The actual values used are printed in the PBGI.LOG file. If you want to change a few equipotential values start with IEQ = 0 or 1, stop the execution and modify the values that will already be present.

0 - Plots potentials at 10 percent increments with additional values at the particle source and at the anode.

1 - Same as above but with 5 percent increments.

2 - Normalized equipotential values must be read in or modified from standard values (see LINE 26 for reading in VCON).

13. **INCR** - Used only if ICT = 6 (used to determine focus of image). Most useful for determining whether a focused image will be delivered for image transfer devices. Default value is INCR = 5, and must be at least 3. A positive value will inject 3 particles at each increment INCR (in trajectory numbers) along the emission surface; a normal particle and two particles at +/- 45 degrees to the normal. A focused image will be obtained when all three particles from a particular point cross the target at a corresponding point.

14. **IRF** - The number of major cycles through the program where strong over relaxation of the voltage matrix will occur. This is most useful for data were there are large areas of almost uniform fields that are slowly convergent. Most useful on the first one or two relaxation cycles. The following four numbers define the region.

15. **NRLO** - The lower radial limit (matrix point number) of the region where the over-relaxation will occur.

16. **NRHI** - The upper radial limit (matrix point number) of the region where the over-relaxation will occur.

17. **NZLO** - The lower axial limit (matrix point number) of the region where the over-relaxation will occur.

18. **NZHI** - The upper axial limit (matrix point number) of the region where the over-relaxation will occur.

19. **IRTD** - IRTD = 1 if the mesh size increment (DR and DZ) has been cut by half (i.e. doubling the mesh resolution).

20. **RATD** - RATD = 2.0 if mesh is doubled. (Other ratios require restarting data from scratch).

4.3.3   LINE 3. FORMAT (8 F10)

1. **SZERO** - Initial guess for current density or current density to be forced, in A/m^2. This number is used when there is a change in the number of trajectories on a restart

(MU = 3 or 4), then it is used to assign an initial current density to any new trajectory starting positions. This is also used to normalize the forced emission current densities for ICT = 3, 4 or 6, for the injected current density of a plasma ion source if the plasma current is zero, or for reflected current densities (ISCS = 2, see above). Otherwise, this number is not used by the program.

2. **VSCALE** - The scaling voltage (in volts) for the device, normally the anode (extraction electrode) voltage. A very safe value is that VSCALE be the potential on the highest voltage electrode. If the high voltage electrode is 9 kV, (or 29 kV) a scaling voltage of 10 kV (30 kV) might make other voltages easier to set. All other voltages read in or printed out must be normalized to this value. This allows one to change the voltages proportionately on all electrodes by changing only one number. No voltage on the matrix, in the vicinity of the beam, should exceed this value by more than 40 percent.

3. **ZSCALE** - The length (in meters) in the device which will correspond to 1.0 in scaled units (all data read in or printed out). This also can be set so that values read in or printed out will be in convenient units, e.g., if ZSCALE = 0.0254 meters, 1.0 unit equals 1.0 inch. This value also determines the grid used for equipotential and trajectory plots, and hence, should be selected with some care.

4. **DZ** - The length of one matrix square (in scaled units. If DZ = 0.1, one scaled unit would be 10 matrix squares long. The program will accept any scaling desired, but for convenience in the formats and formation of useful grids over the equipotential and trajectory plots, it is recommended (but not required) that the axis scaled unit length be kept in the range between 4.0 and 80.0. DZ should be at MOST 0.2 and desirably 0.1 to 0.05. If DZ is greater than 0.2 a reduced density grid will be generated by the plotting routines.

5. **EPSV** - The starting convergence requirement for a voltage matrix relaxation cycle at the beginning of a PBGUNS run. A typical value for this would be 0.00001 (10^{-5}). This is compared to the fractional change at each point of the relaxation from pass to pass through the matrix. If the fractional change is greater than this value the point is considered to be in error. Should the relaxation converge (i.e. the number of errors becomes zero), the program will reduce the value of EPSV by half on the next cycle. This process of checking for no errors and reducing EPSV will continue to a minimum value of 10^{-8} for electron beams and 5×10^{-7} for ion beams. Note that it is not a requirement for a reasonable convergence that the number of errors go to zero if

EPSV is small enough. Also, do not give the program a large number of major (MM) cycles and expect it to converge and terminate itself.

6. **BMAG** - The magnetic field strength (in Tesla's) to which all axisymmetric magnetic field information (see below) must be normalized. This refers to applied magnetic fields, internally generated (self induced) fields are independent of this value.

7. **AMASS** - The average mass of the particles to be used in trajectory computations, normalized to the mass of an electron. This value is used if only one species of ion is to be tracked through the device. Normally this value is 1.0 for electrons. A (positive or negative) proton would have the value 1836. Note that heavier particles (~1820 times atomic weight) can be simulated, but their sign is assumed negative for trajectory computations. Multiple ion values, ratios and energies are assigned below.

8. **E0** - the initial drift energy (not thermal) of the injected (electron or ion) particles in eV. This is also the voltage across the sheath of a sputter ion source (ICT = 14) where it is typically 0.5 to 1.0 kV. Note that the 'cathode' for a plasma sputter ion source is set at the plasma potential for the sputter ion source, the sheath is taken into account by the injection setup routine (CATEMS). E0 = 0 for a beam sputter source.

4.3.4   LINE 4. FORMAT (10 F8)

1. **BETA** - An under relaxation factor for the relaxation of the space-charge densities. The default value is BETA = 1.0 in most cases. BETA is the fraction of the latest computed value for the space-charge densities to be used in the computations. If BETA = 1.0 there is no damping and the changes propagate at maximum rates. In many cases BETA should start at 1.0, exceptions would be high perveance extraction systems (especially Magnetron Injection Guns) where space charge plays a very large role, and some problems where angular spreads in the trajectories are employed; for these devices BETA = 0.5 to 0.8 would be typical. Very fine meshes (INF = 16) frequently require no damping. Reducing BETA from 1.0 to 0.5 may increase execution time. If space charge is not significant, BETA may be greater than 1.0, e.g. 1.2 to 1.3 (higher values tend to be unstable), so that some over relaxation can be employed. If BETA is greater than 1.0, it is reduced by 5-10 percent, down to 1.0, from major cycle to major cycle. If a thermionic electron beam reaches an Excellent Convergence, BETA will be reduced by 10 percent per cycle until the program stops.

2. **DTGT** - If the beam is going to drift for some distance, a linear extrapolation of the trajectories can be made to an arbitrary distance DTGT (in scaled units). At this

point a computation will be made of the current distribution and the emittance plot. This calculation is fairly good for low space charge problems or for short distances, but not too good for space-charge dense beams or over significant distances. The emittance plot will not be produced if 4 plots are already called for by the ZEP values on LINE 5.

3. **STLIM** - The temperature limited current density from a thermionic or space-charge-limited cathode in A/m^2. A computed current density from Child's Law larger than this value will be reduced to STLIM. Default is STLIM = 0.0 and no limit is enforced. Set to value of BCRNT interactively.

4. **ZINE** - If the beam is neutralized at the entrance to the simulation, this is the z location (in scaled units) where the neutralization ends. This would ordinarily be used only for a restarted or injected beam. Default is ZINE = 0.0, no neutralization.

5. **ZITC** - The z location (in scaled units) beyond which the beam is neutralized. This calculation simply wipes out most of the space-charge density, (see BENU). For a positive ion beam this only needs to be approximate, the program will scan backwards (on the axis of the beam) through the beam till it finds a suppression voltage large enough to keep the electrons contained. If INEG = 1 (a negative ion beam), the neutralization will begin at ZITC. Default is ZITC = 0.0 and there is no neutralization. A variation on the above is available by setting ZITC to a negative number. The scan backwards is made for each row of the matrix so that the neutralization takes place over a varying axial position. This is sometimes needed when either a rather large area or a low voltage is involved with the neutralized region. See example in the Injected Beam descriptions of Section 6.9.

6. **BENU** - The fraction of the space-charge density to be left in the neutralized regions specified. This simply wipes out the space charge, but does not do any modeling of the real processes going on. Can be small negative numbers for negative ion beams. The default value is BENU = 0.01 (99 percent neutralized). Negative values can be used for more than 100 percent neutralization, e. g. -0.05 would be 105 percent neutralization.

7. **CEN** - Center of beam. This is generally determined by the program and can be left at its default value CEN = 0.0.

8. **ECAT** - For sputter ion sources ECAT is the mean energy of the particles as they are emitted (ejected) from the surface, before acceleration in the plasma sheath. Typically the order of 25 eV.

9. **EEL** - The multiplier for the emittance ellipse on the emittance plot. Converts RMS Emittance to the Lab. Emittance and plots ellipse. Generally EEL = 1.0 to 6.0. If EEL = 0.0, no ellipse is drawn.

10. **EINT** - Axial point where electrons injected with the ions will be intercepted.

4.3.5   LINE 5. FORMAT (10 F8)

1. 1 - 4. **ZEP** - A matrix four points long specifying the axial locations (in scaled units) for emittance plots to be generated. Note that only four emittance plots can be generated and only one, which must be ZEP(1), can be on the fine matrix. If extrapolated trajectories are computed (see DTGT and DTGTA above), no emittance plot will be generated for the extrapolated position if all four regular emittance plots are used. Unused values should be left 0.0. Current density distributions will be produced for these same cross planes for each value that is negative.

2. 5. **ZSAV** - Z location (in scaled units) where data is to be saved (in a file called PBBMSV.BIN) for restarting the beam in the next portion of beam line. In general, this should not be an edge of the matrix, but should be back far enough that there are little or no end effects, typically 10 to 20 matrix points back from NZ. ZSAV should be a round number, e.g. 12.0, because it will also be the starting z coordinate for the extended simulation.

3. 6 - 9. **ZSKP** - A matrix four points long specifying the axial locations for four planes where relaxation of potentials will NOT be carried out. This is useful for simulating flat screens in low current devices where the screen could be expected to survive. Screens are very useful at the entrance and exit in low distortion Einzel type lenses. The ZSKP value's must be 0.0 or correspond exactly to an axial matrix point. The first value may cross the fine matrix.

4. 10. **ZTARG** - The z location of the target plane. This parameter can be left zero if the beam reaches the right edge of the matrix in the z direction. If there is a target that the beam will hit before it reaches the exit plane, this is the target location in scaled units. If ZTARG = 0.0 (or blank) and an anode crosses the simulation radially, you will be asked for a value. This is what tells the program where to find such things as the target current density distribution. The default value is (NZ-1)*DZ.

4.3.6   LINE 6. FORMAT (8 F8)

LINE 6 is read only if IENJ > 0 (LINE 2).

The following parameters call for the injection of particles any place in the simulation to determine the effect on the particles of a transverse magnetic field in an axisymmetric configuration. This can be used to simulate electrons extracted from (and generated in) a negative ion beam, or for the simulation of electrons generated in a positive ion beam. This is only an approximate calculation, as it uses 2-D calculations with a transverse magnetic field. Note that these are only electron trajectories and carry no current and previous 3-D runs using a similar injection technique (and including space charge) have shown the electron space charge to be negligible. If the beam particles are to be saved in the plasma (see ZSAV), any injected electrons must be defined in the run where the other particles are saved. The axial location of the injected particles can be modified by the restarted data, but their existence must be defined in the initial run. This magnetic field distribution can be read only by the breakpoint method described in LINES 24a, 24b, and 24c.

In axisymmetric solid beams, two electron beams are injected with magnetic fields of opposite signs. When the reversed magnetic field beam crosses the axis the field is again reversed so that one can see how the particles will behave from both sides of the axis.

1. **EINJ** - The energy of the injected particles in eV. May be negative for backward injected particles. If EINJ is negative, the particles are also assumed to be of opposite sign to the primary beam.

2. **PPINJ** - Mass of injected particles - 1.0 for electrons.

3. **ZLENJ** - The lower axial limit of the injection region for particles, in scaled units. This must be outside the region where the plasma surface forms, a small accelerating field is needed to draw the electrons out. If the injection occurs too deep in the plasma, this will not work because the electrons are usually collision dominated there. This will not work if there is a strong magnetic field in the region, because the electrons will simply travel in small circles.

4. **ZHENJ** - The upper axial limit of the injection region for particles, in scaled units. If ZHENJ is the same as ZLENJ then a single plane is used for the injection.

5. **RBBOT** - The lower radial limit, of the injection region for particles, in scaled units. This should ordinarily be RBBOT = 0.0 for an axisymmetric, solid beam simulation.

6. **RBTOP** - The upper radial limit, of the injection region for particles, in scaled units.

4.3.7 LINE 7. FORMAT (I4, F8, 2 I4, 6 F8, 3 I4)

1. **NK** - The number of first electrode surfaces defined by quadratic lines. This includes the cathode and any adjacent focusing electrodes defined by the first cathode electrode.

2. **VLT** - The voltage on this electrode in scaled units (voltage divided by VSCALE). Typically VLT = 0.0 for a cathode, a small number (like 3.0 to 20.0 Volts) for a plasma, but can be any other value. If entered interactively this will be a real world voltage (in Volts). For ion beams, and especially negative sputter sources with converging plasmas, this will be the higher values (5.0 to 20.0 Volts). The plasma potentials are not allowed to go negative (there are some stability problems) therefore the program will put a floor on the potentials. If this happens the behavior of the plasma will be modified and the results may be invalid. The beam axis values are printed out at the end of the PBGI.LOG file and should be checked for any problem with a plasma present. If there are zero values (although a few may be tolerable) VLT should be increased. The potentials on all electrodes in contact with the plasma are important and should be set to this potential except those that have a real potential difference with the plasma. Remember the program always uses negative particles. For non-plasma emitters the voltages may be positive or negative values.

****ALTERNATE DEFINITION OF THIS PARAMETER****

VLT - For injected beams into a drift tube, this is the total injected current.

3. **NEX**(1) - NEX = 1 for electrodes which will cross the fine matrix, 0 otherwise.

4. **ICT** - The particle source type, i.e.,
   1 - electron field emission,
   2 - space-charge limited ion or electron emission,
   3 - forced uniform current emission (SZERO),
   4 - read in current distribution, multiplied by SZERO,
   5 - angular spread (cosine squared current) space-charge limited current (not relativistic), strongly recommended for extraction voltages less than 10 kV,
   6 - image focusing test,
   7 - micro-field emitter,
   8 - Forced breakpoint defined current distribution,
   9 - Injected electron beam in a drift tube.
   10 - not used,
   11 - single ion beam injection in a plasma,

12 - angular spread of particles in a plasma,

13 - negative or positive ion beam angular thermal spread using TNI or TPI,

14 - cosine distribution of negative particles from a sputter cathode.

15 - Maxwellian angular distribution,

16 - Space-charge limited emission,

17 - A restarted ion beam outside the plasma region,

18 - Injected ion beam in a drift tube.

The following four numbers should be set by the graphical routines.

5. **RSTRT** - The r coordinate of the start of the cathode or ion emission area, in scaled units. This is usually 0.0 for most axisymmetric cathodes.

6. **ZSTRT** - The z coordinate of the start of the cathode or ion emission area, in scaled units. For ion beams this should be as far forward as possible to minimize the size of the plasma region.

7. **REND** - The r coordinate of the end of the emission area, in scaled units.

8. **ZEND** - The z coordinate of the end of the emission area, in scaled units.

9. **SLITLN** - The length of the slit (in meters) for two dimensional problems. Default is 1.0 meters. If one uses the real length of the slit, the currents inputted, printed and\or plotted should compare quite reasonably with the real device current.

10. **ZNEP** - Plane in scaled units (must correspond to ZEP value) where it is desired to compute an x-x' plot from the r-r' emittance plot.
The following three parameters allow a second emission region along the first 'cathode' electrode (either cathode or ion injection). This allows injection of current from a secondary emission region such as the rim around a plasma injection aperture. Not generally used.

11. **NROFF** - In the case of an injected beam, the number of break points in the current distribution, up to a maximum of NROFF = 20.

12. **NZOFF** - Negative axial offset for the second emission region relative to ZLENJ (the lower axial limit of the injection region for particles, in scaled units) in units of fine grid spacing (or matrix columns).

13. **NMAX** - Maxwellian distribution:

   0 - uniform,

   1 - tapered to axis.

4.3.8   LINE 8a. FORMAT (5 F8) (FIELD EMITTER)

LINE 8a is read only for field emitters (ICT = 1).

1. **WORK** - The work function in eV for the field emitter. This value is usually between 4.0 and 5.0 eV for most metals. Default value is WORK = 4.5.

2. **GAMMA** - The field enhancement factor for field emitted currents. Seldom are real field emitters as smooth as the simulation, and this value is a multiplier to increase the field at the surface of a real world field emitter. Typical values for this parameter would be between 2.0 and 3.0. If larger values are needed one should ask if the model being simulated is good enough.

3. **ESTRT** - The electric field below which the field emission current density will be assumed 0.0. A typical value would be on the order of 10^{-7}. This is to eliminate extremely low current trajectories (nano-Amp) along the shank of a field emitter.

4. **DTGTA** - Distance to target from exit plane where the beam is being accelerated by a uniform field to some voltage VTGTA. Most useful for low current problems (micro-field emitters), where additional acceleration is being done in simple parallel configurations. The voltage at the exit plane, the target voltage (VTGTA) and this distance are used to determine the electric field.

5. **VTGTA** - Voltage on target (in Volts), DTGTA from the end plane of simulation. Both DTGTA and VTGTA must be non-zero for this calculation to be carried out.

4.3.9   LINE 8b. FORMAT (I4, 2 F8) (ELECTRON BEAM THERMAL SPREAD or BEAM SPUTTER EJECTION)

LINE 8b is read only if ICT = 5 or ISCS = 2.

   Thermal spreads become important at low (< 10 kV) voltages, and can dominate the current distribution at 1 kV. This spread should be run for one to three cycles (with BETA = 1.0) restarting from a converged (no thermal spread) run. This effect is difficult to use if no experimental data is available. The thermal energy of injection (E0) is used to inject all

the particles and the effects are a strong function of both the energy and the angular spread. A strong spike on or near the axis seems to indicate that the energy may be too high. This effect should be examined for most non-relativistic electron beams. For thermal spreads most of the beam current is in the particle spread, not in the primary beam. The angular spread in ion beams is most impressive when an x-x' plot is to be generated to compare with experimental data. Before running an angular spread (ICT = 5) it would be wise to obtain a converged solution with no angular spread. Three cycles are more than sufficient with the thermal spread. Beam sputter injection follows a cosine current distribution from the surface.

1. **ISPRD** - The number of beams, typically 3 to 10, in the angular spread to be added to the primary beam. If ISPRD = 0, only the primary beam is injected.

2. **AINC** - The angular increment between injected beams (in degrees).

3. **SKEW** - The skew energy in the nominally non-skew particles, typically 0.05 to 0.1. This is used to keep particles from crossing the axis, particularly in plasma region.

The following LINEs 9a-12 are read only if 10 < ICT < 17, for positive or negative ion beams.

4.3.10   LINE 9a. FORMAT (F8, 6 I4, 2 F8, I4, 2 F8) (ION BEAMS)

1. **PCRNT** - Plasma or sputter source current for ion beam injection. Particles striking the ion source walls will be lost, reducing the current that gets into the beam. This parameter determines the plasma density of the extracted particles. If PCRNT = 0.0, SZERO (LINE 3) will become the plasma current density for the injected particles. For slits this is the current for one meter of depth, or it is the current for a slit depth specified by SLITLN, e.g. PCRNT = 1.0, and SLITLN = 1.0 is the same as PCRNT = 0.01 and SLITLN = 0.01, for a 10 mm slit.

2. **ISPRD** - The number of beams in plasma or sputter source angular spread. Can be left zero even if other numbers defining the spread are present. If ISPRD = 0, only the primary beam is injected. The larger this number, the longer the program will take to run. Also remember only 10,000 particles can be traced. For plasma ion sources it is usually desirable to solve the problem first without the angular spread, adding the spread on a restart of the data set. For plasma-sputter sources the angular distribution MUST always be used.

3. **NBSP** - The number of beams in each angle spread. May be either 3 or 5 depending on whether or not a radial (or y) directed spread is desired with NO SKEW energy. Default is NBSP = 3. The forth and fifth beams in the spread are injected with 10 percent of the primary beam current.

4. **ISPN** - If SKEW energy is desired, ISPN = 1. ISPN = 0, will have no SKEW energy.

5. **ITBP** - The number of breakpoints in the current distribution at the injection plane (up to a maximum of ITBP = 20) (See LINEs 10, 11, and 12 below). If ITBP = 0, the plasma injection is uniform over the injection plane.

6. **IPLBL** - This (and IPLBH below) are used to prevent calculations of the boundary conditions on the fine mesh where there is no physical boundary, i.e., places where the plasma would be in the adjoining region. Ordinarily this would be the plasma injection plane and adjacent plasma regions. These are the numbers of the line segments forming such boundaries on the fine mesh. For a standard axisymmetric ion beam IPLBL = 1.

7. **IPLBH** - This is the number of the last line segment defining the plasma boundary conditions. Typically IPLBH = 2 or 3 (see IPLBL above and examples).

8. **AINC** - The angular increment for the spread in degrees. Each new particle spread will have this increment added to the preceding particle spread. The angular spread for the ejected ions in plasma sputter ion sources is smaller (2 to 5 degrees) than for other types of plasma sources.

9. **SKEW** - The percent skew energy for the nominally NON-skew particles. Typically 0.05 to 0.1. This supplies a weak force (if SKEW > 0) to keep particles from crossing the axis and causing space-charge to unrealistically build up on the axis of symmetry. This value varies with the problem and is usually started at 0.1 and varied to obtain the most realistic results.

10. **ITBPS** - Number of axial breakpoints in the background plasma density in a plasma sputter source. This has been added because an H- source at LANL has a relatively low amount of electrons injected with the ions. The suggestion is that the plasma density is much lower at the beam extraction plane than it is back at the ion source generator. This is after the relatively small channel through which the beam must pass through before extraction and/or a magnetic field across the extraction hole from the plasma. (up to a maximum of ITBPS = 10)

11. **VBIASC** - The potential that must be attained, on the axis of the beam, to suppress secondary particles in a positive ion beam. This has a default value of VBIASC = 20 eV, set only if ZITC ≠ 0.0 and VBIASC = 0.0.

12. **VBIASE** - The potential that must be attained on the axis of the beam to suppress secondary particles from the left, in a positive ion beam. This has a default value of VBIASE = 30 eV, set only if ZINE ≠ 0.0 and VBIASE = 0.0.

4.3.11   LINE 9b. FORMAT (8 F8) (ION BEAM)

1. **ZDIV** - The z location of the plane where the fine matrix ends and the regular matrix calculations start (in scaled units). ZDIV = 0.0 if no plasma region is present. Remember that the plasma region should be kept as small as possible.

2. **ZSURF** - The approximate location on the z-axis where the plasma surface is expected to form. The default value of ISURF (which is computed from ZSURF) is at 0.6*NFZ.

3. **TE** - The electron temperature for the background electrons of the source plasma. The program runs and converges rapidly when this value is 8 to 10 eV, becomes less stable, but should still converge at 5 eV. Below 5 eV the calculations tend to become less stable, but usually can be made more stable by increasing INF. At very low energies (1-2 eV) the plasma region behind the plasma surface should be minimized and an even finer matrix may be needed. At TE = 1 eV for either electron or ion energies, INF (LINE 2) may need to be increased to 8 or larger. For INF = 1 very high electron and ion energies are needed to obtain a stable result.

4. **TPI** - The positive ion temperature (in eV) in the plasma region when a negative ion beam is being extracted, or the thermal energy when a spread is added to a positive ion beam. Default value is TPI = 2.0, for a negative ion beam, and TPI = 0.0, for a positive ion beam. Low values (∼1.0 eV) may require damping of the plasma calculations with lower values of BETA, e.g., 0.5. The location of the plasma surface for a negative ion beam becomes a strong function of this parameter below 2.0 eV.

5. **PIR** - This is the ratio of positive ion space-charge density present in the plasma to the total negative space-charge density (electrons and ions) when negative ions are being extracted (INEG = 1). The more intense the plasma, the higher this number may be. Default for negative ions is PIR = 2.0. For intense plasmas this number could be 10.0 to 100.0. If a transverse magnetic field is employed in the plasma extraction region

PIR may be as small as 1.0, if ALL of the electrons are stopped back in the plasma. This number is not used for positive ion beams.

6. **TNI** - Temperature of negative ions. Used for thermal energy of a negative ion angular spread in the plasma.

7. **RHIN** - The increase in space charge density in the plasma needed to allow for ion stripping (or neutralizing) in the acceleration region. This is used primarily for negative ions and is of the order of 0.25 for negative H- beams. The stripping percentage is decreased linearly from the plasma surface to RHEND (see below). Default is RHIN = 0.0. See ISURF, above. The effect of this parameter is to increase the space-charge density in the plasma and in the acceleration region, pushing the plasma surface forward.

8. **RHEND** - The point on the z-axis, in scaled units, where the "stripping" ends.

The following three groups, LINEs 10-12, are read only for plasmas with more than one ion mass present, i.e. NION > 1, and with IRST = 0, up to a maximum of NION = 20.

4.3.12   LINE(S) 10. FORMAT (10 F8)

1. 1-10. **PP** - The relative mass divided by the charge state, for up to the first 10 ions.

2. 11-20. **PP** - The relative mass divided by the charge state, for ions 11 up to a maximum of 20 (read only if NION > 10).

4.3.13   LINE(S) 11. FORMAT (10 F8)

1. 1-10. **RCUR** - The relative current carried by ions, for up to the first 10 ions.

2. 11-20. **RCUR** - The relative current carried by ions, for ions 11 up to a maximum of 20 (read only if NION > 10).

4.3.14   LINE(S) 12. FORMAT (10 F8)

1. 1-10. **EPP** - The initial energy of ions (eV), for up to the first 10 ions.

2. 11-20. **EPP** - The initial energy of ions (eV), for ions 11 up to a maximum of 20 (read only if NION > 10).

The following three groups, LINEs 13-15, are read for ion beams and forced current electron beams only if ITBP (or NROFF) > 1, up to a maximum of ITBP (or NROFF up to 20). Cannot be used with plasma density variations along axis (see below).

Linear variations of the current density and angular variation are made between the points specified by XS. This is useful for non-uniform plasma distributions and forced current distributions from cathodes.

4.3.15   LINE 13. FORMAT (10 F8) (ION BEAM)

1. 1-10. **XS** - The radial coordinates (in scaled units) for the break points in the plasma distribution.

2. 11-20. **XS** - The radial coordinates (in sealed units) for the break points in the plasma distribution. Read only if ITBP (or NROFF) > 10.

4.3.16   LINE 14. FORMAT (10 F8)

1. 1-10. **SC** - The relative current density at each XS point along the injection surface.

2. 11-20. **SC** - The relative current density at each XS point along the injection surface. Read only if ITBP (or NROFF) > 10.

4.3.17   LINE 15. FORMAT (10 F8)

1. 1-10. **ANG** - The variation from the normal (in degrees) to the injection surface at the points specified by XS. ANG = 0.0 for a hard surface.

2. 11-20. **ANG** - The variation from the normal (in degrees) to the injection surface at the points specific by XS. ANG = 0.0 for a hard surface. Read only if ITBP (or NROFF) > 10.

The following two groups, LINEs 16 and 16a, are read for plasma source sputtered ion beams only if ITBPS > 0, up to a maximum of ITBPS = 10. This allows a variation of the plasma density in the axial direction. Cannot be used with current density variations along emitting surface.

4.3.18   LINE 16. FORMAT (10 F8) (ION BEAM)

1. 1-10. PIRZ - The axial coordinates (in scaled units) for the break points in the plasma density distribution in the plasma sputter source.

4.3.19   LINE 16a. FORMAT (10 F8)

1. 1-10. PIRP - The ratio of the positive ion density to the negative ion density at each breakpoint along the axis on the fine matrix.

The following sections for LINEs 17-21 contain the description of the electrodes. The electrode boundary segments are joined head to tail around the cathode or plasma injection electrode. All electrodes are defined in a counter clockwise direction. The electrodes must terminate at a boundary of the matrix if they begin at a boundary, and must close on themselves if they do not start on the boundary. If the electrode does not begin and end on the boundary, the first and last segments must NOT join on the fine matrix (the region near the particle emission surface(s). The total number of electrodes is defined by ICAT (LINE 1). The first electrode must have the particle emission area somewhere on its line segments. Multiple emission areas cannot be defined. For beams restarted from data saved in the plasma, the usual 'cathode' electrodes must be defined. Be sure that any electrode crossing the fine mesh is described as a cathode electrode.

Boundary planes and cylinders should NOT be defined as electrodes if they correspond exactly to the matrix boundaries. It is essential that the (non-zero) potentials be set on the boundaries if the boundary is an electrode. While the program will set most potentials on electrodes, it may not set all of them. Presetting electrodes and inter-electrode voltages will significantly speed convergence of the program. If some boundary is not set as desired, sometimes it is a small electrode at the end of the region that is not being set correctly (See small electrode in the 2.2 micro-perveance electron gun simulation of Section 6.2.1.

Small gaps between electrodes (such as the gap between a thermionic cathode and the adjacent focusing electrode) should be ignored if they are less than three (fine) matrix squares wide. Gaps three matrix squares or larger should be included (especially at the edge of the cathode). Small details (less than one regular matrix square in length) near the cathode may be skipped by the regular relaxation routines but will be taken into account on the fine matrix. Note also that if all the emission area limits are zero, a Laplace solution can be obtained. In this case EPSV might be made smaller and the number of errors must be small (or zero) at convergence.

4.3.20   LINE(S) 17. FORMAT (A3, 9 F8)

1. **SYMB** - One of six types of easily definable line segments. This must be all lower case or all capital letters and be one of the following values;

   TCN or tcn - A truncated cone (sloping line),
   PLA or pla - A plane (vertical line),
   CYL or cyl - A cylinder (horizontal - axial line),
   SPH or sph - A circle,

   $$(r - rc)^2 + (z + zc)^2 = ro^2 \tag{2}$$

   PAR or par - A horizontal parabola,

   $$(r - rc)^2 = 4ro(z - zc) \tag{3}$$

   ELL or ell - An Ellipse.

   $$\frac{(r - rc)^2}{ro^2} + \frac{(z - zc)^2}{zo^2} = 1.0 \tag{4}$$

   GEN or gen - A general quadratic function is implemented in LINE 18.

2. **ZB** - z or x coordinate of the beginning of this line segment in scaled units.

3. **RB** - r or y coordinate of the beginning of this line segment in scaled units.

4. **ZZ2** - z or x coordinate of the end of the line segment in scaled units.

5. **RR2** - r or y coordinate of the end of the line segment in scaled units.

6. **ZC** - z or x coordinate of the center of a circle or ellipse, or vertex of a parabola, in scaled units. This will be zero for a straight line.

7. **RC** - Radial or y distance to the center of a circle or ellipse, or vertex of a parabola, in scaled units. This will be zero for any straight line.

8. **RO** - Radius of the circle or the half length of r axis of an ellipse or the distance from the vertex to the focus of a parabola in scaled units. This will be zero for a straight line.

9. **ZO** - Radius of the circle or half length of z axis of an ellipse or the distance from the vertex to the focus of a parabola in scaled units. This will be zero for a straight line.

NOTE

There is redundant information above because the end of one line segment is the beginning of the next line segment. After the first line segment on each electrode it is only necessary to list the end of each succeeding line segment. The end of the line segment is put in instead of RB and ZB and the remainder of the line can be left blank if one is defining a straight line. Both ends of a line segment are necessary after a general line segment is defined (see Section 4.3.21).

For a cylinder RB must equal RR2 and for a plane ZB must equal ZZ2.

10. **CX** - The spacing between trajectories along this segment of the cathode in terms of a fraction of a matrix square. In general should have CX $\leq$ 1/INF, the fine mesh increment. The default on a cathode electrode is CX = 1/INF. The maximum value must be 1.0, with smaller values (e.g. 0.5 or 0.25 for thermionic emitters and typically 0.01 or less for field emitters) for more trajectories (2, 4, 100 per matrix square). This can be left 0.0 for non-emitting surfaces. The program can handle increases or decreases in the number of trajectories by a factor of two on a restarted run, i.e., increasing or decreasing CX by a factor of two. See also SZERO on LINE 3.

The following LINEs are used to define line segments not capable of being done with the simple types above. SYMB can probably be defined as SPH for some quadratics.

4.3.21 LINE(S) 18. FORMAT (A3, 11 F7)

1. **SYMB** - GEN or gen

2. **ZB** - The starting axial coordinate of the line segment in scaled units. ZB must correspond exactly to ZZ2 of the previous line segment on this electrode.

3. **RB** - The starting radial coordinate of the line segment in scaled units. RB must correspond exactly to RR2 of the previous line segment on this electrode.

4. **ZZ2** - The ending axial coordinate of the line segment in scaled units. ZZ2 must correspond exactly to ZB of the next line segment defined after this electrode.

5. **RR2** - The ending radial coordinate of the line segment in scaled units. RR2 must correspond exactly to RB of the next line segment defined after this electrode.

6. 6-11. **SP**(1)...**SP**(6) - A, B, C, D, E, F; the coefficients of the quadratic equation

$$Ar^2 + Bz^2 + Crz + Dr + Ez + F = 0, \qquad (5)$$

which describes the line segment or values defined for SYMB. Remember scaled units must be employed.

7. 12. **CX** - The spacing of trajectories along cathode, Must be 1.0 or less (see above).

LINE 19, followed by a combination of LINEs 20 and/or 21, are repeated for each electrode (after the first electrode, described by LINE 7 and a combination of LINEs 17 and/or 18).

4.3.22   LINE(S) 19. FORMAT (I4, F8, I4)

1. NK - The number of simple line segments defining an electrode.

2. VLT - The voltage on this electrode normalized to VSCALE.

3. NEX - 0 for electrodes that do not cross the fine matrix, 1 for those that do.

4.3.23   LINE(S) 20. FORMAT (A3, 9 F8)

1. This is identical to LINE 17.

4.3.24   LINE(S) 21. FORMAT (A3, 11 F7)

1. This is identical to LINE 18.

4.3.25   LINE 22. FORMAT (A80)

This is a comment line that will be printed out in the PBGI.LOG file and on the trajectory plot. Anything can be typed on this line.

Most input data sets will terminate at this point. Beyond this point, only special equipotentials and magnetic fields will be read.

If data is to be restored (MU = 3 or 4), it is done at this point (following the reading in of LINE 22).

4.3.26   LINES 23. FORMAT (10 F8)

If IBMAG = 1 or 4, normalized values of the magnetic fields as they vary at each point along the axis are read here. If IBMAG = 2, the normalized magnetic field matrix is read at this time from a binary file named MAGB.DAT. The normalization is important for visualization because the axis field is plotted from the normalized field and is assumed normalized to 1.0.

The following three LINEs (24a, 24b, and 24c) are read if IBMAG = 6 or 7.

4.3.27   LINE 24a. FORMAT (I4)

1. **IBB** - The number of breakpoints used to describe the magnetic field along the axis of the beam. Allowed values are $2 \leq \text{IBB} \leq 20$.

4.3.28   LINE(S) 24b. FORMAT (10 F8)

1. 1-10. **XS**(k) - The location along the z-axis of the breakpoints in the values of the magnetic fields, in scaled units.

2. 11-20. **XS**(k) - The location along the z-axis of the breakpoints in the values of the magnetic fields, in scaled units. Read only if IBB > 10.

4.3.29   LINE(S) 24c. FORMAT (10 F8)

1. 1-10. **VY**(k) - The (normalized to BMAG) values of the magnetic field at the breakpoints specified above.

2. 11-20. **VY**(k) - The (normalized to BMAG) values of the magnetic field at the breakpoints specified above. Read only if IBB > 10.

Example of uses of LINES 24a-24c, a localized solenoid (IBMAG = 6) or transverse magnet (IBMAG = 7) centered at 18.0 on a simulation 30.0 units long.

```
  6
    0.0      15.0      17.0      19.0      21.0      30.0
    0.0       0.0       1.0       1.0       0.0       0.0
```

4.3.30   LINES 25. FORMAT (10 F8)

1. If IRST $\leq$ 0 and ICT = 4 (forced cathode emission), then the cathode current densities (normalized to SZERO) are read for each trajectory point.

4.3.31   LINES 26. FORMAT (10 F8)

1. 1-40. **VCON** - The normalized values of equipotentials to be plotted. There may be up to 40 values. The values to be plotted should be in increasing order. Slightly different values are plotted for electron and ion beams. The scan of this matrix is stopped when there is a zero value. Usually there is an electrode with the normalized voltage of 1.0, this should be plotted with the value 0.9999 or 1.0001 to avoid any problem. If IEQ = 0 (LINE 2) the values are set automatically. If IEQ = 1, the increment in the acceleration region is reduced to 5 percent. If IEQ = 2, four lines of data will be read in the specified format. These are best modified after execution of the program has started.

4.3.32   LAST LINE. FORMAT (A1)

1. **X** - Must appear in the first column of the last line if the interactive capabilities are to be utilized.

5   PBGUNS Output

Output from the program comes in four forms. The most useful outputs are the graphical results presented on the interactive screen and the final plot files. Plot files of the trajectories, equipotentials, emittance and current distributions are produced. Graphical output is directed at the screen and will give a running picture of the results being obtained from the program.

More output is written to the ASCII PBGI.LOG file which can be examined after it is finished. Additional output can be added to this file by use of the parameters on the first input data line. In general the massive amounts of data available are not of great use except for those produced by IDG = 1, which prints the setup data produced by the input routines. This can be useful in debugging an input data set.

The third form of output consists of data saved for restarts. This data can be saved for restarting the same data (PBGDD.BIN) or for restarting the beam (PBBMSV.BIN) in an additional section of beam line. For restarting the same (or somewhat modified) data the voltage and space charge matrices are saved along with the beam borders and cathode current densities and a few parameters that are useful in restarting the problem. If the problem is relativistic the z-directed current distribution matrix is also saved. The program does NOT do an exact restart, as several parameters can be varied by the input data. Be aware that PBGDD.BIN may be several Mbytes long when large matrices are employed. The program will tolerate significant changes in acceleration or focusing electrodes on a restart.

It is also possible to save the space-charge density matrix (RHOSP.BDT, RHOSS.BDT) so that beam-sputter ion sources can be simulated. RHOSP.BDT contains the space charge from the primary beam and RHOSS.BDT contains the space charge for the secondary beam. The matrix of space charge may be reversed left to right and its sign reversed. The secondary ions must be of opposite sign and the configuration may or may not be reversed.

The beam data can be saved at any plane of the simulation, but it is not wise to save it too close to the end of the simulation where end approximations (the zero field assumption or a fixed potential) may effect beam parameters. Saved in PBBMSV.BIN is all the beam information needed to restart the beam in a new section of beam line. Beam data saved includes the initial conditions at the cathode including current densities, initial radius and initial magnetic field parameters. Also saved is the voltage distribution at the saved plane. On the restart the voltages are restored for the initial plane which may be on either a coarser or a finer mesh, but must be related to the original mesh by an integer number. If the beam data is saved on the fine mesh, the restart must have the same fine mesh size. Note that the real world voltage (V(I,J)*VSCALE), and not the scaled voltage (V(I,J)), must be consistent

for the two sections of beam line at the restart plane. Therefore the voltages can be re-scaled.

5.1   PBGI.LOG File

In addition to the plots, the program generates an ASCII log file summarizing the results of the run. The first thing the program prints is the values in the parameter statement defining the fixed array dimensions in the program. This will be followed immediately by error statements if any input variables require values larger than defined in the parameter statement. This can be followed by printouts of all the line segments (IDG = 1) from the input data in the format (coefficients of the quadratic equations) that the program uses. Some initial checking of this data is done as they are read in, and more checking is done after they have been read. A conditional error will ask if you want to continue if the end of a line segment does not agree with the specified endpoint. In general if the error is small, you might want to continue to see if the error is significant. A fatal error occurs if the end of one segment does not correspond to the beginning point of the next segment on the same electrode. If the input data is entered interactively this will not be allowed.

After information about each electrode is read in and printed out, a summary of the data is printed. This includes the number of simple surfaces, the number of general surfaces (usually 0) the axial coordinate where the electrode starts, the total number of line segments, the electrode number and the normalized voltage on the electrode.

The data is then scanned to determine where each axial section of the configuration begins and ends. These can be then printed as the REGION BOUNDARIES and should correspond to the end points of all the equations, and are printed in order from right to left, e.g., the first point will correspond to the right edge of the matrix (grid) and the last point (0.0) to the left edge of the matrix (grid). Each section is then scanned for the electrode surfaces present in each region and determine the logical description needed to establish if a point is inside or outside of an electrode. Many possible configurations are already built into the program (over 280). The geometry associated REGION TYPES are then printed out, if any are 0 (zero), and not associated with input data errors, it will be necessary to add a new logical description to the XLOC subroutine and a means of getting to it in the GEOM subroutine. To do this you will need to contact FAR-TECH, Inc. at support@far-tech.com for assistance.

Some of the tables used to set up the logic are the STRAIGHT LINE CONFIGURA-TION and the CIRCLE CONFIGURATION. The program can handle up to 18 straight line segments or up to 10 circles in one region. Again, be aware that not every possible combination has been incorporated in the program.

NEY and NEYF (points/electrode) are used in the shading routines to tell the program to which of the electrodes that the points in the IJCAT and IJCATF matrices correspond (matrix points along each electrode).

If IDG (I DiaGnostic) is 1 a great deal of additional information generated in the set up routines is printed. The first data is the starting points for the trajectories along the emission surface, this is useful if there is an error in the end point of the emission area. Included also are the point by point outline of the electrodes; an error in the equations not detected by the GEOM routine can cause a failure and dump of the part of the matrix which was completed, (the last point should give an idea where the problem is located). The matrices set up to do the relaxation are then printed, before being modified for the fine matrix. Once the input data is working properly, IDG should be set to 0.

The input parameters are then printed. Most (but not all) parameters initially left zero (or blank) will be assigned a default value. The integer matrices which describe most of the electrodes, and are used in the voltage matrix relaxation are then printed. Basic relaxation is done between the lower (odd numbered) and upper (even) matrices. Before the smoothing of the electrodes was added, these integer matrices defined all the relaxation regions, now they define the first matrix point on or outside the electrodes. The beam boundary matrices are printed next. This is the program's initial guess where the beam will be on an initial run, or will be the final beam border computed on a previous run if a run is being restarted (the initial beam border does not effect the results, don't worry if this is not too good).

Cycle by cycle results are then printed out as the program progresses. Printed are the number of "errors" on the voltage matrix, the currents computed, and the beam boundary (expressed in matrix squares) computed for each cycle. The integer values give discrete values that can be conveniently compared from cycle to cycle. Most of these values are self evident, but the CMAG current is the average over many cycles of the current extracted from the cathode (the sum of the target and anode current) and may be used in relativistic calculations to determine the magnetic field in the region of the cathode. One condition of convergence for electron beams is that the emitted current must be very close to CMAG.

After the last cycle, the current densities at the cathode corresponding to each trajectory are printed. If the calculation is relativistic, a radial listing of the induced magnetic field is printed (in Tesla or Gauss) at the $j = NZ/3$ column and the current densities along the beam axis are also printed.

If one has not followed the results as they come out on the screen plots, this file should be examined to see if the program is adequately converged. Early in the design process it is usually sufficient to have the current emitted and current transmitted (CMAG) within a few percent of each other, with 10 or fewer changes in the beam border. As the final results

are approached, the currents should be within a percent and the changes in the beam border should be in 0 to 3 locations. At program convergence the currents must be within 0.01 percent, there must be no changes in the beam border, and the relaxation is converging (NE near 0).

One of the last things printed out is the current density distribution at the exit plane. Here the first column is the current densities computed from the space-charge matrix. The second column is the current densities computed from the trajectories on the last cycle. The third column is the current density at an extrapolated distance (DTGT) from the exit plane, if the extrapolated distance is zero, column 3 will be zero. The final column is the integrated current distribution starting at the axis, this should be in fair to good agreement (0 to 2 percent error) with the current printed for the last cycle if the beam is reasonably parallel to the axis and/or there is no magnetic field at the exit plane.

For ion beams, a sampling of the radial current density distributions on the fine matrix at various points along the axis of the beam are printed. And finally the potentials along the axis of the beam are printed for both the fine and regular matrices.

5.2   Plots

PBGUNS produces several types of plots. The most prominent is the trajectory and/or equipotentials plot. The usual form is shown in Fig. 2 for the case of a low energy (non-relativistic) electron gun, where the combined trajectory-equipotentials plot includes full annotation, showing scale, current and voltages. For engineering purposes a full grid is supplied to facilitate measurements of the results.

While the plot on the computer screen uses black and colored lines, the plot produced on paper by the printer program reverses black and white. If a screen capture program is used the plot will be white on black and will use enormous amounts of black ink.

The complete plot can also be split into separate trajectory and equipotentials plots. These are seen in Figs. 3 and 4. These plots are made by setting IOVL = 2 (if IOVL were equal to 1 then the equipotentials plot would not have the electrodes shaded). It is also possible to produce these plots in "viewgraph" mode (IGRF = 1 or 2). As shown in Fig. 5, the grid and some of the annotation can be removed, so that a cleaner plot can be generated. IOVL is also used in viewgraph mode so that separate plots can be obtainable. Fig. 6 shows the equipotentials in viewgraph mode, here without the shaded electrodes. Shading of electrodes can be obtained with IOVL = 2. Even more annotation can be removed by setting IGRF = 2.
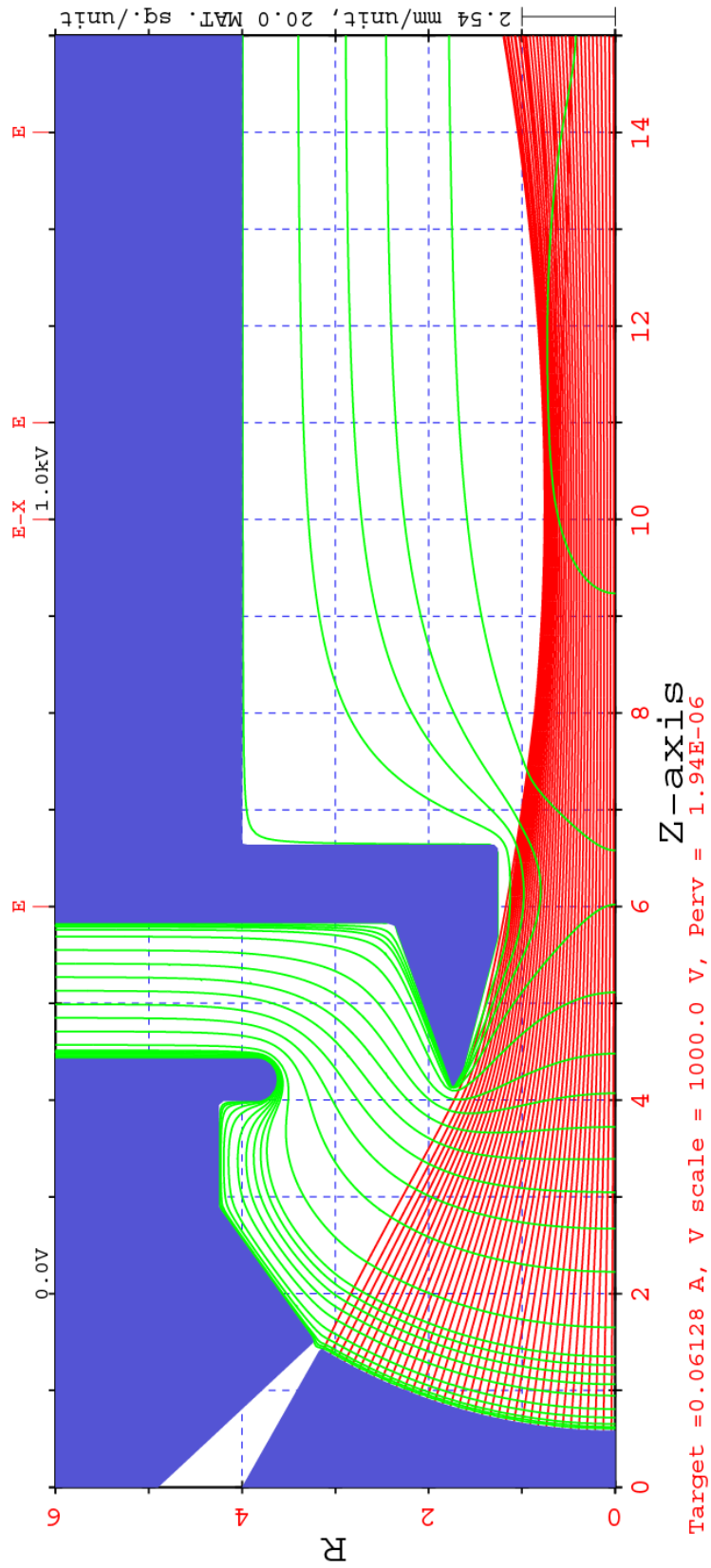
Figure 2: Basic trajectory and equipotential plot for electron beam
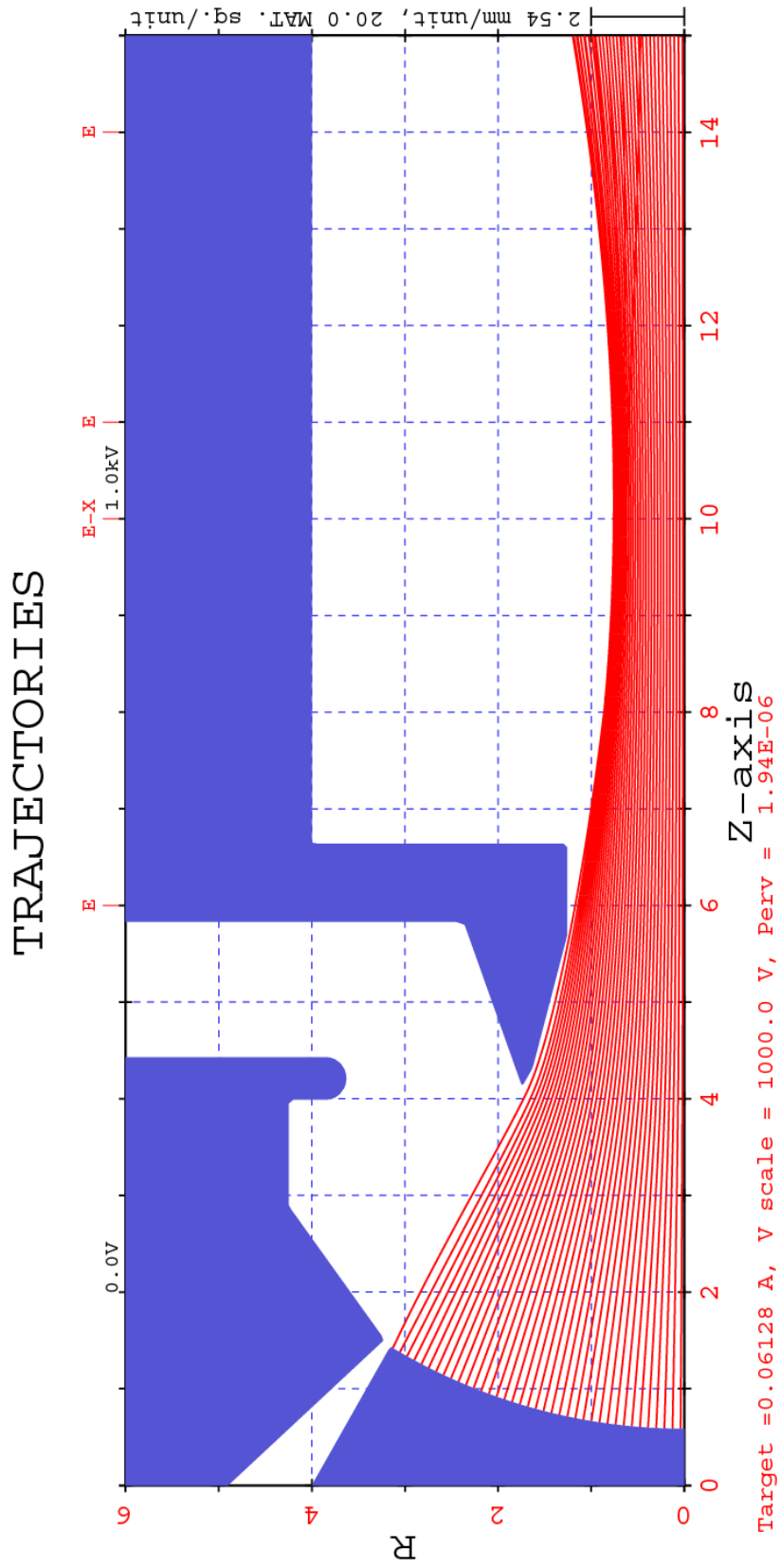
Figure 3: Trajectories without equipotentials.
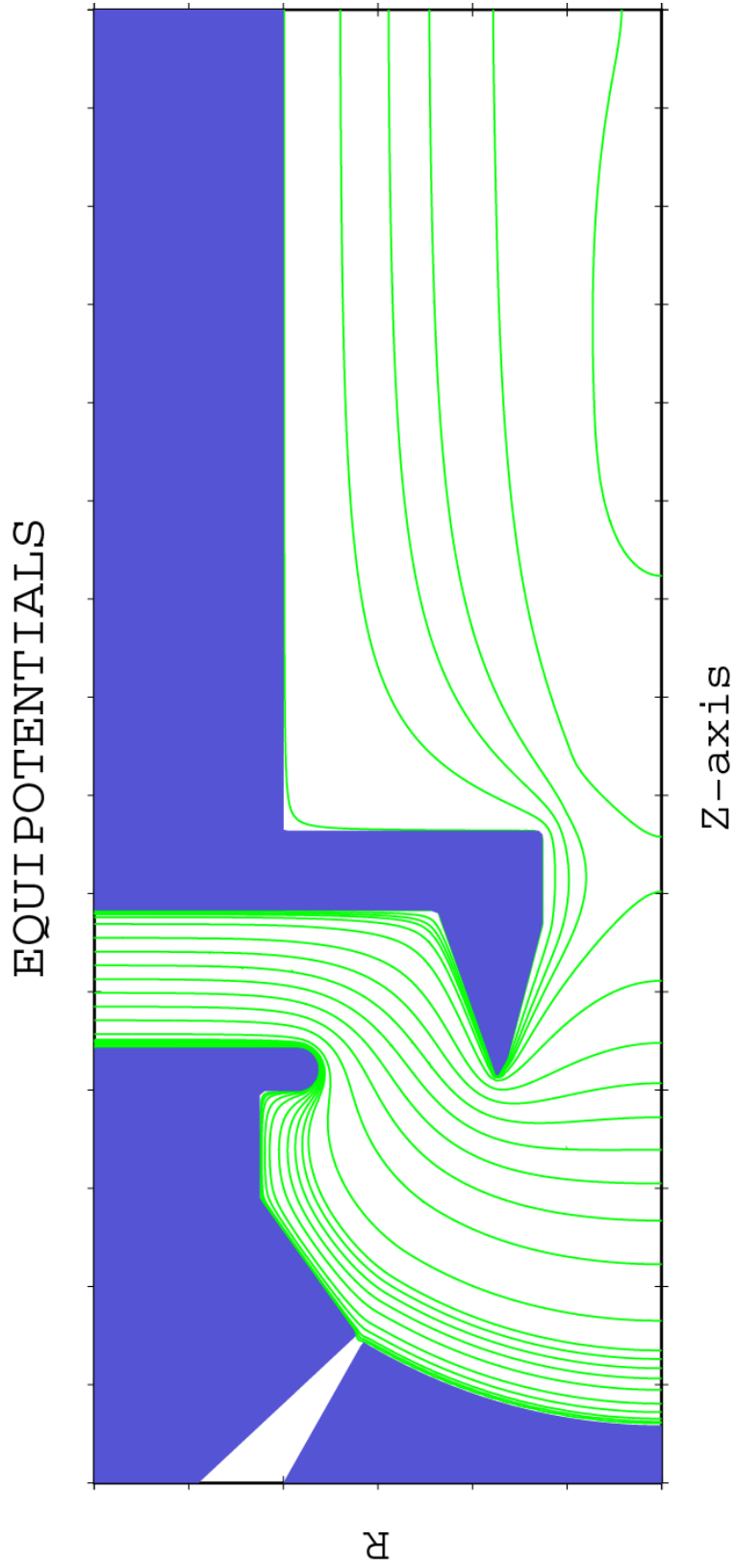
Figure 4: Equipotentials with shaded electrodes
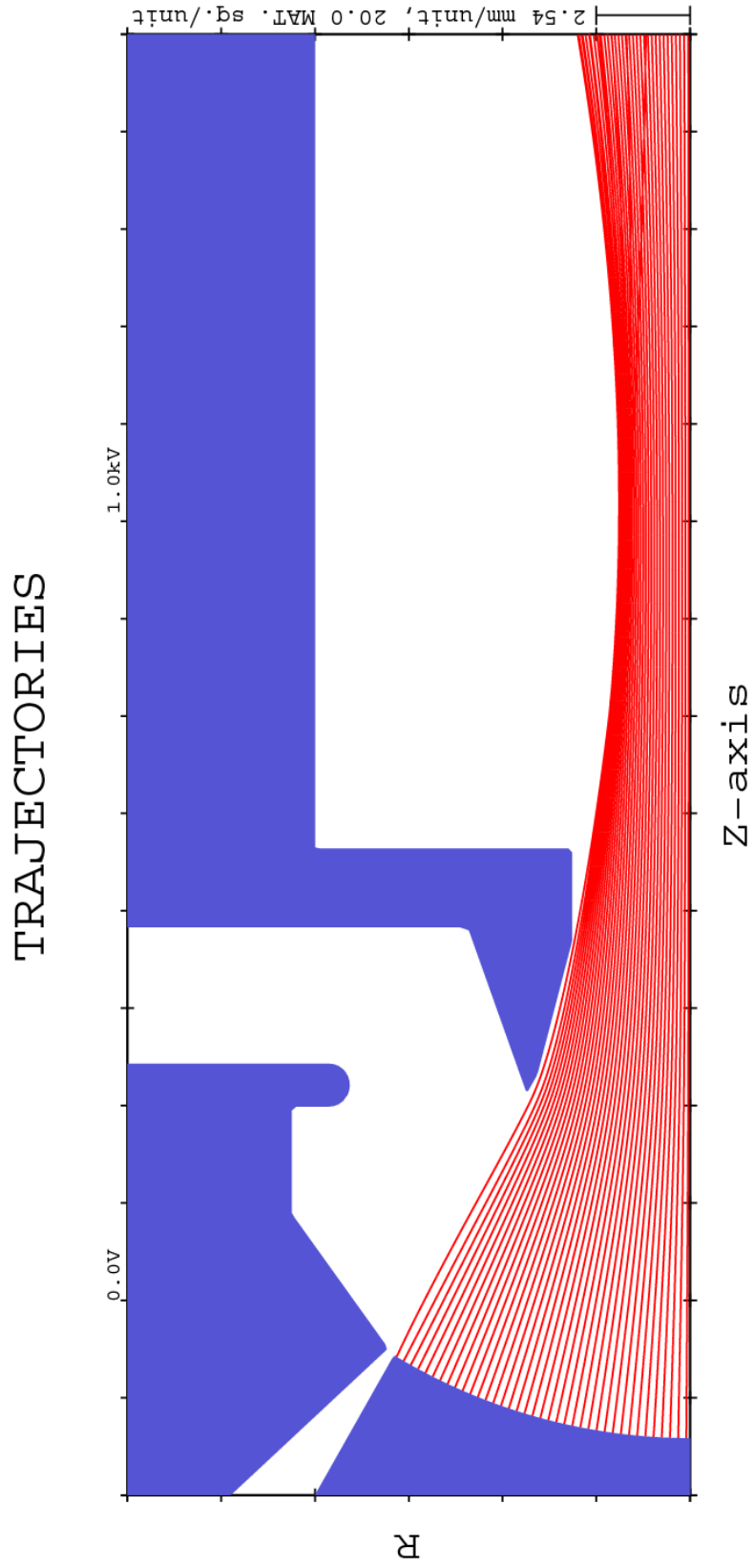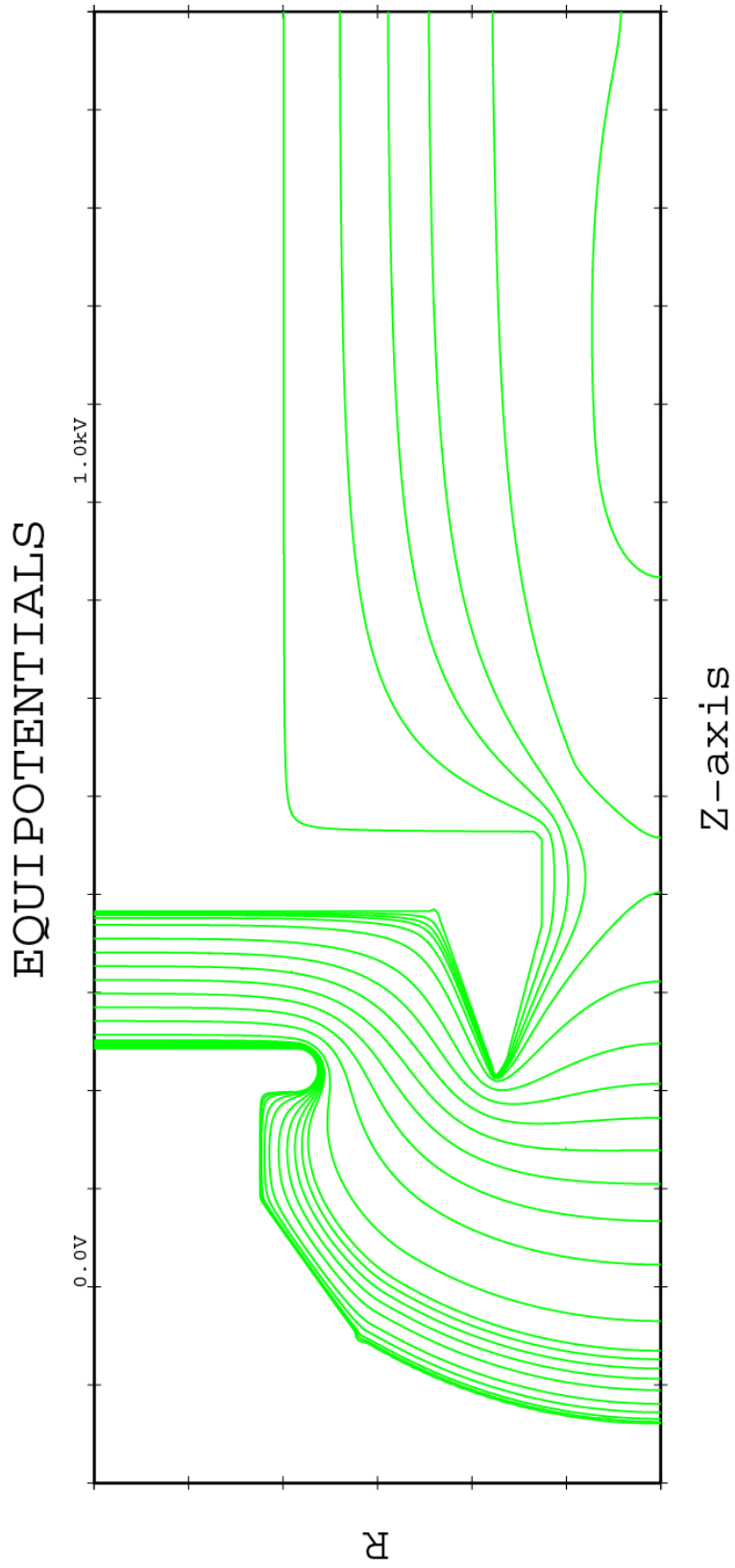
Figure 5: Trajectories in viewgraph mode

Figure 6: Equipotentials in viewgraph mode

The target current density distribution is shown in Fig. 7. This under most circumstances is simply the current density at the exit plane from the gun. Shown as the solid line is the long-term average current density obtained from the space-charge density matrix. The crosses are the current densities as computed on the last cycle. For a well converged solution the x's should fall on or very close to the line. If the target is not at NZ and/or is not flat the current density plot will follow the target shape. This can cause some distortion of the current density distribution plot as the points are not necessarily spaced the same as the radial position and the last cycle current density will only be available where trajectories reach the target plane (ITARG).

It is also possible to over plot an extrapolated current density distribution some distance downstream of the exit plane. This extrapolated distribution can be computed in one of two ways. The most straight forward calculation is the straight line extrapolation a distance DTGT (in scaled units) from the exit plane. For a beam with significant space charge effects the value of the extrapolation deteriorates rapidly with distance. This will be plotted on the same scale using triangles. An example of a target current density plot is shown in Fig. 7.

A second form of extrapolation is possible for low current beams, typically from micro-field emitters. Here it is possible to compute trajectories in the uniform field region between the field emitter and the accelerator anode, usually a fraction of a millimeter away. The program assumes a uniform field from the simulation exit plane to the anode at real voltage VDTGA a (scaled) distance DTGTA downstream. An emittance plot will be produced at the anode if four emittance plots have not already been used, as shown in Fig. 9.

One can save the beam data at any point in the configuration and then restart the beam on a second matrix. This also permits the re-scaling of the matrix (either finer or coarser mesh) on the restart. For long beam lines or long acceleration columns this can be repeated as many times as necessary.

A plot of the equipotentials on the fine mesh is also produced and allows a better resolved view of the emission area. The fine matrix is generated automatically by the program with at least the same resolution (INF = 1) of the regular voltage matrix. As the resolution increases (INF>1), the thermal isolation gap typically found at the edge of the cathode should be included in the simulation, as this will typically cause a sharp variation in current density there. The smaller the cathode area, the higher the resolution should be. A typical electron beam should use at least an 8 to 1 ratio to obtain optimum resolution of the cathode. This plot is shown in Fig. 8.
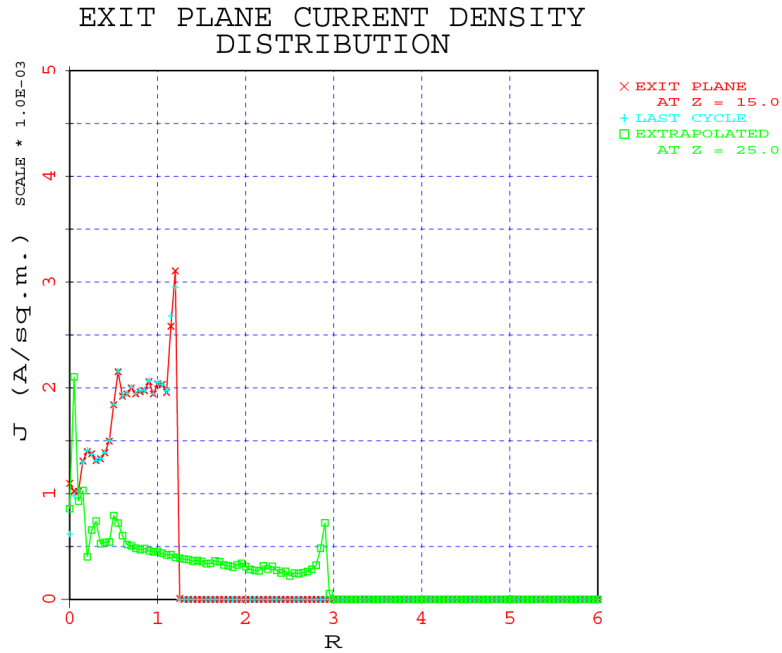
EXIT PLANE CURRENT DENSITY
DISTRIBUTION

Figure 7: Current density distribution at exit plane and 10 units downstream
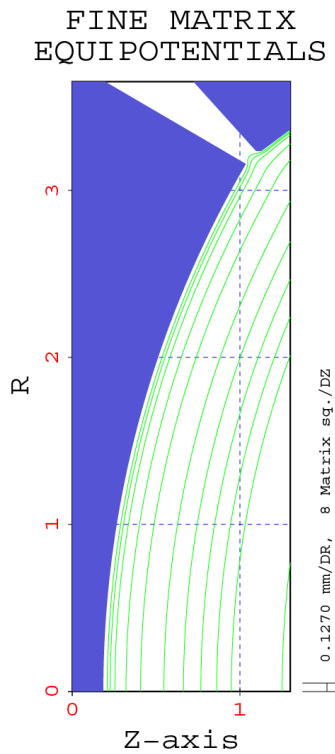
FINE MATRIX
EQUIPOTENTIALS

Figure 8: Fine matrix equipotentials

The emittance plots are the third type of plot that the program can produce. This is a plot of the slope of the trajectory (in milli-radians) vs. the relative radial position (usually

in mm, but scaled to microns or nanometers if necessary) of the particles in the beam. This computation of the emittance was originated by Joe Sherman of LANL (originally in the SNOW code). It is sometimes easier to see what is going on in the beam on the emittance plot than on the trajectory plot. An example of an emittance plot near a beam waist is seen in Fig. 9. Here the small errors in the trajectories generated at the cathode are visible.

Without the fine mesh at the cathode the fluctuations were as large as 1 mrad about the smoothed emittance line, but with the 4 to 1 fine mesh the fluctuations are seen to be the order of 0.25 mrad, a linear reduction with mesh size. These fluctuations occur as the curving cathode crosses axial matrix columns. Reducing the mesh size increases the frequency of the fluctuations but decreases their amplitude. There is some error in computing trajectories near the axis, however this is small compared to normal emittance variations.

In addition for a hollow beam (such as that from a Magnetron Injection Gun), the first emitted particle along the cathode is marked with a double size + so that one can determine whether or not the beam has crossed over or has formed a waist.

Since the cathodes can come in such diverse shapes there was a problem in generalizing the display of the current density variations along the surface. The solution was to plot normals to the cathode proportional to the current densities there. This gives a good qualitative feeling for the current density distribution, while the final, exact numerical values are available in the PBGI.LOG print file. Small fluctuations occur in the current density where the curved cathode crosses matrix columns. This is the price of computing the current densities near enough to the cathode surface to obtain an accurate distribution near the edges of the cathode. A plot of the cathode current distribution is seen in Fig. 10. When angular distributions are injected the plot becomes very complex and probably not too useful.

The current density printed on the plot is the actual current density carried by one particle and may show little relationship to the values printed in the log file when distributions are employed. Note that even when no distribution is present this current density is reduced by CS(K) the spacing specified on the line(s) that define the cathode. The initial current distributions are not plotted for ion beams injected in a plasma.

Current distributions across the beam can also be generated at planes where emittance plots are generated. These can be generated by making the Z location (ZEP(I)) negative for any emittance plot. This is useful when there is a great deal of experimental data to be compared, or when the variations themselves are of interest.
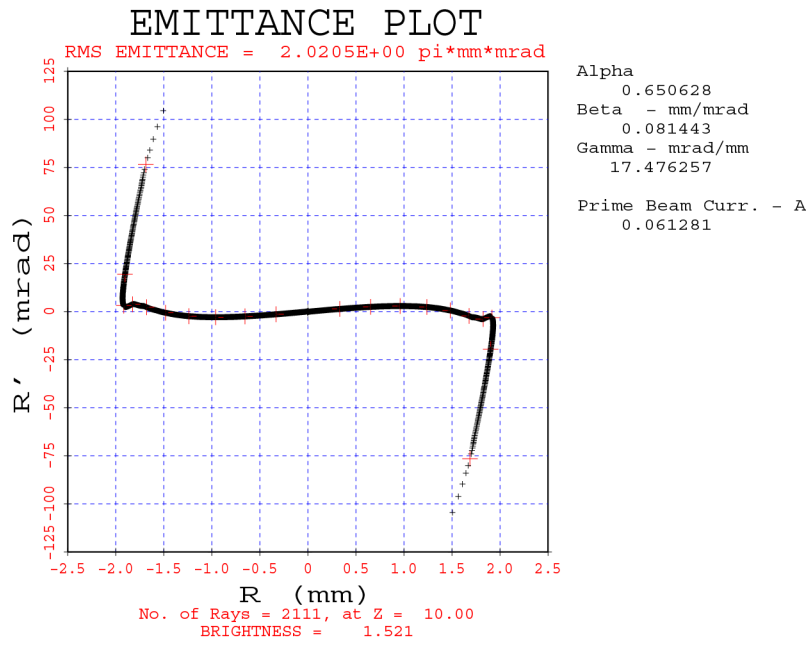
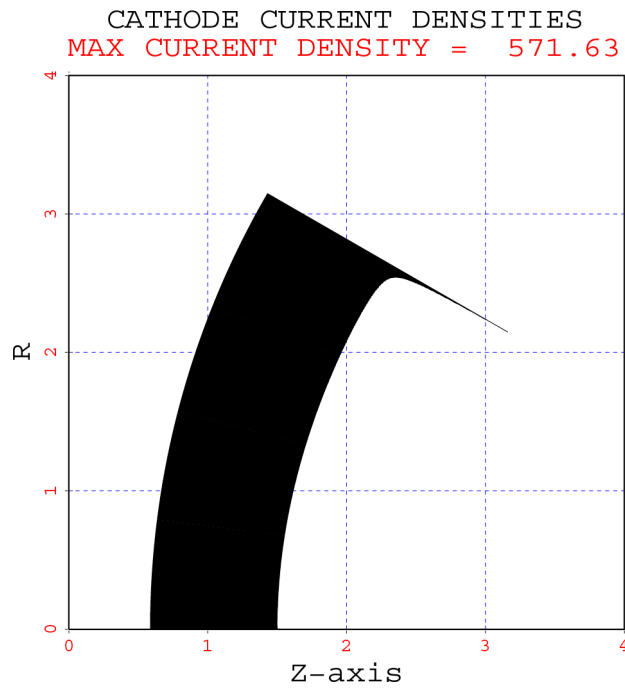Figure 9: Emittance plot at beam waist with Alpha, Beta, and Gamma and beam current totals.

Figure 10: Current density distribution along a curved thermionic cathode.

6   Simulation Examples

Example data sets and their results will be displayed and discussed in following Sections. The important features of these data sets are the ability to accurately predict the total current obtained, the cathode current density distribution, the location and size of the beam waist, the emittance of the beam and the ability to trace the particles well past the beam waist. Several examples will be presented here and compared with experimental results where possible.

Most beam designers are developing a gun for a specific purpose and with specific parameters in mind. The ability of the program to trace the beam to and past the beam waist and accurately predict the current, beam size, and emittance are essential. Sufficient memory should be available to simulate the gun on a reasonable mesh, although the use of a fine mesh has helped this issue significantly. For thermionic cathodes there should be at least twenty fine matrix points across the cathode, with many more desirable. Passable results seem to be obtainable from field emitters with tips having at least a 5 fine matrix increment radius but much more soul satisfying results are obtained with 10 to 20 matrix increment radii. At the beam waist there should be at least 3 or 4 matrix points across the beam, with 8 to 10 desirable. When a beam (with significant space-charge density) is focused within one matrix square of the axis the results beyond that point are questionable, but low current (i.e. low space-charge) beams are usually OK.

The PBGUNS example data sets presented in this manual are listed in Tables 6 - 8, organized by the problem type, typically given by the particle source type (ICT).

Section	Simulation	ICT	Filename	Configuration
6.1	Electron Field Emitters	1	mfe.dat	
6.2.1	2.2 Micro-Perveance Electron Gun	2	neg.dat	
6.2.2	1.9 Micro-Perveance, Low Energy Electron Gun	2	leeg.dat	
6.3	Relativistic Electron Gun	2	reg.dat	
6.4.1	Relativistic Slit Electron Beam Gun	2	rsb.dat	
6.4.2	Non-Relativistic Hollow Beam Electron Gun	2	hbeg.dat	
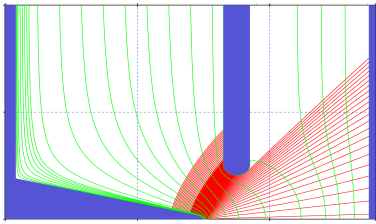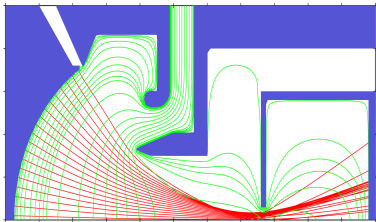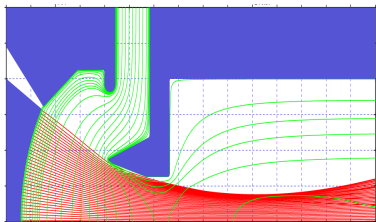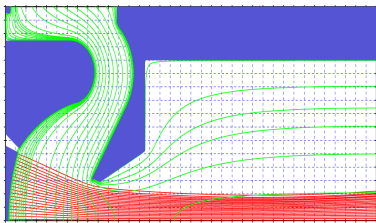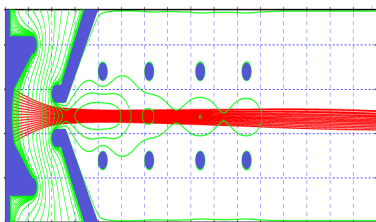
Table 6: Available Example Data Sets (Part 1 of 3)

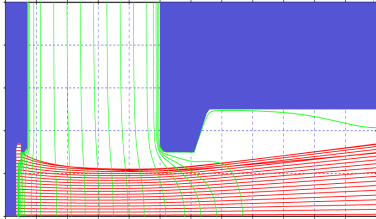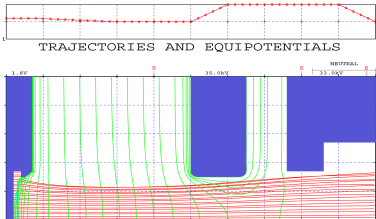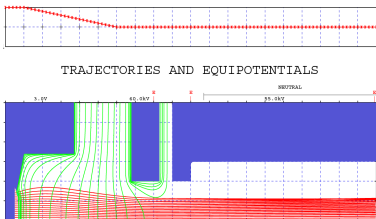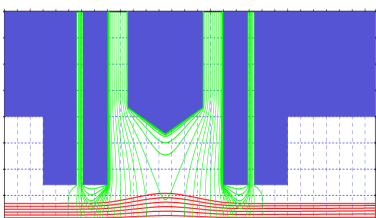| Section	Simulation	ICT	Filename	Configuration
6.5	Magnetron Injection Electron Gun	2	mig.dat	
6.6.1	Negative Ion Sputter Source	14	iss.dat	
6.6.2	Primary Beam Sputter Ion Source	5	pbbs.dat	
6.6.3	Secondary Sputtered Ion Beam from Target	5	sbt.dat	
6.7	CRT Guns	11	crt.dat	
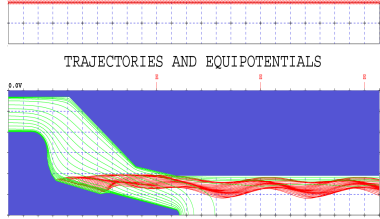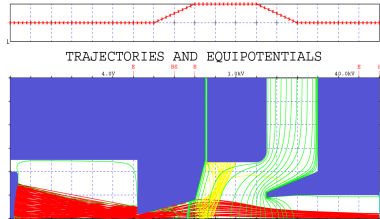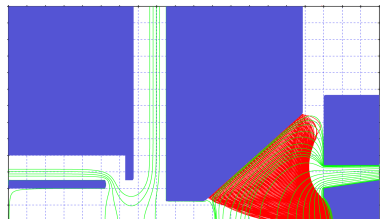
Table 7: Available Example Data Sets (Part 2 of 3)

Section	Simulation	ICT	Filename	Configuration
6.8.1	Negative Ion Beam Extraction From a Plasma	11	nib.dat	
6.8.2	Positive Ion Beam Extraction From a Plasma	12	pib.dat	
6.8.5	Emittance Plots for Multi Ion Beams	11	ecris.dat	
6.9.1	Injected Beam Through a Lens	18	lens.dat	
6.9.2	Low Energy Ion Beam Neutralization	18	leb.dat	
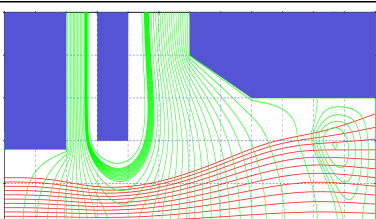
Table 8: Available Example Data Sets (Part 3 of 3)

6.1   Electron Field Emitters

Here we use a Spindt micro-cathode [8] as an example to show the simulation of field emission cathodes. These cathodes typically operate at around 100 to 200 Volts on the anode and 1 to 10 μAmps of current. The simulation here uses the Fowler-Nordheim equation to compute the current density, and requires a field enhancement factor the order of 3.2 to obtain the experimental current. Users of these emitters report "bright" spots on these cathodes, and we suspect there are some small emission area thermal effects. The experimental current vs. voltage curves agree only qualitatively with the simulation curves, if this was purely field emission, we believe the agreement would be much better. It would be interesting to compare these simulation results with measured current distributions at some distance from the cathode.

The input data set is seen in Table 9. A 5 nm tip uses 95 Volts to extract the current from the cathode. Note that the scaled length is 1 micron (10^{-6} m).

```
   111200 141 101    0    3    0   16    0    0                          0    0    0    0    0    0
      2    8    0    0   -1    1    0    0    0    0    1    0    0    0    0    0    0    0    0 0.0
   0.0000000      100.0 0.0000010   0.02000 0.0000020    0.00000     1.000     0.300
     0.8000   0.0000      0.0    0.000    0.000 0.00000   0.0000   0.0000
     1.900    0.000    0.000    0.000    0.000    0.010    0.000    0.000    0.000    2.800
        3     0.00    1    1   0.0000   1.5000   0.0875   1.2500      0.0
     4.5000   3.2000 0.1D+09   0.0000       0.0
PAR  1.5000   0.0000   1.4000   0.0500   1.5000   0.0000   0.0000  -0.0063 0.01000
TCN  0.0800   0.3800                                                  0.06250
PLA  0.0800   2.0000
     3   0.9500    0
PLA  1.6500   2.0000   1.6500   0.5100
SPH  1.8500   0.5100                      1.7500   0.5100   0.1000   0.0000
PLA  1.8500   2.0000
     1    1.00    0
PLA  2.7500   2.0000   2.7500   0.0000
   MICRO - FIELD EMITTER
X
```

Table 9: Micro field emitter with 95 volt extraction and parabolic emitter

The extraction of the beam is seen in Fig. 11. Here the extraction is obtained from the cathode by placing a voltage on the flat electrode with a round hole that the beam passes through.

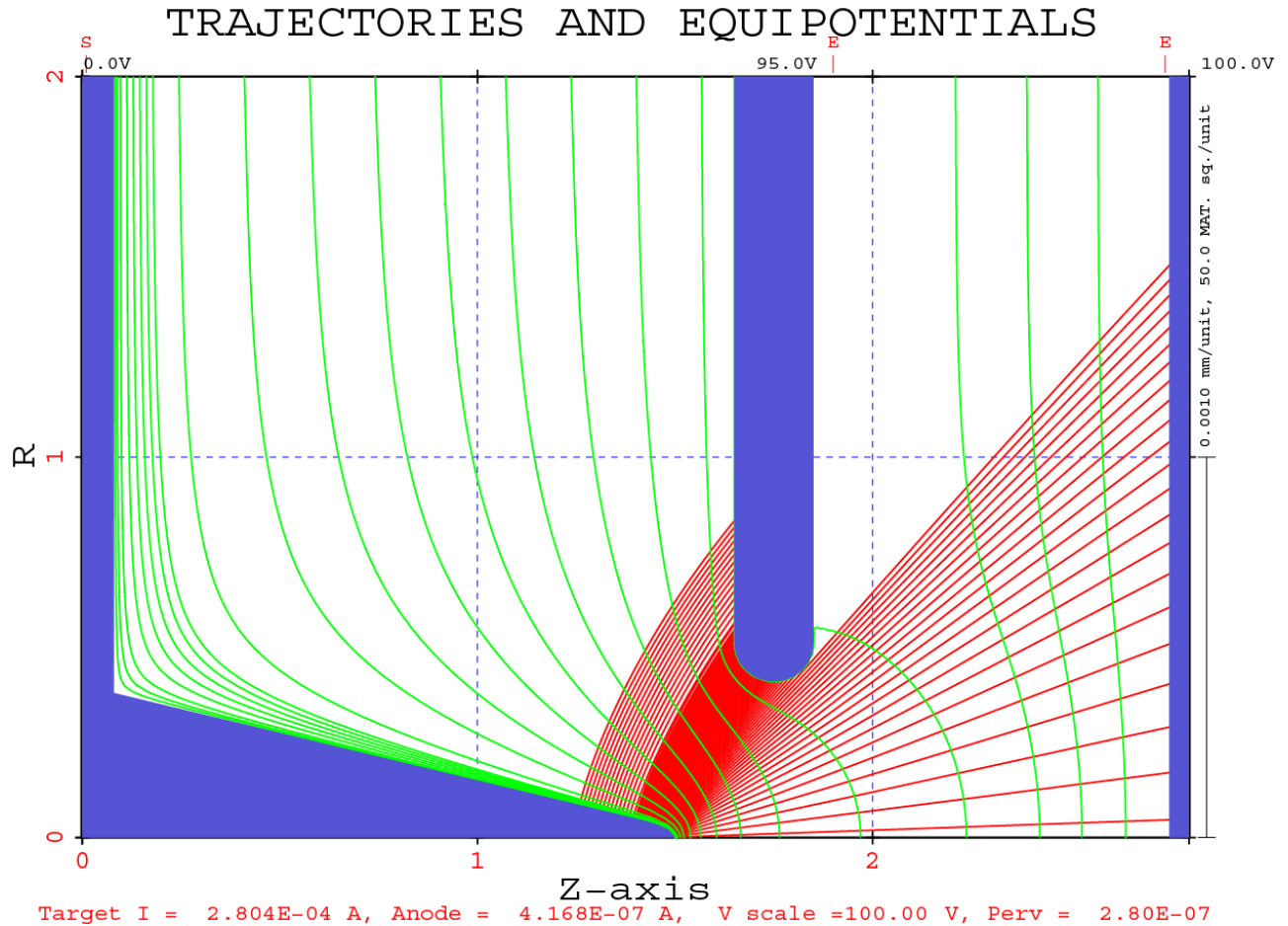The field emission current densities from the cathode are shown in Fig. 12 where the

Figure 11: Spindt type micro field emitter

finite grid effects seen in the thermionic case are still present. As the ratio of the fine matrix to the regular matrix increases, the emission will become smoother.

The current distribution at the right edge of the device is shown in Fig. 13. The current is peaked at the center and falls off rapidly away from the axis, remember this current is distributed over a 2 micron radius.

The current density distribution at the exit plane displays the same rapid fall off as the emitted current shown in Fig. 12.

Fig. 14 shows the fine matrix equipotentials around the field emission tip.

The emittance plot at the exit plane of the simulation is shown in Fig. 15. The relatively wide divergence indicated should be counter balanced by the extremely small diameter of the beam.
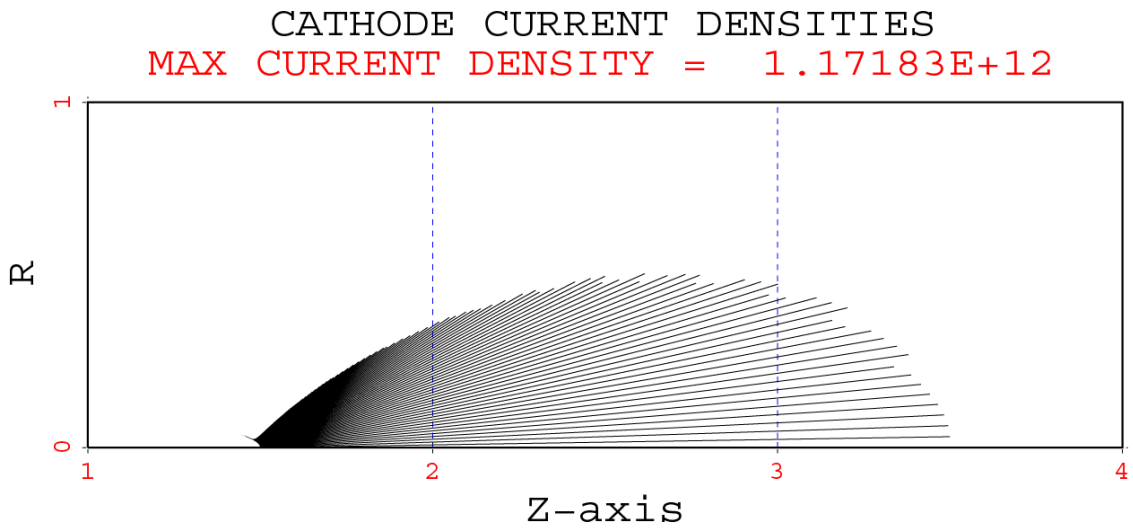
CATHODE CURRENT DENSITIES
MAX CURRENT DENSITY =   1.17183E+12

Figure 12: Current densities from field emitter cathode

TARGET CURRENT DENSITY
DISTRIBUTION
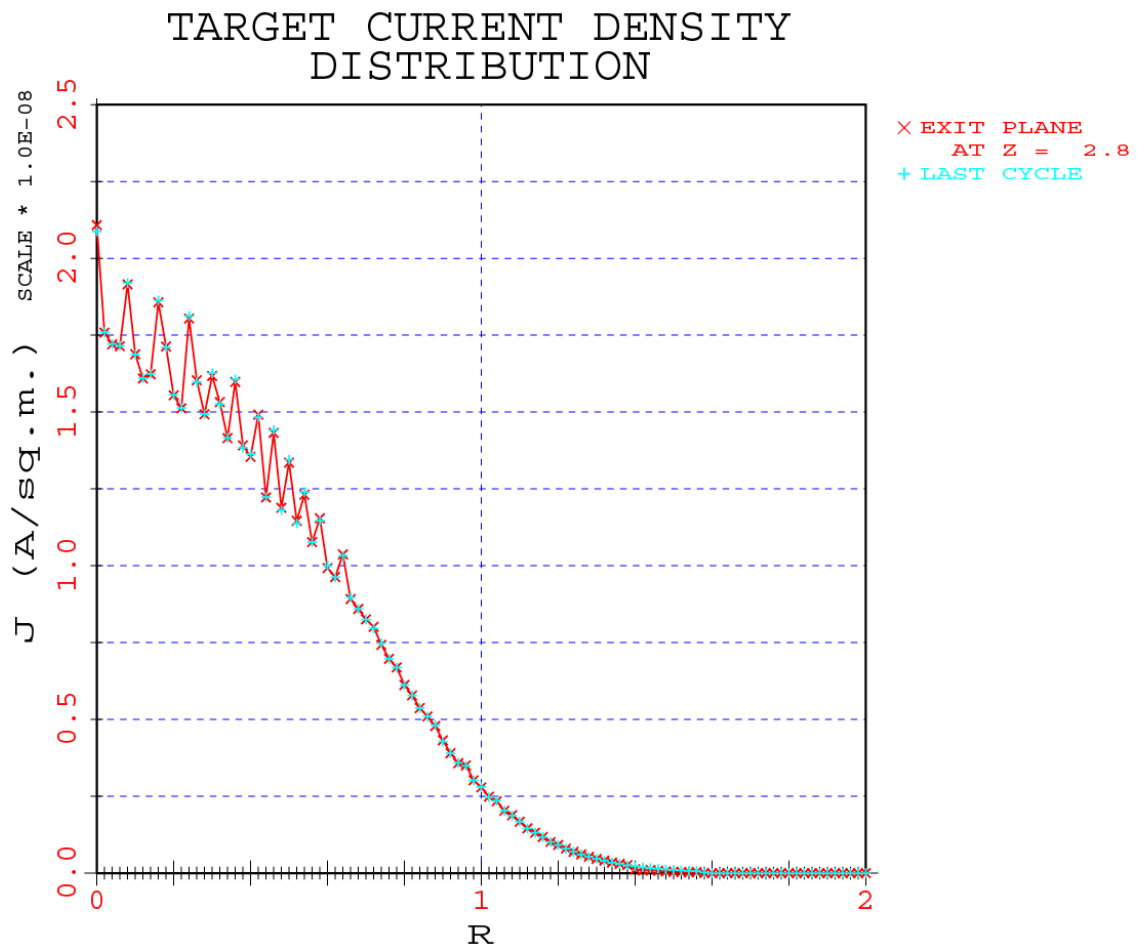
Figure 13: Current density distribution at exit plane of the field emitter

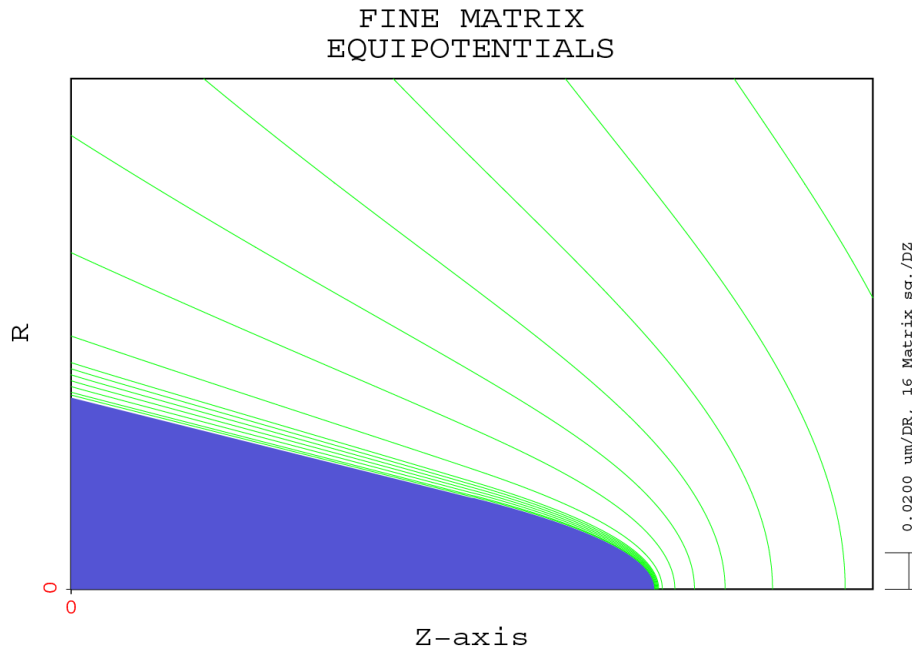FINE MATRIX
EQUIPOTENTIALS

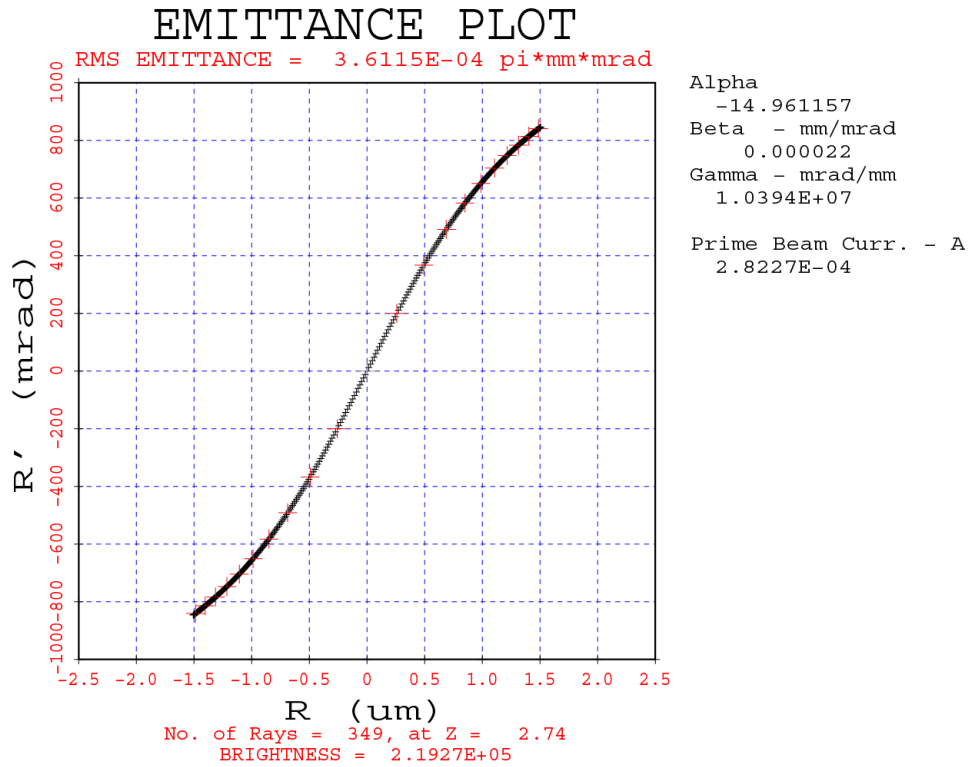Figure 14: Fine matrix equipotentials for micro field emitter.

Figure 15: Emittance plot at exit plane for micro field emitter.

6.2   Non-Relativistic Electron Guns

Non-relativistic electron beams almost always require the addition of thermal effects at the cathode as the initial energy of the electrons is significant with respect to the acceleration voltage. An example will be shown below of a gun described by Frost and Purl in 1962 in the proceedings of the IRE. They made detailed measurements on two guns, one of which had a perveance of 2.2×10^{-6} a high number for a solid, axisymmetric beam gun. The second gun had a perveance of 1.9×10^{-6} and was discussed in Chapter 5.

6.2.1   2.2 Micro-Perveance Electron Gun

The higher perveance gun (2.2×10^{-6}) has proven to be a good test for PBGUNS. The input data for this gun is seen in Table 10 below. There are some differences between their experimental results and the PBGUNS results presented here, however, they may be related with experimental measurement errors. Fig. 16 shows the rough layout of their experimental setup.

This is a very high convergence gun and the particles from the edge of the cathode cross the axis at a fairly steep angle The emittance plot seen in Fig. 17 gives a slope of about 280 mrad (about 17 degrees) for particles in the edge of the beam. It is these electrons that may not have made it into either the current distribution or angular distribution measurements. The unusual shape of the emittance plot has been consistent through 30 years of running this problem.

The most disturbing feature of this gun is seen in Fig. 18, where the current density distribution from the cathode is displayed. Here, there is a greater than 3 to 1 variation in the current density (becoming nearly 5 to 1 if the matrix is doubled again) with the peak at the outer edge of the cathode. This means that most of the current comes from the edge of the cathode where the electrons have the worst angles with the axis. It also means that if you build a higher voltage, higher current version of this gun the cathode could become temperature limited if the current density extracted is too high at the outer edge of the cathode.

While generating these plots it was observed that the beam was only 3 matrix squares wide at the target, breaking the nominal rule that the beam should be 5 to 10 matrix squares wide at the beam waist. Rerunning the problem with double the matrix size indicated that the results are reasonable. Fig. 19 shows the high resolution run (without pinhole in target). The emittance plot for the high resolution run is shown in Fig. 20.

The data was rerun with an angular spread from the cathode. The particles were injected at +/- 20 degree increments with 3 increments from the normal. The initial energy was left

at 0.4 eV. The emittance plot is shown in Fig. 21 and indicates a diameter of about 0.9 mm and a convergence ratio of 100. The thermal energy estimate may be a little high.

```
  311400 221 101    0    4    0    8    0    0    0    0    0    0    0    0    1    0    0    0
     6    9    0    1   -1    1    0    0    0    0    1    0    0    2    1   60    4   76    0  0.0
  500.0000     2000.0    0.00254   0.05000 0.0000010   0.00000       1.000       0.400
   0.8000  0.0000     0.0    0.000    0.000 0.00000  0.0000  0.0000
    6.750   7.000    7.150   0.000    0.000   0.000   0.000   0.000   0.000   7.200
     4     0.0    1    2 0.00000 0.26100 3.54353 2.25081     0.0                    1
SPH  0.2610  0.0000   2.2615  3.5500   4.411     0.0    4.15           0.12500
TCN  2.2123  3.6000
CYL  2.0000  3.6000
TCN  1.0000  5.0000
  10     0.0   1
TCN  1.5000  5.0000   2.3115  3.5500
TCN  2.7045  4.3200
CYL  4.5123  4.3200
PLA  4.5123  3.0100
CYL  4.3100  3.0100
SPH  4.1225  2.8225                      4.31   2.8225   0.1875
SPH  4.3100  2.6350                      4.31   2.8225   0.1875
CYL  4.5123  2.6350
SPH  4.8870  3.0100                    4.5123    3.01    0.375
PLA  4.8870  5.0000
   8    1.0     0
PLA  5.6100  5.0000   5.6100  2.0350
CYL  4.9900  2.0350
TCN  3.8990  1.6700
PLA  3.8990  1.6300
TCN  4.3100  1.5000
CYL  6.0100  1.5000
PLA  6.0100  4.0000
CYL 11.0000  4.0000
   3    1.0     0
CYL 11.0000  3.0000   7.3000  3.0000
TCN  7.2000  2.9000
PLA  7.2000  0.0000
  FROST 2.2 MICRO PERV
X
```

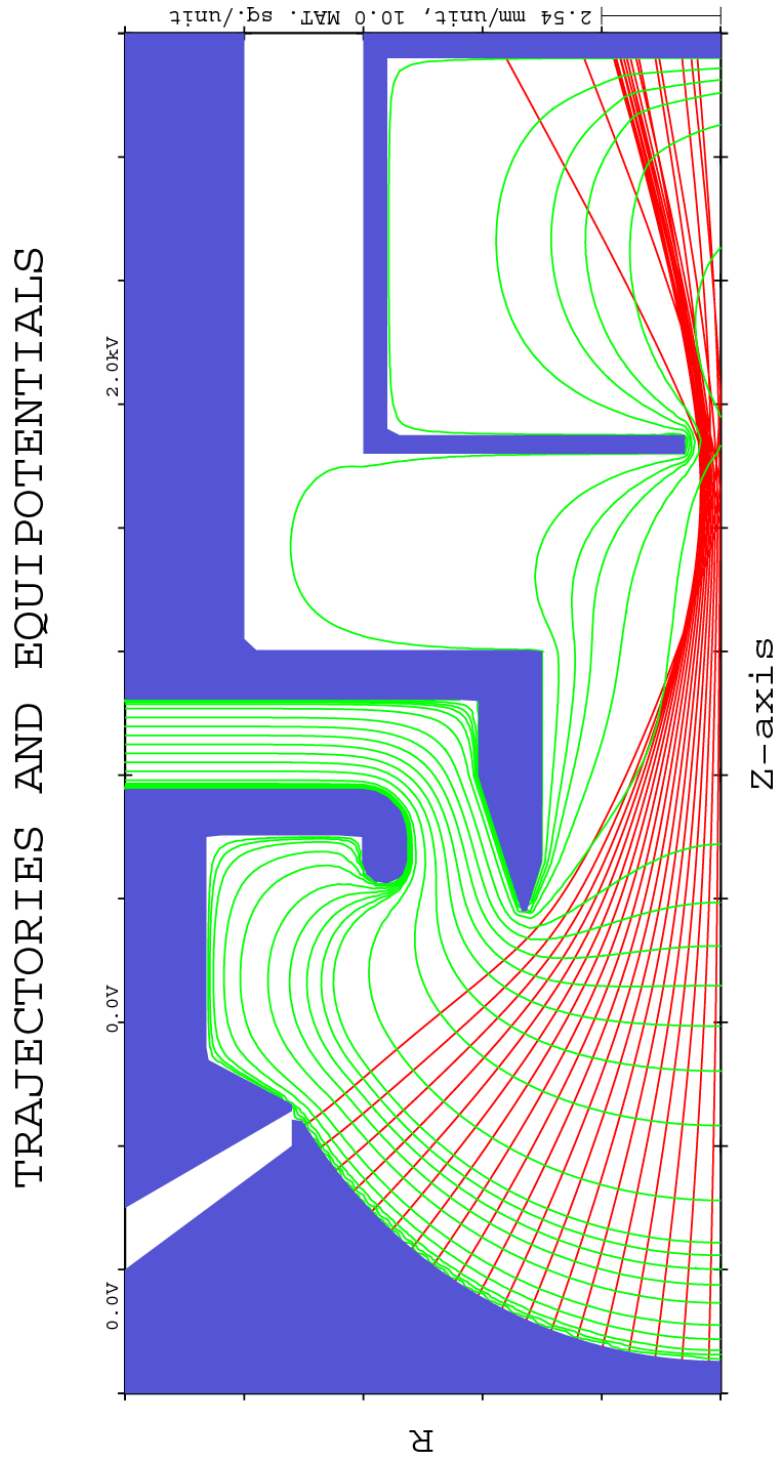Table 10: Input data for 2.2 micro-perveance electron gun

TRAJECTORIES AND EQUIPOTENTIALS

Figure 16: Frost and Purl 2.2 micro-perveance gun with oversized pinhole collector

EMITTANCE PLOT

RMS EMITTANCE = 4.2692E+00 pi*mm*mrad

Alpha
   0.136421
Beta - mm/mrad
   0.001914
Gamma - mrad/mm
 532.117004

Prime Beam Curr. - A
   0.200416

No. of Rays = 681, at Z = 7.15
BRIGHTNESS = 1.114
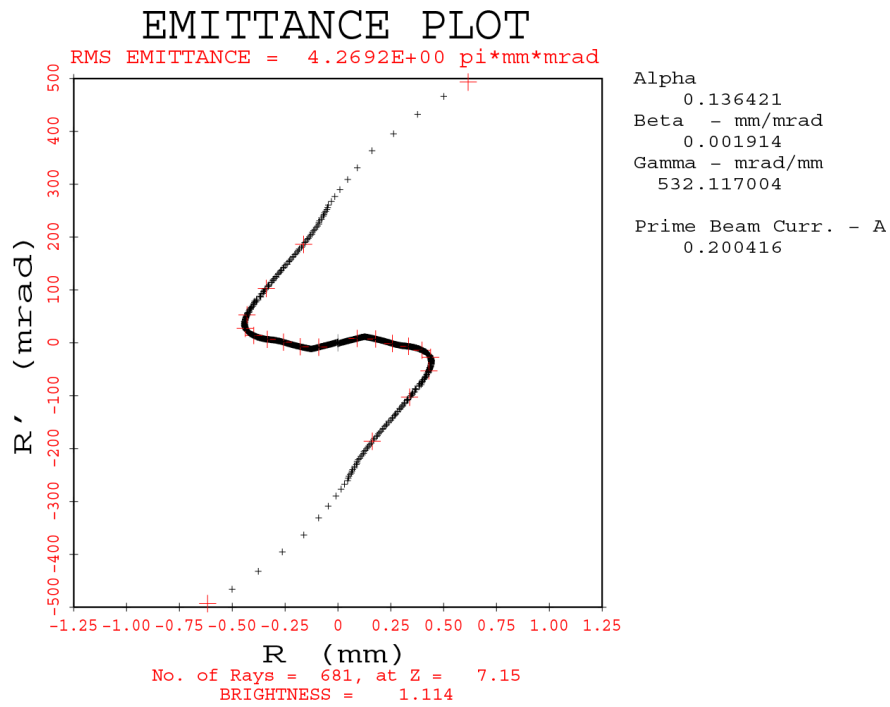
Figure 17: Emittance plot near entrance to pin hole

CATHODE CURRENT DENSITIES
MAX CURRENT DENSITY = 1283.53
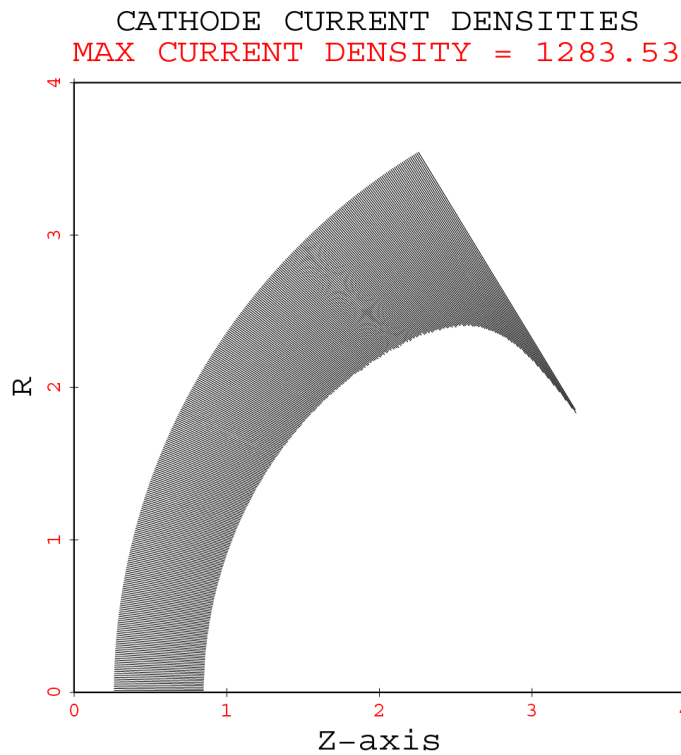
Figure 18: Current density distribution at the cathode of 2.2 micro-perveance electron gun
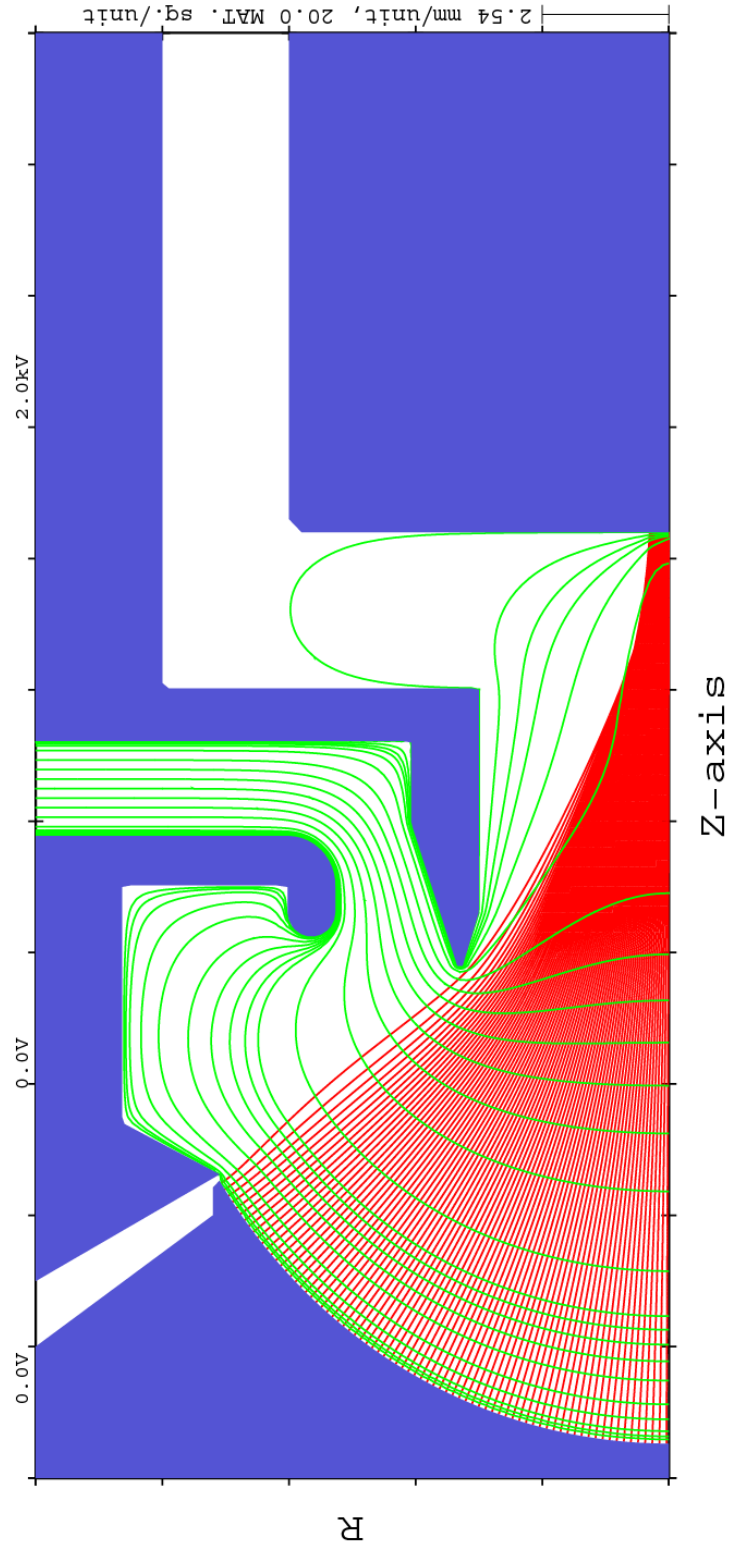
Figure 19: 2.2 micro-perveance beam at 4 times the resolution as shown in Fig. 16 (without pinhole in target).
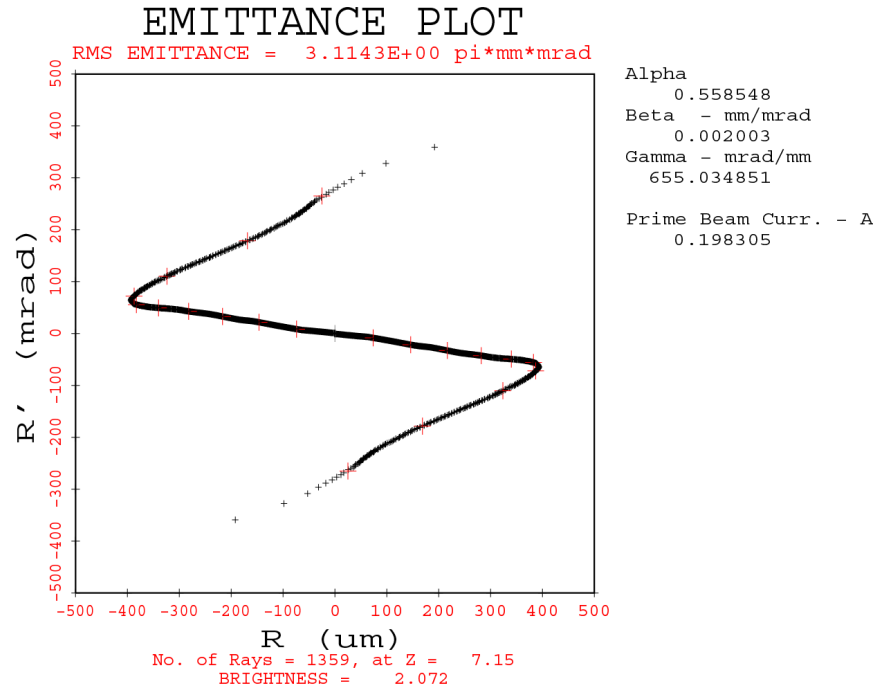
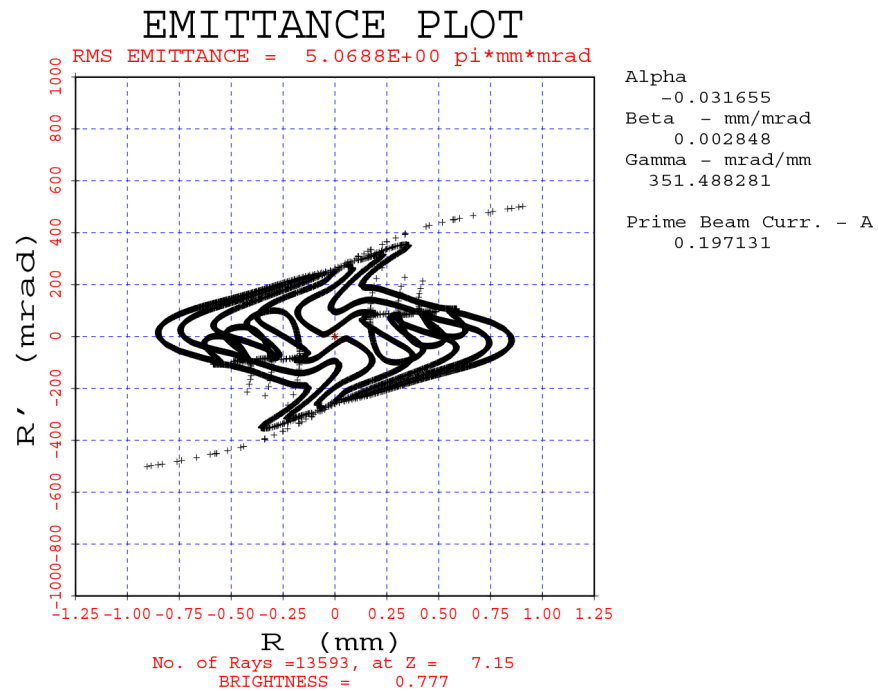Figure 20: Emittance plot at target for the high resolution run

Figure 21: Emittance plot for micro-perveance 2.2 gun with thermal spread added at the cathode

79

6.2.2   1.9 Micro-Perveance, Low Energy Electron Gun

Another example of a non-relativistic electron gun is the following low energy electron gun, the 1.9 micro-perveance case of Frost, et al. This case was highlighted in the PBGUNS Output chapter. For completeness, the input data, and the associated basic trajectory and equipotential plot is included here as Table 11.

```
 100 900 301 121    0    3    0    8    0    0    0    0    0    0    0    2    0    0    0    0
   3   28    0    1   -1    1    0    0    0    0    1    0    0    2    1   99   15 151    0 0.0
   500.0000     1000.0    0.00254    0.05000 0.0000010    0.00000         1.0        0.350
   1.0000 10.0000      0.0    0.000    0.0000.000000   0.0000   0.0000     0.00       0.0
  -6.000 -10.000 -11.000   14.000    0.000    0.000    0.000    0.000    0.000   15.000
   2 0.00000    1    2 0.00000 0.58500 3.14719 1.42873 0.00000     10.00    0    0    1
SPH   0.5850    0.0000    1.4350    3.1580    6.8764    0.0000    6.2914           0.06250
TCN   0.0000    4.0000
   7    0.000    1
TCN   0.0000    4.9000    1.4965    3.2350
CYL   1.5265    3.2350
TCN   2.8900    4.2500
CYL   3.9900    4.2500
PLA   3.9900    3.8500
SPH   4.4300    3.8500                    4.21     3.85     0.22
PLA   4.4300    6.0000
   8      1.0    0
PLA   5.8300    6.0000    5.8300    2.3700
TCN   4.1500    1.7500
PLA   4.1500    1.7300
TCN   4.3200    1.6300
TCN   5.6900    1.2600
CYL   6.6400    1.2600
PLA   6.6400    4.0000
CYL 15.0000    4.0000
    FROST ET AL "1.9"
X
```

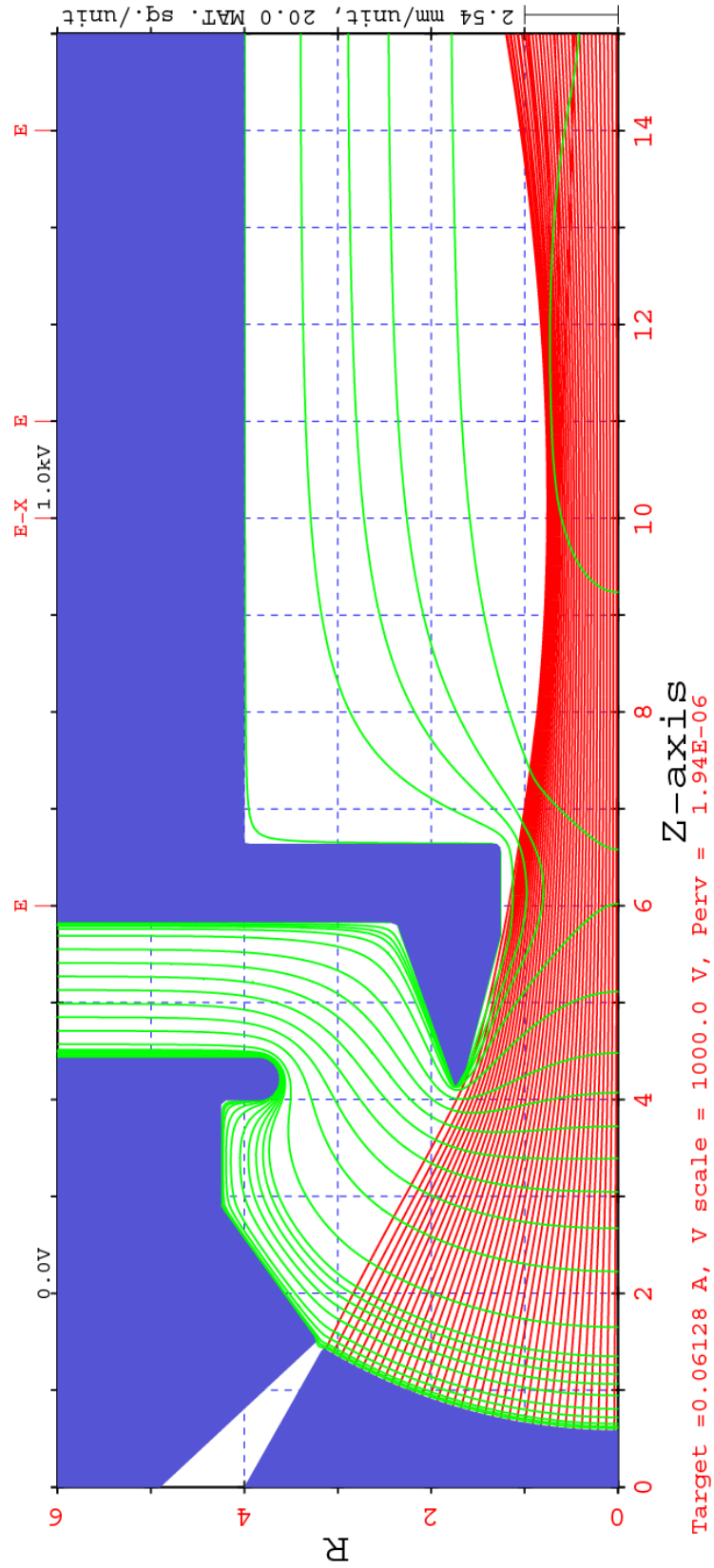Table 11: 1.9 micro-perveance low energy electron gun input data

Figure 22: Basic trajectory - equipotential plot for electron beam

6.3   Relativistic Electron Gun

This example is a relativistic, 600 kV electron gun, designed and built for the Phermex accelerator at Los Alamos National Laboratories. It has a perveance (current over the voltage to the 1.5 power) of just over 1 μPerv, a current of 500 Amps and is shown in Fig. 23. The beam forms a waist at about the 250 mm point on the z axis and the beam is calculated out to 350 mm so the end effects are remote (the long waist is aided by the self induced magnetic effects of this relativistic problem). The mesh used to simulate this device is 181 points long by 81 points wide. This yields 50 points along the cathode (for a 2 to 1 fine mesh over the cathode) and 10 across the beam at the waist, both of which are adequate. Use of a fine mesh ratio of at 8 to 1 seems to be the optimum for electron beam guns, producing the best output in the least amount of time.

The input data for this simulation is displayed in Table 12. The data consists of 28 lines with four electrodes defined using a total of 18 line segments. The cathode and adjacent focusing electrode have been defined as separate parts, as they would be experimentally to obtain thermal isolation, the gap having a significant effect on the current density at the outer edge of the cathode.

The same simulation was carried out with 2 to 1, 4 to 1, 8 to 1, and 16 to 1 fine meshes. It is very easy to change the mesh size, requiring the changing of only a few parameters (DZ, the matrix point number dependent parameters NR and NZ, and the intense relaxation region). Changing the fine mesh resolution requires changing only INF, the regular to fine mesh ratio. The advantage of the 2 to 1 fine mesh is that the program runs much faster for early design variations, while the progressively finer meshes give better resolution and accuracy. For cathodes with more curvature, larger values of INF should be used. The best results were obtained by doubling the regular mesh to 361 by 161 and using an 8 to 1 fine mesh ratio.

```
   21 900 181  81    0    4    0    8    0    0    0    0    0    0    0    2    0    0    0    0
    3  10    0    1   -1    0    0    0    0    0    0    0    0    1    1   36    4   85    0    0
   0.60E+05  600000.0    0.01000    0.20000 0.0000020    0.00000           1.0     1.0000
   0.9000 20.0000  0.0000  0.0000  0.0000 0.00000
   24.700  35.000    0.000    0.000  30.000    0.000    0.000    0.000    0.000   36.000
    2      0.0    1    2   0.0000   0.3010   5.0983   1.2097    0.0
SPH  0.3010  0.0000  1.2140  5.1100  15.155     0.0  14.854            0.12500
TCN  0.0000  5.6000
    5      0.0    1
TCN  0.0000  6.5000  1.3400  5.3800
SPH  6.8750  8.7990                         9.13    -1.0   10.07
SPH  8.6400 11.0860                         6.26  11.086    2.38
SPH  6.2600 13.4660                         6.26  11.086    2.38
CYL  0.0000 13.4660
    9      1.0    0
PLA 10.8300 16.0000 10.8300 14.6400
SPH 12.4500 11.0400                         7.65   11.04     4.8
SPH 11.8000  8.6100                         7.65   11.04     4.8
TCN  8.4260  3.1900
PLA  8.4260  3.1600
TCN  9.1740  2.8860
TCN 13.5500  5.1900
PLA 13.5500 12.0000
CYL 36.0000 12.0000
    2  0.0000    0
CYL  0.0000 15.5000  0.5000 15.5000
PLA  0.5000 16.0000
  PHERMEX INJECTOR 600KV
X
```
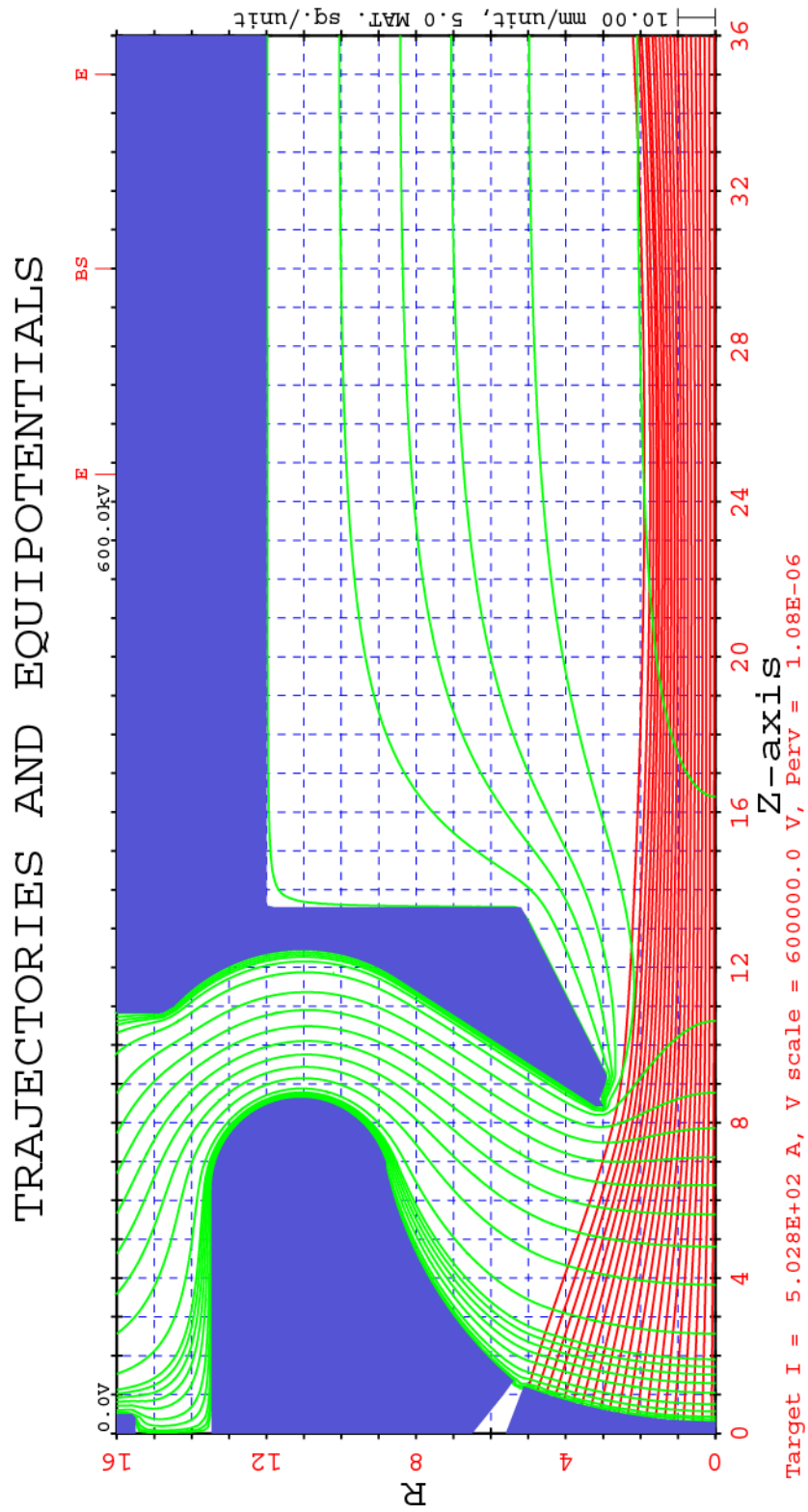
Table 12: Input data for Phermex injector simulation

Figure 23: Relativistic electron gun with micro-perveance of one, simulated on a 181 by 81 point matrix with a 4 to 1 fine mesh over the cathode.
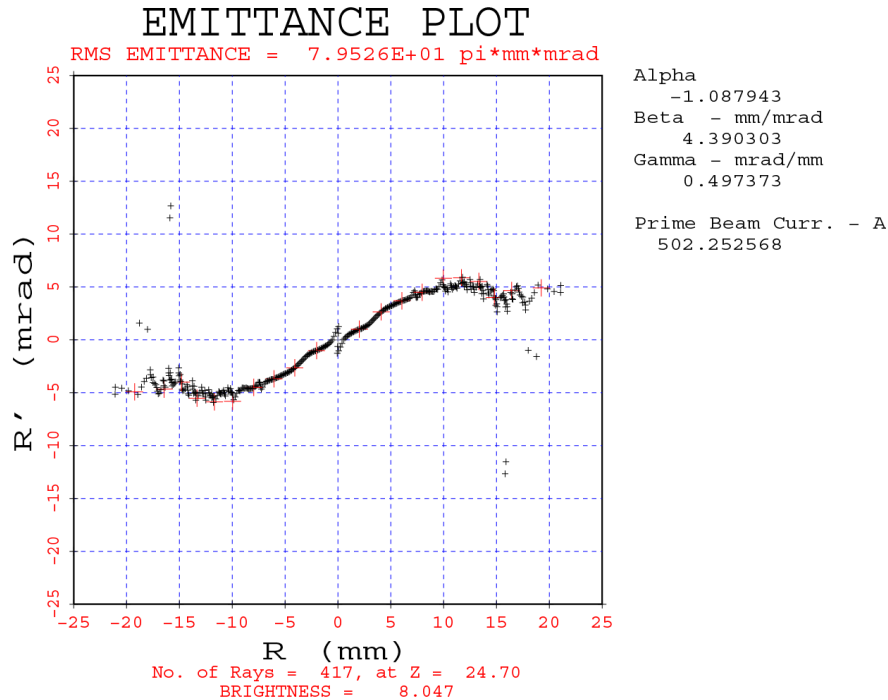
Figure 24: Emittance plot at waist for 2 to 1 fine mesh ratio

This optimization result has been seen before with other electron beam simulations and it is suggested that the fine mesh not be more 8 times finer than the regular mesh for electron beams.

The results of the errors in the potentials along the cathode are seen in the emittance plots at the beam waist shown in Figs. 24 - 28. Here the overall angular variation is within the 5 mrad scale and variations the order of 1 mrad can be seen with radial position for the 2 to 1 ratio fine mesh. The results for 4, 8 and 16 to 1 meshes show the rapid reduction in these errors as the mesh becomes finer. These smaller fluctuations in the emittance plots can be traced back largely to the cathode where the curving electrode crosses matrix columns or rows. Variations in cathode current densities also can be correlated with these points. The fluctuations can be seen to get smaller, but more frequent, as the mesh increment gets smaller. Most of these variations are no longer visible as the emittance plot scale becomes larger, i.e., usually these can only be seen in a plot at the beam waist. The application of a fine mesh over the cathode or plasma region means that the accuracy of large mesh solutions can be obtained in much shorter times. The most interesting emittance plot is seen in Fig. 28 where the regular mesh has been doubled and the fine mesh ration is 8 to 1 making the fine mesh the same as the fine mesh seen in Fig. 27. The additional smoothing is a result of the doubling regular mesh. It is recommended that the fine mesh ratio for electron guns not exceed 8 to 1. Additional resolution can be obtained by increasing the regular mesh size.
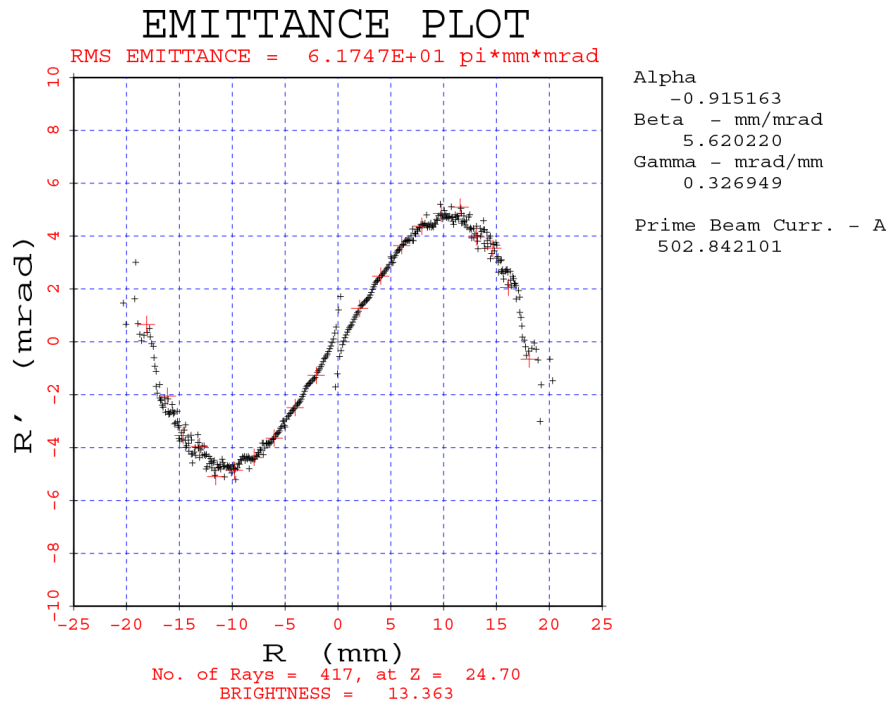
Figure 25: Emittance plot at beam waist for 4 to 1 fine mesh ratio
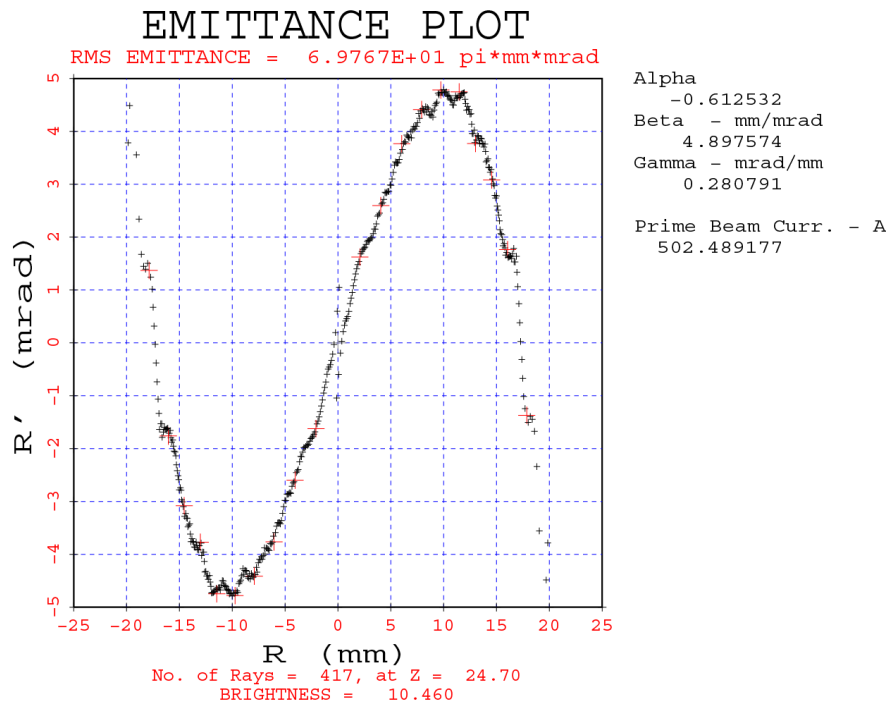

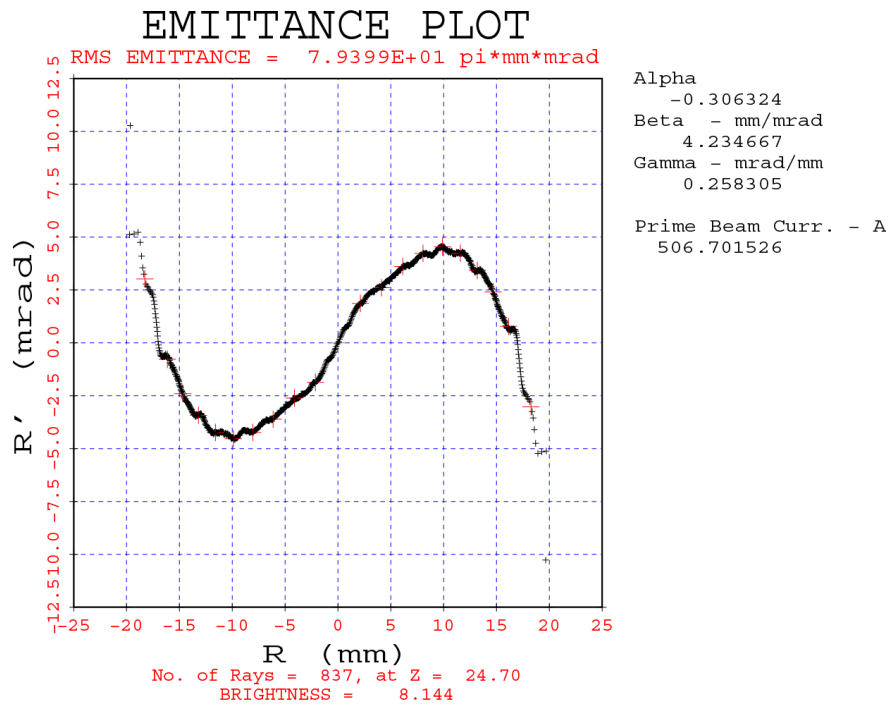Figure 26: Emittance plot at beam waist for 8 to 1 mesh ratio

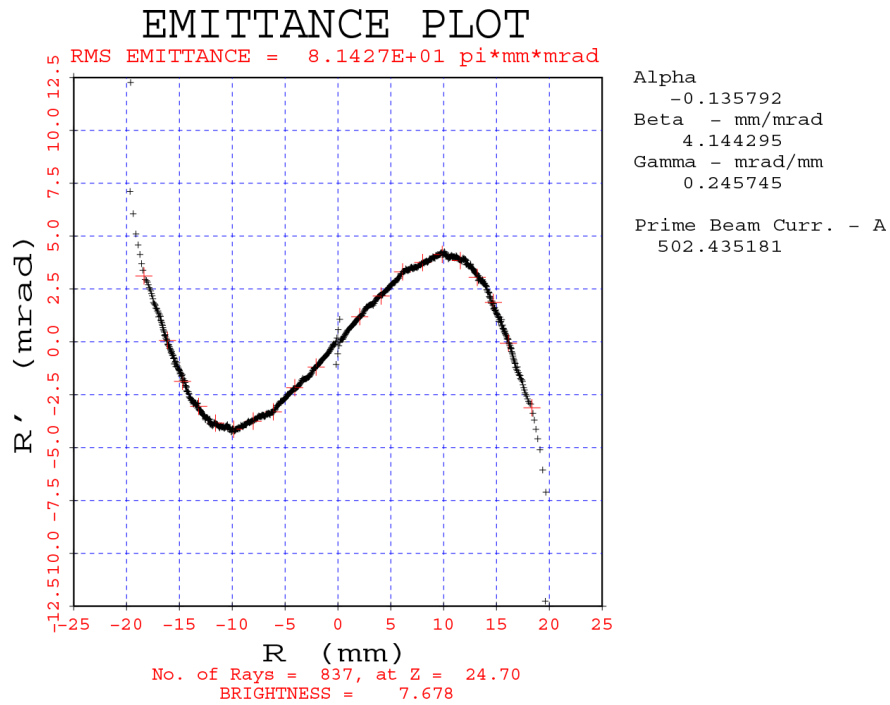Figure 27: Emittance plot at beam waist for 16 to 1 fine mesh ratio

Figure 28: Emittance plot at beam waist for 8 to 1 mesh ratio with doubled regular mesh dimensions

Initial relaxation cycles may contain some strange emittance plots for relativistic electron beams while the self-induced magnetic fields fluctuate wildly. The self-induced fields will not stabilize until the beam current stabilizes, which can take 8 to 12 relaxation cycles. Even then another 5 to 20 cycles may be needed to clean up the emittance plots.

There is also a variation in the current density distribution at the exit plane as the mesh is made progressively coarser. Fig. 29 shows the current density at the exit plane for the finest mesh. The differences between the finest mesh and an intermediate mesh (Fig. 30) are small while the coarsest mesh (Fig. 31) shows a somewhat larger beam with correspondingly lower current densities. The finest cathode mesh also produces the smoothest current density distribution.

The importance of the mesh increment is also seen in the cathode current density distributions in Fig. 32. Here the length of the lines is proportional to the current density at each point along the cathode. There is a 2 to 16 ratio in the mesh increment on the fine mesh and a corresponding decrease in the distance over which the Child's Law voltage is computed. The sharp rise on the finest mesh has been substantially masked when the current density is computed on the coarsest mesh much farther from the cathode. The 2 to 1 mesh produced a total current about one percent higher than the other meshes. The maximum current density shown in each plot is at the outer edge in all cases and rises steadily as the mesh gets finer. The plots are all scaled to the highest current density (at the outer edge of the cathode), which essentially doubles in going from the lowest to the highest fine matrix ratio.

Ultimately (in theory) the current density would become infinite as the mesh approaches zero length, experimentally the cathode would become temperature limited at some finite current density. The masking effect of the longer distances used to compute the current densities is quite evident even with the small distances employed here. Two matrix squares on the coarsest mesh represent about 2 percent of the anode-cathode gap. If one uses a distance of 20, 10 or even 5 percent of the anode cathode gap, the rise at the outer edge would not be evident.
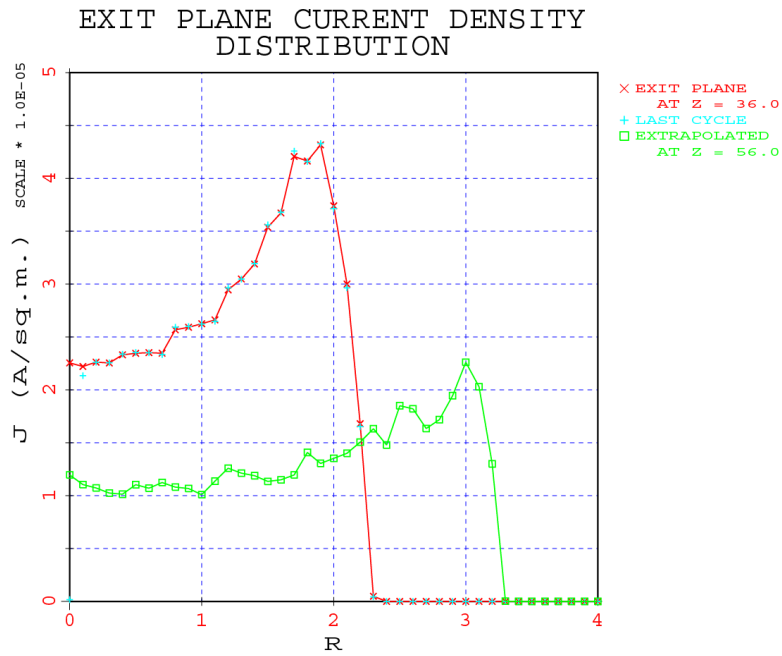
Figure 29: Current density distribution at the exit plane and extrapolated 20 units down stream for doubled regular voltage mesh and 8 to 1 fine mesh
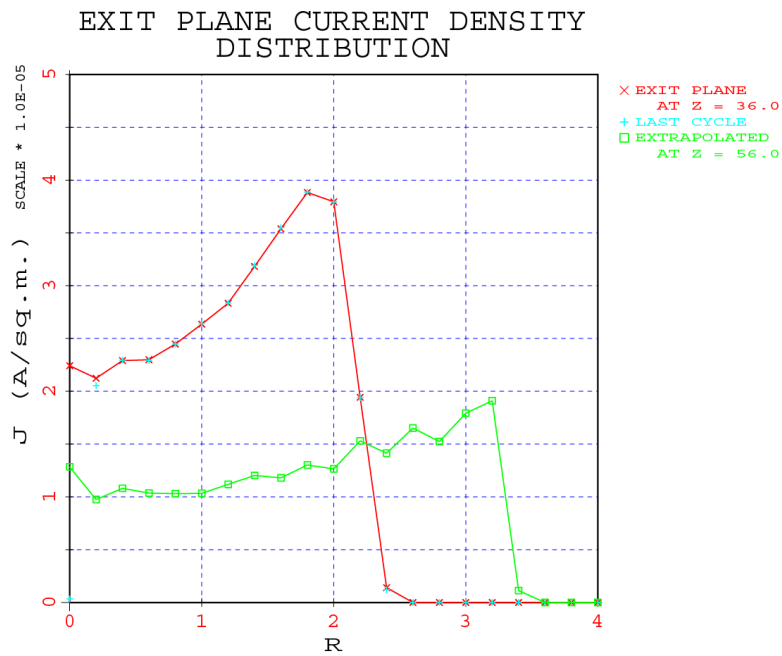

Figure 30: Current distribution at exit plane and extrapolated 20 units downstream for 8 to 1 fine mesh
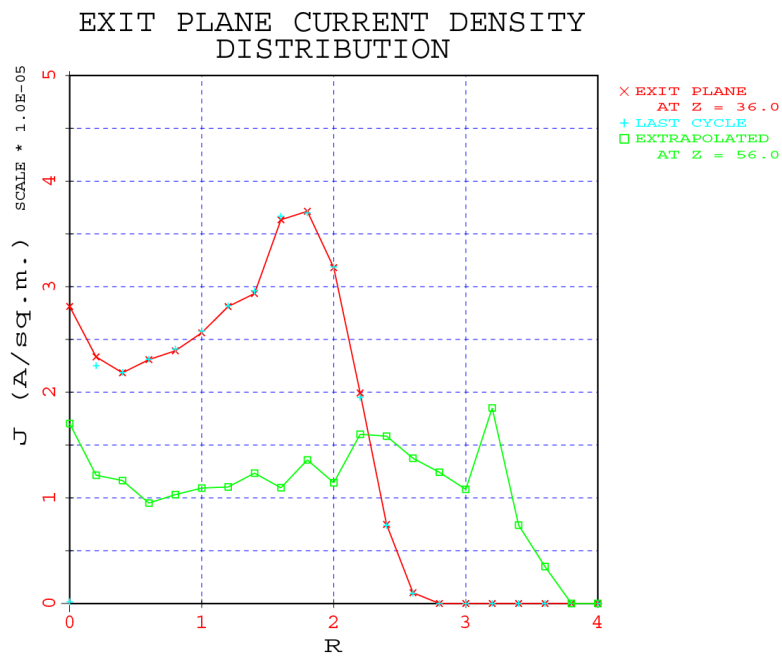
Figure 31: Current distribution at exit plane for 2 to 1 fine mesh

CATHODE CURRENT DENSITIES
MAX CURRENT DENSITY =   8.88580E+04

R

Z-axis
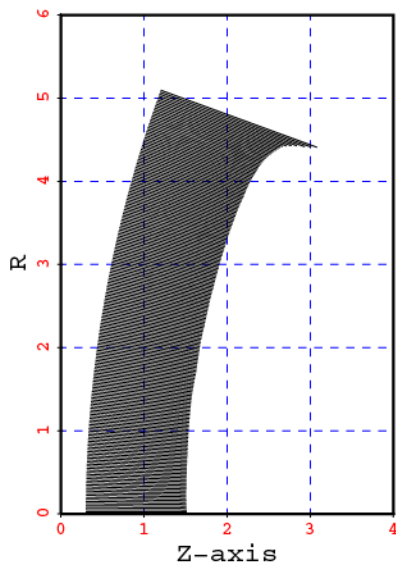
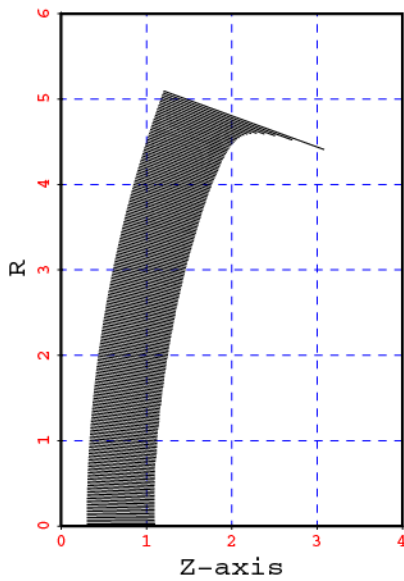2 to 1

CATHODE CURRENT DENSITIES
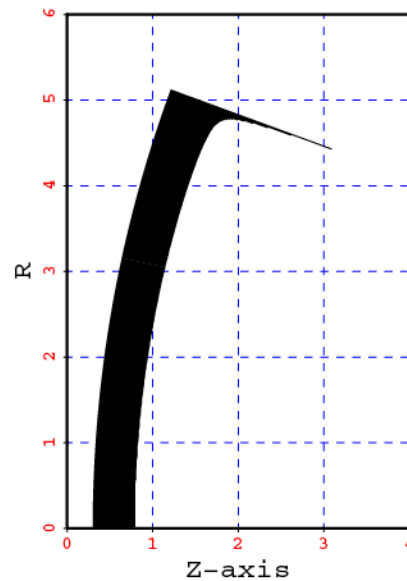MAX CURRENT DENSITY =   1.06658E+05

R

Z-axis
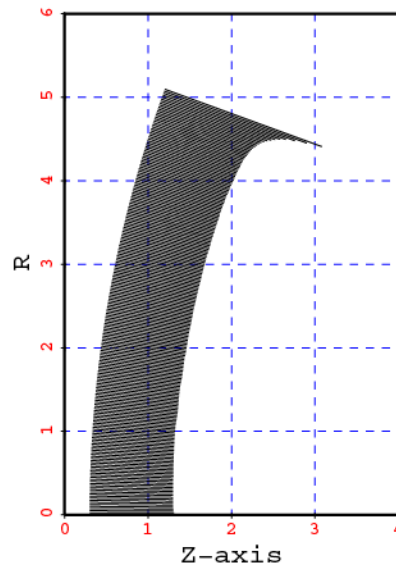
4 to 1

CATHODE CURRENT DENSITIES
MAX CURRENT DENSITY =   1.33355E+05

R

Z-axis

8 to 1

CATHODE CURRENT DENSITIES
MAX CURRENT DENSITY =   2.12656E+05

R

Z-axis

16 to 1

Figure 32: Current density distributions for 2, 4, 8 and 16 to one fine mesh ratios

6.4   Slit and Hollow Electron Beam Guns

6.4.1   Relativistic Slit Electron Beam Gun

PBGUNS can also simulate two dimensional (strip beam) electron guns, and an example is shown in Fig. 33. The program assumes an infinitely long slit but numbers printed out will be for 1.0 meter or the slit length specified in the input data. Here a relativistic 75 kV, 41.7 Amp electron beam, 0.1 meter in depth, is shown. This design was developed to test the program and its ability to handle complex configurations and has not been experimentally built. The input data file is shown in Table 1 below. A 401 by 121 matrix is employed with a 8 to 1 fine matrix over the cathode.

The cathode current density distribution is shown in Fig. 34 along with the distribution obtained with a mesh of 801 by 241 and an 8 to 1 fine mesh ratio in Fig. 35. Small fluctuations in the current density caused by errors in the potentials near the cathode are visible and are more noticeable on the coarser mesh especially at the edges of the cathode. The effect can be reduced to almost any arbitrary level by making the cathode mesh fine enough.

The fluctuations are caused by the extremely high space charge densities close to the cathode as well as errors in the calculations near the cathode. Errors in the potential relaxation are typically proportional to the mesh length.

The equipotentials for the fine mesh are shown in Fig. 36. These are the potentials used to compute all parameters near the cathode.

Some of the magnetic capabilities of the program are seen in Fig. 37. Here a rather idealized wiggler magnetic field, with a peak value of 0.02 Tesla (200 Gauss for non SI people), is applied to the slit beam. The program is still fully relativistic and includes the self induced magnetic field. The x-varying, z-directed magnetic field distribution is seen at the top of the plot, again this was created to test the program and is not experimental data.

The effects the errors near the cathode are seen in the emittance plot, Fig. 38, near the end of the beam in Fig. 33. The small fluctuations in the center part of the plot are caused primarily by the fluctuations near the cathode, but can also result from errors on the regular mesh. If you are counting on the accuracy of the results it would always be wise to increase the regular mesh resolution and repeat the problem.

The emittance plot for the 801 by 241 resolution plot are displayed in Fig. 39, and are somewhat smoother than shown in Fig. 38. The emittance plot at the end of the beam with the magnetic field as shown in 33, is seen in Fig. 40.

The Exit plane current density distribution is displayed in Figs. 41 and 42. The distribution is seen to be somewhat smoother and more symmetric for the finer mesh.
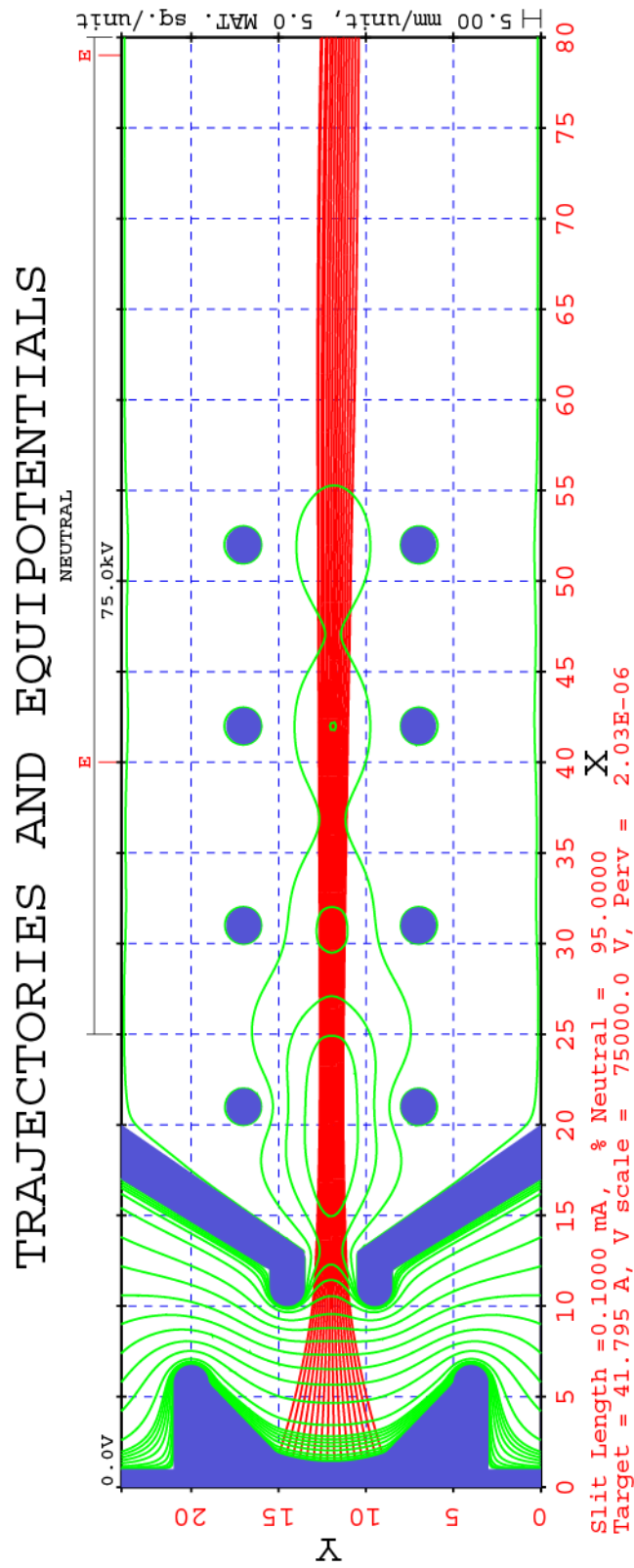
Figure 33: Relativistic slit beam
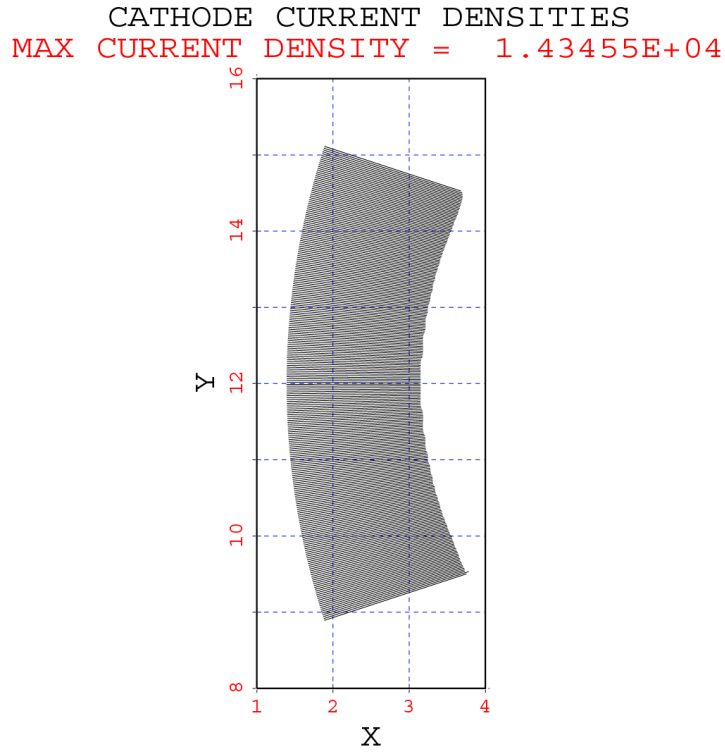
Figure 34: Cathode current densities for 402 by 121 mesh

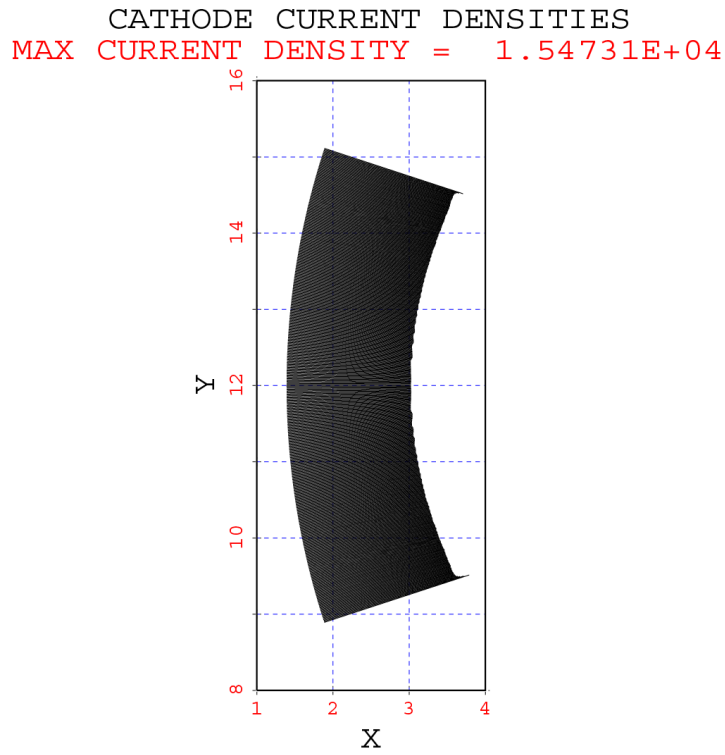Figure 35: Cathode current densities for 801 by 241 mesh

```
  311000 401 1219999  11    0    8    0    0    0    0    0    0    0    0    0    0    0    0
     6  16    0    1   -1    0    0    0    0    0                    2   41  281   21  141    0
   0.70E+05   75000.0    0.00500   0.20000 0.0000100      0.02000      1.000      1.000
   0.8000  0.0000      0.0   0.000   25.000 0.05000   0.0000   0.0000     0.00
   40.000  79.000    0.000   0.000    0.000   0.000    0.000    0.000    0.000  80.000
      9     0.0    1    2 8.89288 1.8761015.10712 1.87610     0.1
PLA   1.0000  0.0000   1.0000   3.0000
CYL   5.7500  3.0000
SPH   5.7500  5.0000                         5.7500   4.0000      1.0
TCN   1.8800  8.8810
SPH   1.8800 15.1190                        11.3910 12.0000     10.0          0.12500
TCN   5.7500 19.0000
SPH   5.7500 21.0000                         5.7500 20.0000      1.0
CYL   1.0000 21.0000
PLA   1.0000 24.0000
      5     1.0
TCN 20.0000   0.0000 13.0000 10.5000
CYL 11.0000 10.5000
SPH 11.0000   8.5000                        11.0000   9.5000      1.0
CYL 12.0000   8.5000
TCN 17.0000   0.0000
      5     1.0
TCN 17.0000 24.0000 12.0000 15.5000
CYL 11.0000 15.5000
SPH 11.0000 13.5000                        11.0000 14.5000      1.0
CYL 13.0000 13.5000
TCN 20.0000 24.0000
      3     1.0
SPH 43.0000   7.0000 42.0000   8.0000 42.0000   7.0000   1.0000
SPH 41.0000   7.0000                        42.0000   7.0000   1.0000
SPH 43.0000   7.0000                        42.0000   7.0000   1.0000
      3     1.0
SPH 43.0000 17.0000 42.0000 18.0000 42.0000 17.0000   1.0000
SPH 41.0000 17.0000                        42.0000 17.0000   1.0000
SPH 43.0000 17.0000                        42.0000 17.0000   1.0000
      3     1.0000
SPH 22.0000 17.0000 21.0000 18.0000 21.0000 17.0000   1.0000
SPH 20.0000 17.0000                        21.0000 17.0000   1.0000
SPH 22.0000 17.0000                        21.0000 17.0000   1.0000
      3     1.0000
SPH 22.0000   7.0000 21.0000   8.0000 21.0000   7.0000   1.0000
SPH 20.0000   7.0000                        21.0000   7.0000   1.0000
SPH 22.0000   7.0000                        21.0000   7.0000   1.0000
      3     1.0000
SPH 53.0000 17.0000 52.0000 18.0000 52.0000 17.0000   1.0000
SPH 51.0000 17.0000                        52.0000 17.0000   1.0000
SPH 53.0000 17.0000                        52.0000 17.0000   1.0000
      3     1.0000
SPH 53.0000   7.0000 52.0000   8.0000 52.0000   7.0000   1.0000
SPH 51.0000   7.0000                        52.0000   7.0000   1.0000
SPH 53.0000   7.0000                        52.0000   7.0000   1.0000
      3     1.0000
SPH 32.0000 17.0000 31.0000 18.0000 31.0000 17.0000   1.0000
SPH 30.0000 17.0000                        31.0000 17.0000   1.0000
SPH 32.0000 17.0000                        31.0000 17.0000   1.0000
      3     1.0000
SPH 32.0000   7.0000 31.0000   8.0000 31.0000   7.0000   1.0000
SPH 30.0000   7.0000                        31.0000   7.0000   1.0000
SPH 32.0000   7.0000                        31.0000   7.0000   1.0000
   RELATIVISTIC SLIT TEST 0.1 M SLIT LENGTH
   14
    0.000  20.000  24.000  28.000  34.000  38.000  46.000  50.000  58.000  62.000
   66.000  70.000  75.000  80.000
    0.000   0.000   0.500   0.500  -1.000  -1.000   1.000   1.000  -1.000  -1.000
    0.500   0.500   0.000   0.000
X
```

Table 13: Relativistic strip beam data set
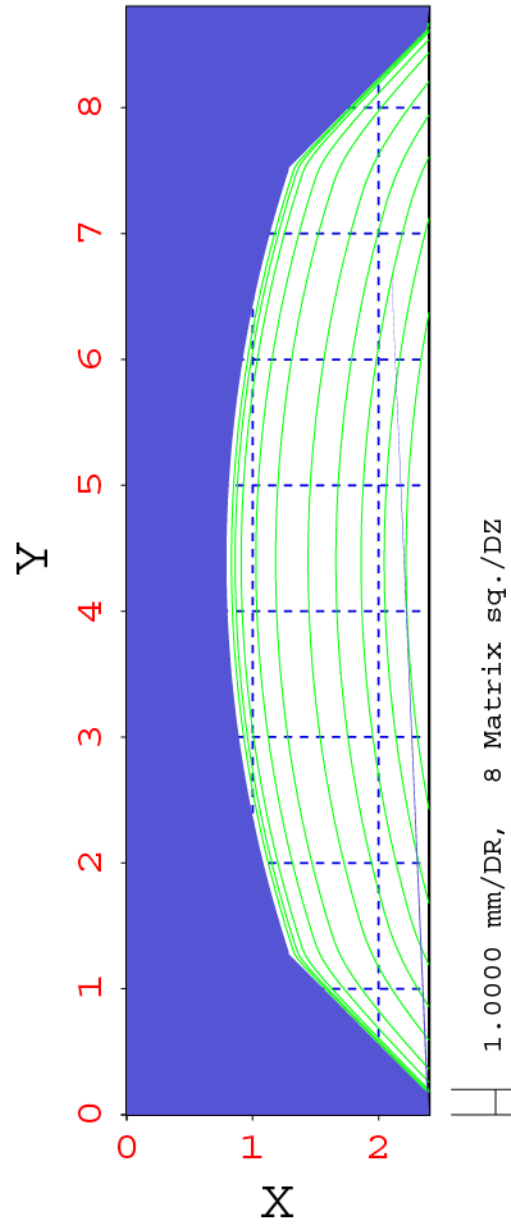
FINE MATRIX EQUIPOTENTIALS

Figure 36: Fine matrix equipotentials for slit beam
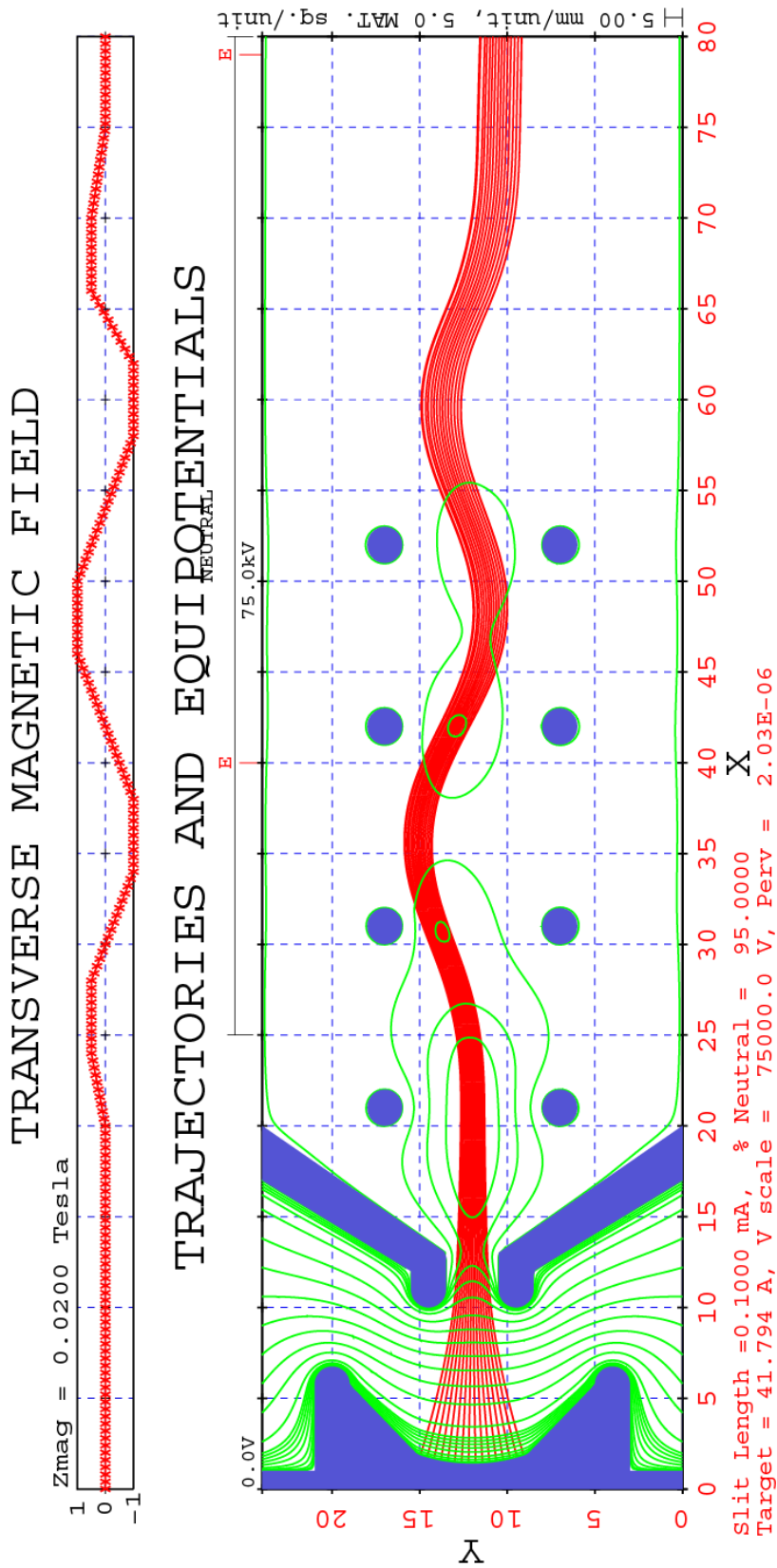
Figure 37: Strip beam from Fig. 33 with applied wiggler magnetic field shown at top
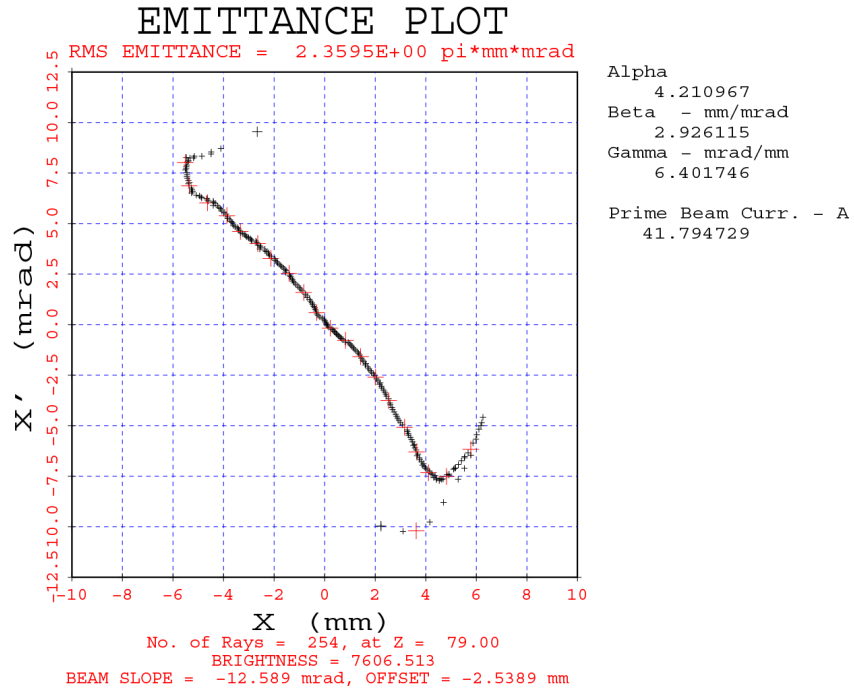
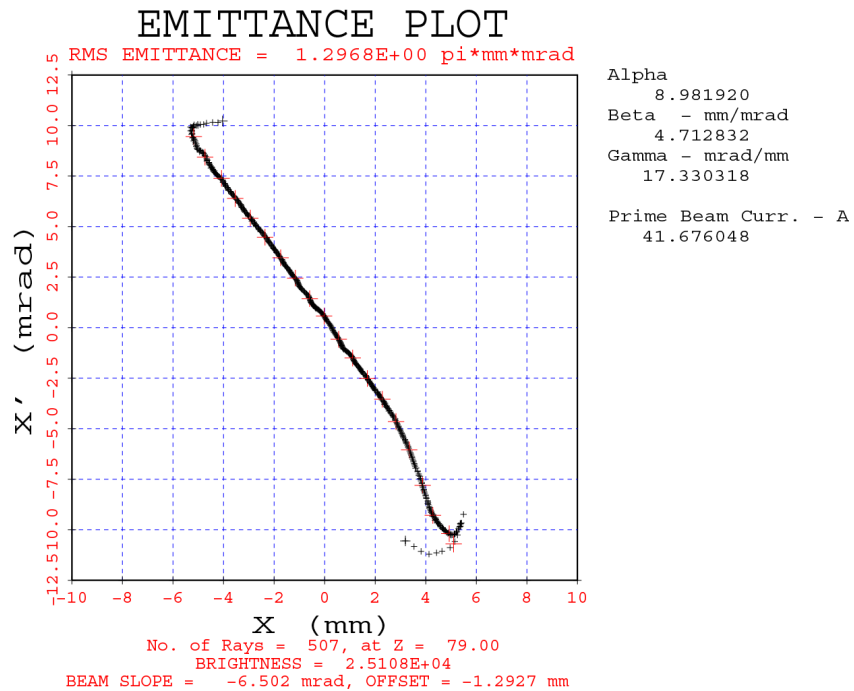Figure 38: Emittance plot near end of beam of Fig. 33

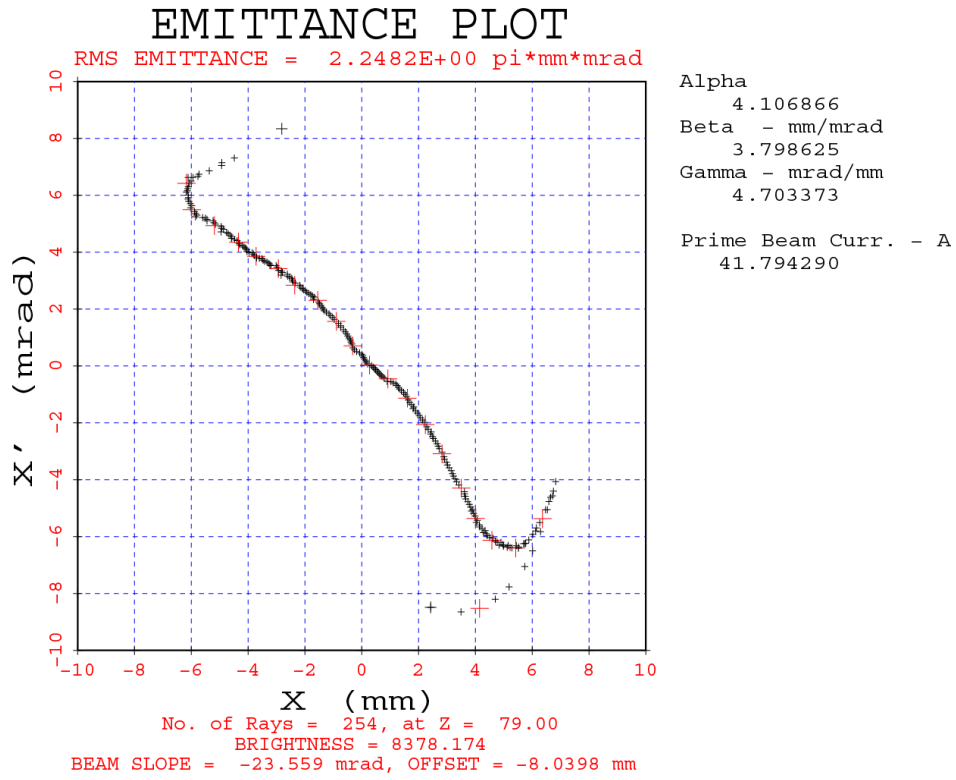Figure 39: Emittance plot for 401 by 241 mesh

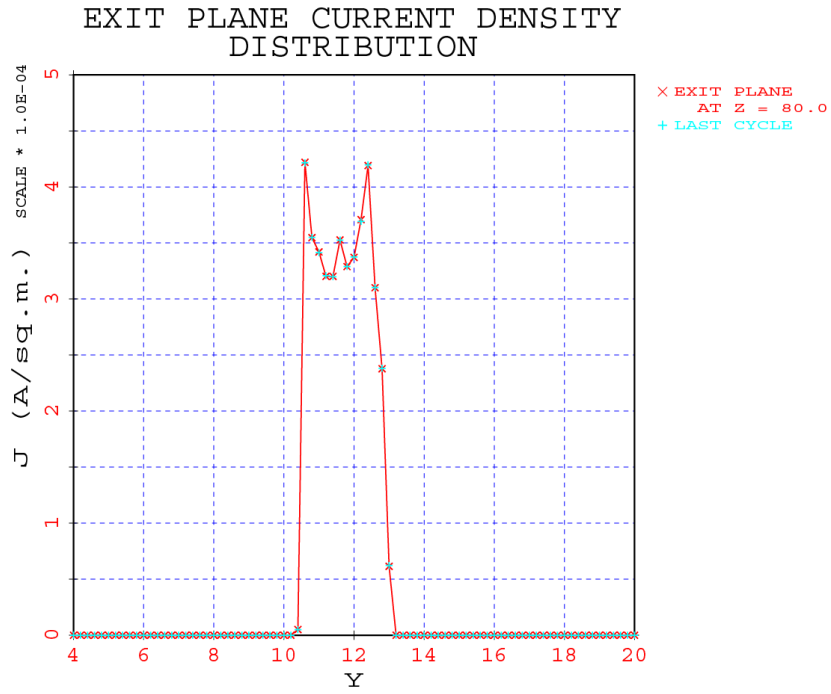Figure 40: Emittance plot for beam with magnetic field

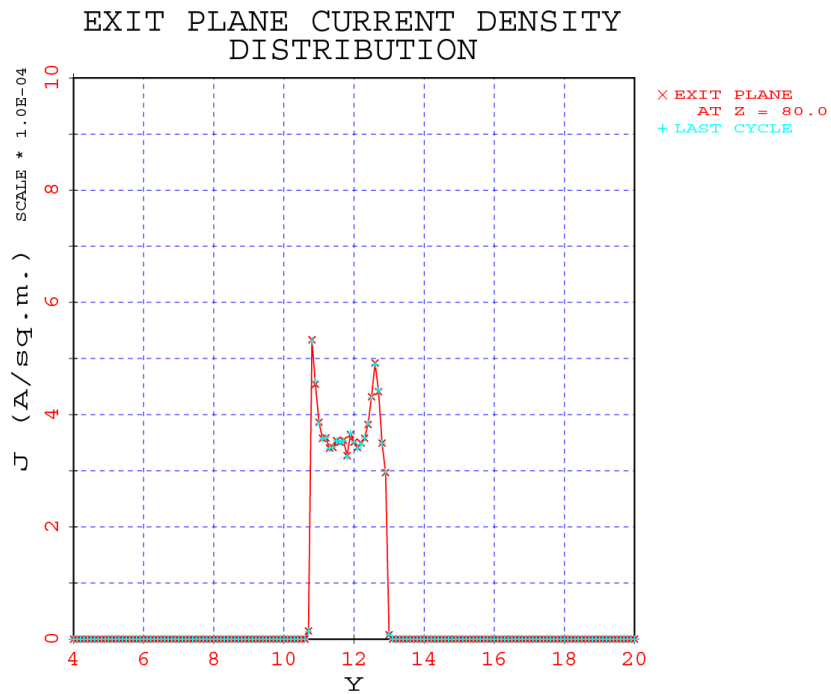Figure 41: Current density distribution at exit plane for 201 by 121 mesh

Figure 42: Current density distribution at exit plane for 401 by 241 mesh

6.4.2 Non-Relativistic Hollow Beam Electron Gun

Hollow beam guns can also be simulated using PBGUNS. A simple example is shown below. The input data is shown in Table 14. The fifth number on the first line is 100, the offset from the axis in matrix squares. The configuration and beam are shown in Fig. 43. The fine matrix equipotentials are seen in Fig. 44. Slight asymmetries can be seen in the beam, these are caused primarily by the symmetry about the axis which is below the bottom of the plot. This design was generated interactively with the PBGUNS in less than half an hour on the computer, it obviously needs some refinements but the basic design is done.

```
 100 800 121  61 100   7   0   4   0   0
   2   4   0   1  -1   1   0   0   0   0
 0.0000000     5000.0   0.00254   0.10000 0.0000020    0.00000       1.0     0.3000
   1.0000 15.0000      0.0   0.000    0.000 0.00000  0.0000  0.0000    0.00
   10.000   0.000    0.000   0.000    0.000   0.000   0.000    0.00  0.000  12.000
     5     0.0   1    2 2.41233 0.99793 3.58767 0.99793     0.0
 PLA  2.0000  0.0000  2.0000  1.0000
 TCN  1.0000  2.4000
 SPH  1.0000  3.6000                    4.5750  3.0000  3.6250        0.25000
 TCN  2.0000  5.0000
 PLA  2.0000  6.0000
     5     1.0   0
 PLA  6.0000  0.0000  6.0000  2.6000
 CYL  4.0000  2.6000
 PLA  4.0000  2.0000
 CYL  5.0000  2.0000
 PLA  5.0000  0.0000
     5     1.0   0
 PLA  5.0000  6.0000  5.0000  4.0000
 CYL  4.0000  4.0000
 PLA  4.0000  3.4000
 CYL  6.0000  3.4000
 PLA  6.0000  6.0000
     3     1.0   0
 PLA 11.6000  0.0000 11.6000  2.5000
 CYL 11.0000  2.5000
 PLA 11.0000  0.0000
     3     1.0   0
 PLA 11.0000  6.0000 11.0000  3.5000
 CYL 11.6000  3.5000
 PLA 11.6000  6.0000
     3  0.4000   0
 PLA  9.0000  0.0000  9.0000  2.4000
 CYL  8.0000  2.4000
 PLA  8.0000  0.0000
     3  0.4000   0
 PLA  8.0000  6.0000  8.0000  3.6000
 CYL  9.0000  3.6000
 PLA  9.0000  6.0000
   NON-RELATIVISTIC HOLLOW BEAM
 X
```

Table 14: Input data for basic hollow beam gun
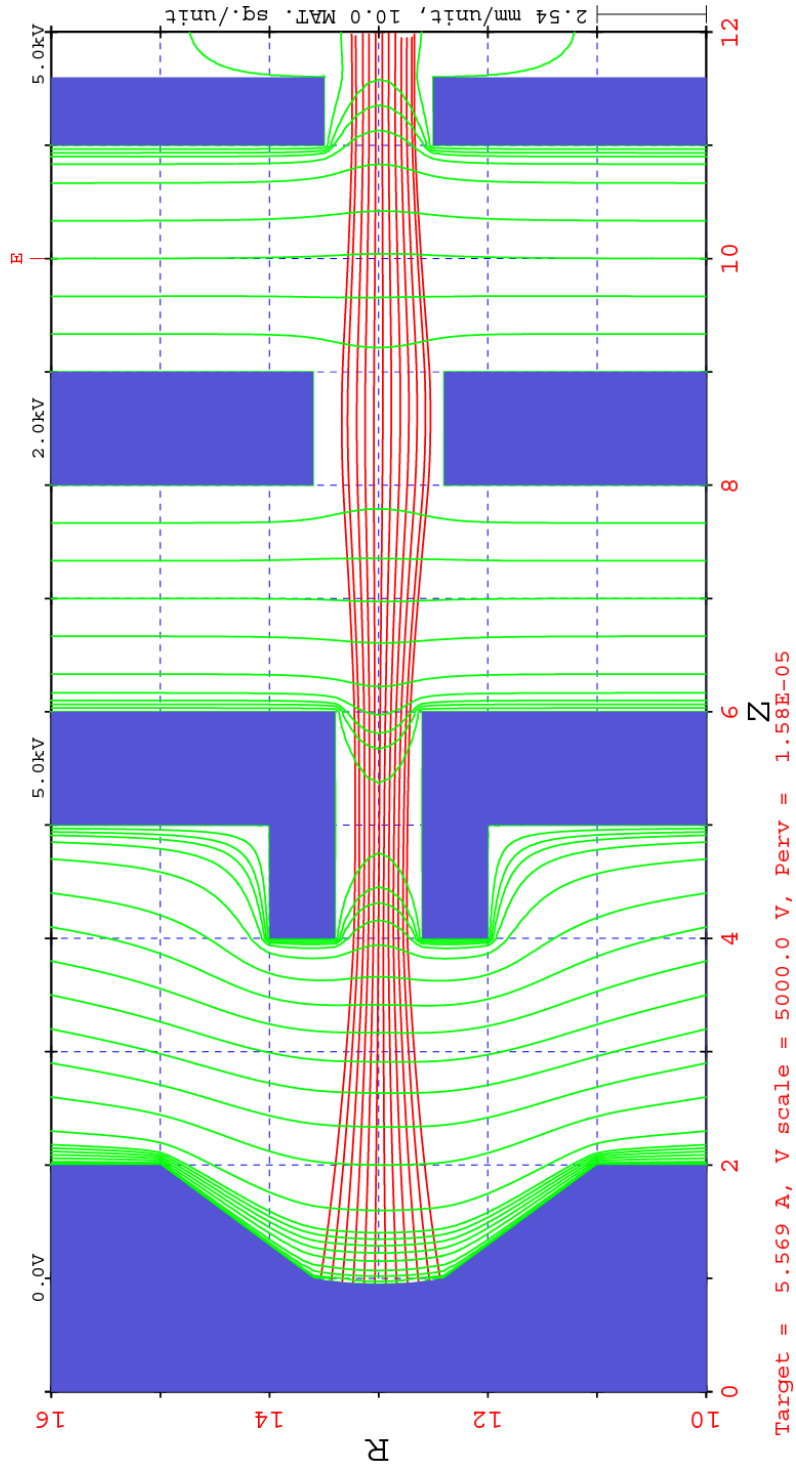
Figure 43: Hollow beam electron gun example
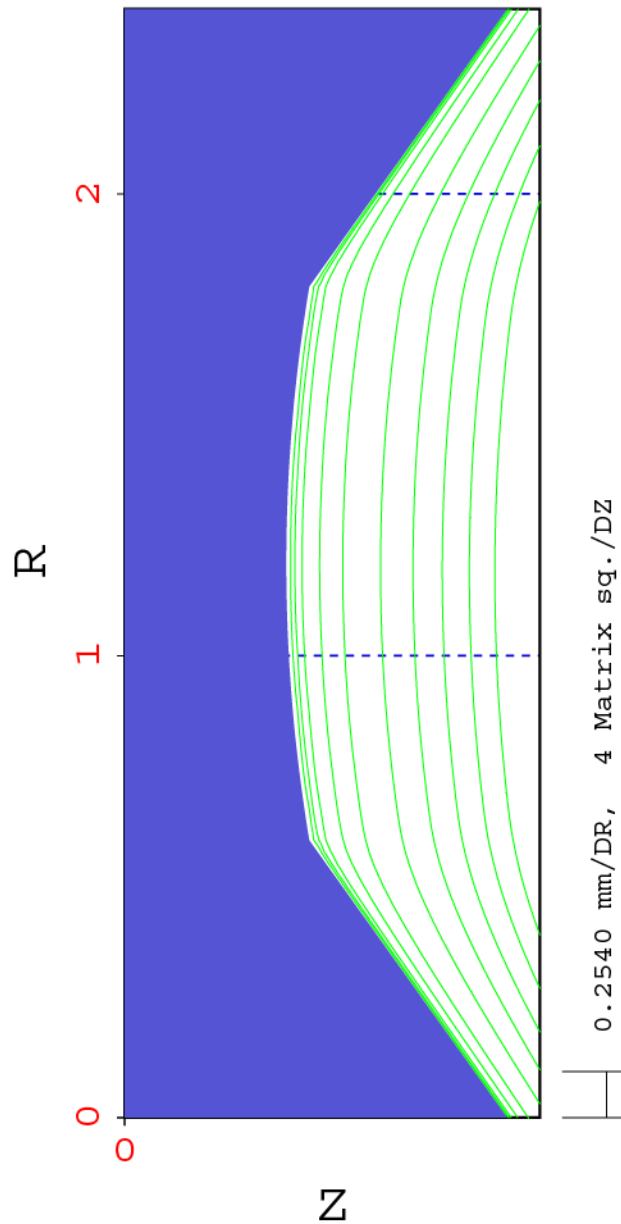
Figure 44: Fine matrix equipotentials for hollow beam gun

Figs. 45 and 46 display the asymmetries caused by the symmetry about the axis more clearly. A 2-D slit beam would not display such asymmetries. Finally the Emittance plot, Fig. 47, is the only plot that fully shows the symmetry about the axis.
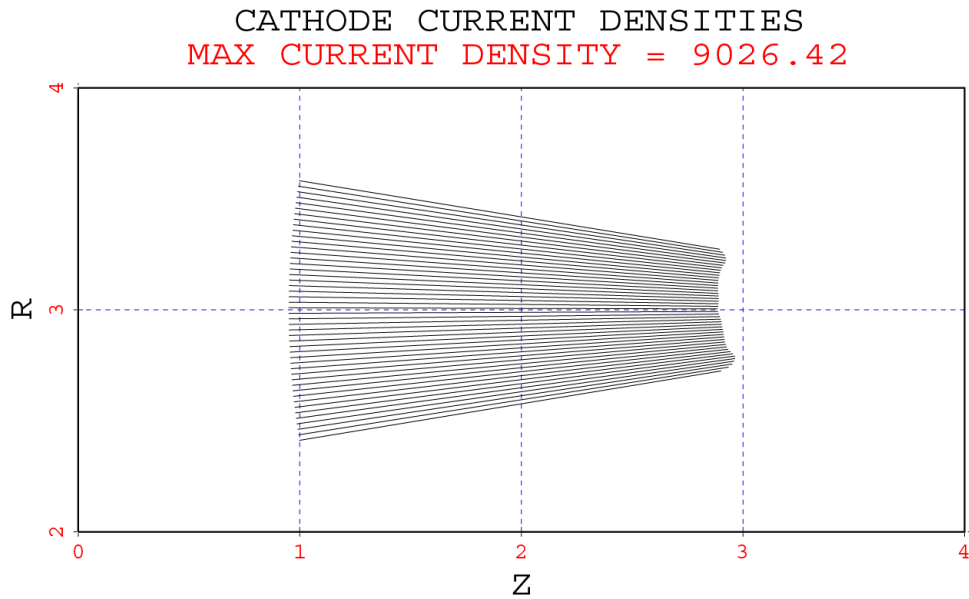
Figure 45: Cathode current density distribution for hollow beam gun. The asymmetry in the current density is caused by the axial symmetry
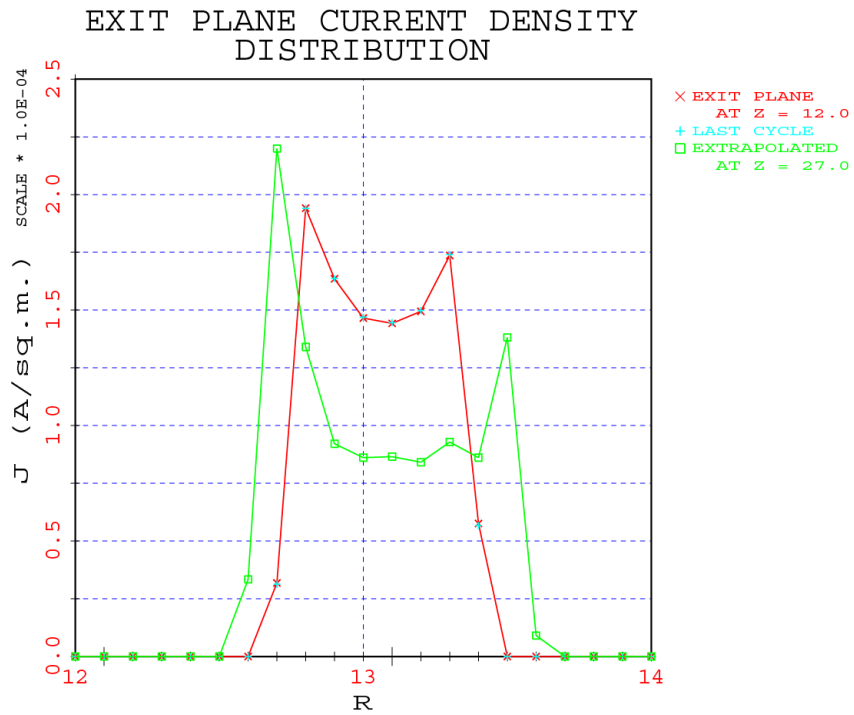
Figure 46: Exit plane current density distribution for hollow beam gun
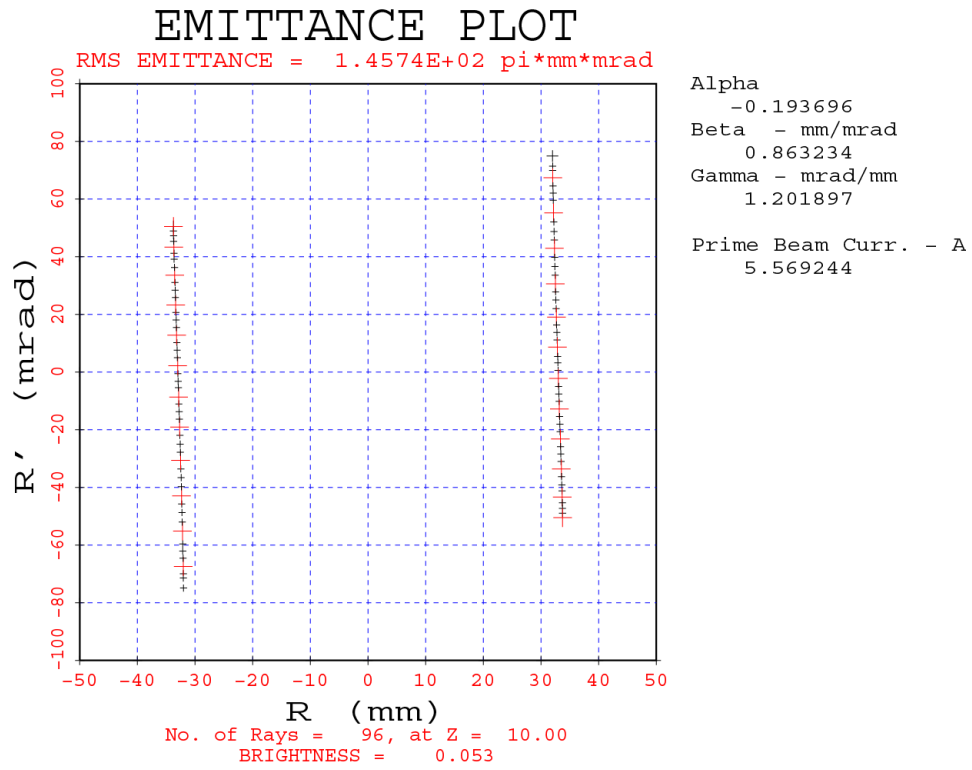
Figure 47: Emittance plot for hollow beam gun. The symmetry about the axis is quite clearly seen

6.5   Magnetron Injection Electron Gun

Magnetron injection guns are extremely difficult to run. Cathodes with a cone half angle of less than about 15 degrees tend to be very unstable as electrons from the back of the cathode cycloid over the front of the cathode. It is not uncommon for PBGUNS to require 200 heavily damped cycles to reach any kind of convergence. Damping can consist of small values of the damping factor (BETA = 0.2) and small numbers of cycles ($\sim$200) through the voltage matrix relaxation. After a steady, but not necessarily fully converged beam has been obtained, the damping factor can be increased to respond faster to changes in the configuration.

Obtaining good reasonably laminar beams require maintaining the Pierce angle (67.5 degrees to the cathode) at both the front and back of the cathode. The electrode at the front, while starting near the Pierce angle, must rapidly pull back from the beam, while the electrode at the back must curve forward to maintain focusing of the beam at the back. It is difficult to reduce the ripple in the beam although a transformer of similar cones for the snout on the cathode and the accelerating electrode seem to help. From past experience, the truncated cone for the cathode must not be too long or have too small a cone angle. Either condition can allow cycloiding in front of the cathode and will make the program unstable (and possibly the real device). Increasing the magnetic field will probably reduce the ripple, but will likely make the cathode calculations more unstable.

The simulation should be done on a rather fine regular mesh with at least an 8 to 1 fine mesh ratio. The changes in the current density from cycle to cycle are heavily damped. After the 4th cycle the number of passes through the mesh are reduced by a factor of 4 and the damping factor is reduced by a factor of 2. Typical starting conditions would be 800 to 1200 passes through the mesh and BETA set between 0.4 and 0.6. After a few more cycles the number of passes should be reduced to 200. Larger meshes are usually offer more stability.

Typically the convergence of the cathode current densities begins at the left edge of the cathode. This is accompanied by bad transients which usually start at the right edge of the cathode. It is not unusual for this to require 300 or more cycles through the program.

A magnetron injection gun operating at 5 kV and 2.54 Amps is shown in Fig. 48. This was developed over a long period of time while developing the code and could use much more work. The input data is shown in Table 15. Note that the mesh size is 501 by 121, much larger than would be used for most other simulations.

The cathode current density distribution is shown in Fig. 49. The current ramps up toward the front of the cathode as the radial gap decreases and field strength increases. The small ripples correspond to the radial matrix increments along the cathode. The bump in the current density at the back is the effect of the still incorrect focusing electrode at the

back of the cathode.

```
 140 800 501 121    0    2    0   16    6    0    0    0    0    0    0    0    0    0    0
   6  32    0    1   -1    1    0    0    0    0    1    0    0    0    0    0    0    0  0 0.0
   700.0000     5000.0    0.00254  0.050000 0.0000100    0.09900      1.000      0.500
   0.5000   0.0000 40000.0    0.000    0.000 0.00000   0.0000   0.0000      0.0      0.0
   10.000   17.000   24.000    0.000    0.000    0.000    0.000    0.000    0.000   25.000
   11 0.00000    1    2 1.00000 6.20000 1.64000 3.20000 0.00000 0.00000    0    0    0
SPH 11.5000   0.0000 11.2703   0.2500 11.2491   0.0000   0.2509
TCN  6.9000   1.0500
CYL  6.5500   1.0500
TCN  6.2000   1.0000
TCN  3.2000   1.6400                                              0.06250
TCN  2.9000   1.9400
TCN  2.6900   2.3800
TCN  2.6000   2.8000
PLA  2.6000   3.0000
SPH  1.6000   4.0000                    1.6000   3.0000   1.0000
CYL  0.0000   4.0000
    4      1.0    0
CYL  0.0000   5.7000   4.1000   5.7000
TCN  8.6000   2.3500
TCN 11.3000   1.9000
CYL 25.0000   1.9000
  NON-RELATIVISTIC BEAM
    2
    0.000   25.000
    1.000    1.000
X
```

Table 15: Demonstration MIG data set

AXIAL MAGNETIC FIELD

Bmag = 0.0990 Tesla

TRAJECTORIES AND EQUIPOTENTIALS

2.54 mm/unit, 20.0 MAT. sq./unit

Z-axis

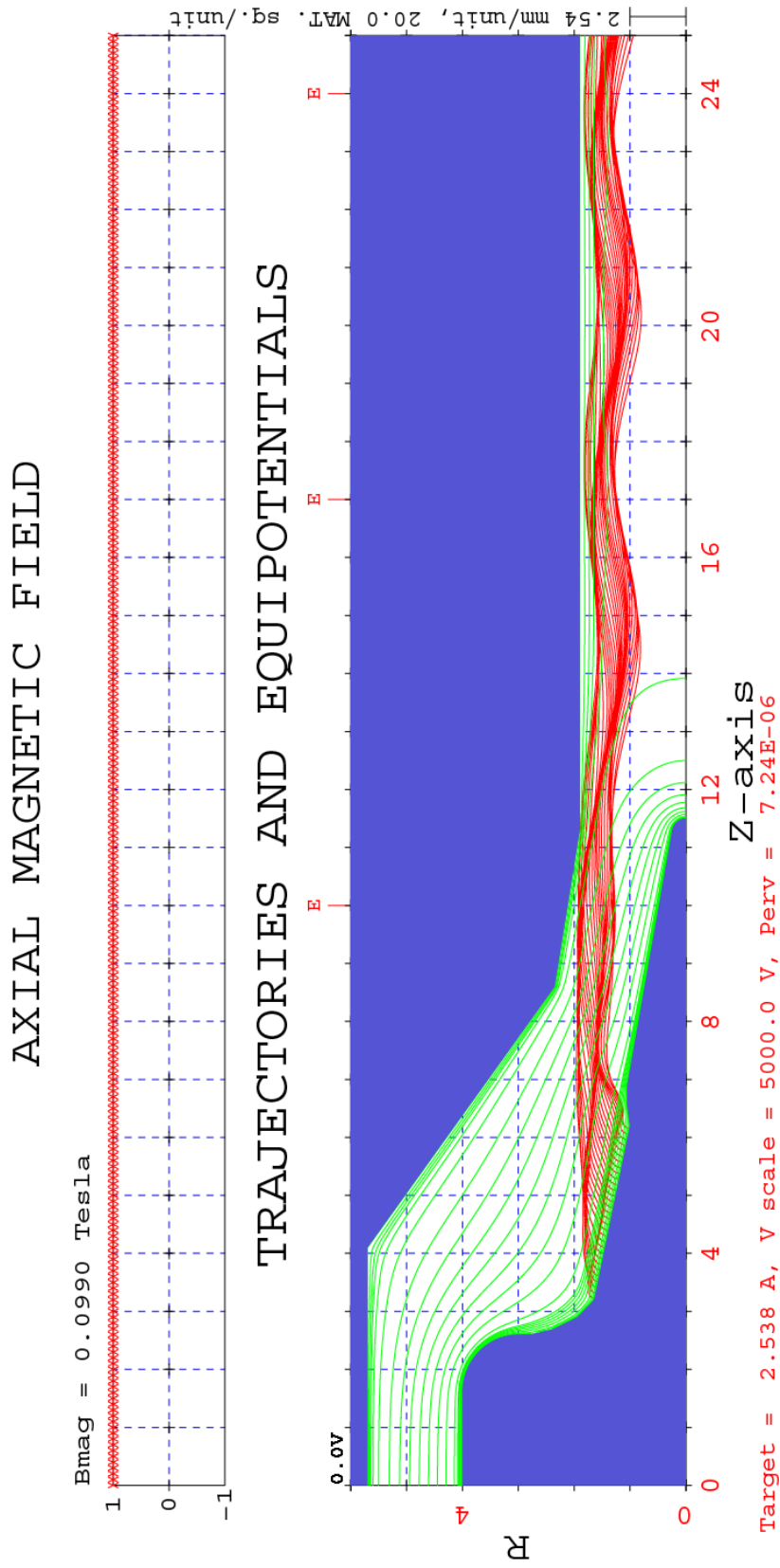Target = 2.538 A, V scale = 5000.0 V, Perv = 7.24E-06

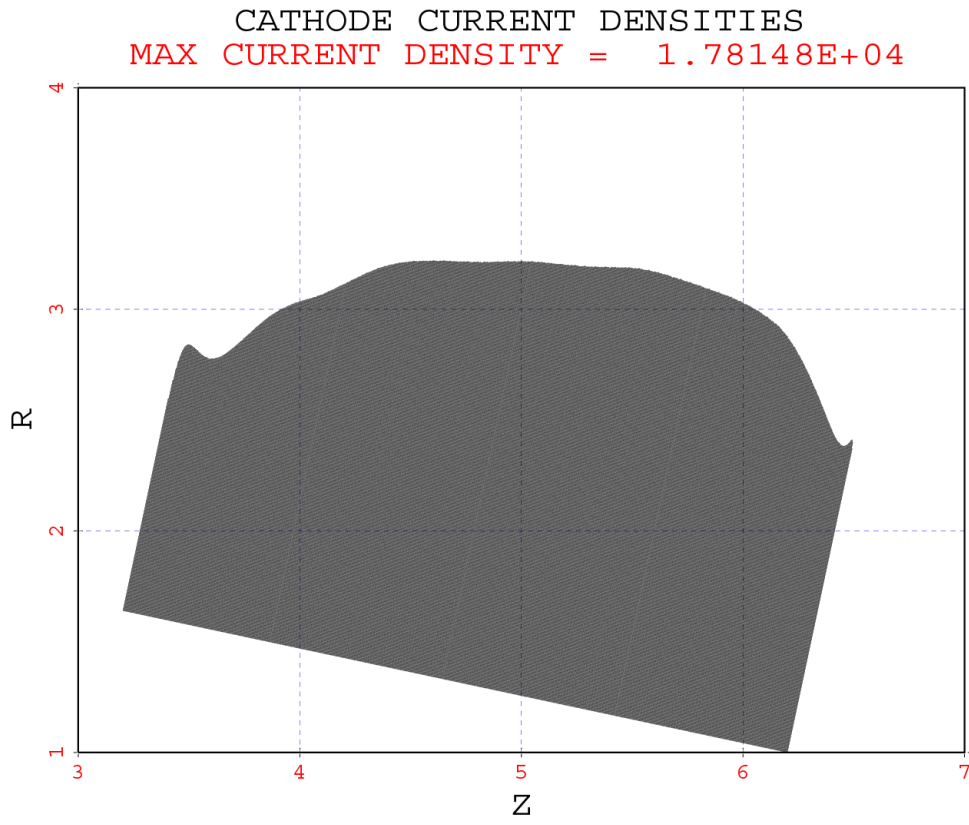Figure 48: Demonstration MIG electron gun

Figure 49: Emission current density distribution from MIG cathode

6.6   Beam and Plasma Sputter Ion Sources

PBGUNS can also simulate many types of ion beams. It can simulate positive or negative ions extracted from a plasma, sputtered from an electrode in a plasma or emitted from a space charge limited electrode.

6.6.1   Negative Ion Sputter Source

The first example is a negative ion sputter source similar to those developed at Oak Ridge National Laboratories. This consists of a spherical electrode with a 1.5 cm radius in a dense plasma between 0 and 9.7 on the z axis. This electrode is held between -250 and -1000 Volts below the chamber voltage. Ions from the plasma bombard the electrode and depending on the material of the electrode negative ions, such as gold, copper or oxygen, are emitted with an energy of 15 to 25 eV with a cosine distribution from the normal to the surface. These ions are accelerated by the 250 to 1000 Volts on the electrode and then drift to the aperture at 9.7 on the axis and are then accelerated by the electrodes on the right. The ions are assumed to be accelerated through a sheath formed on the surface of the spherical electrode. The angular spread of the emitted particles is reduced by this acceleration so that the injected particles have a smaller angular distribution as they leave the sheath. The particles in this case are injected (from the surface) with 7 beams at 2.3 degree increments with 25 eV of energy, transformed through the sheath with 0.9 kV of acceleration. It is *essential* that a distribution of injected particles be used with this type of ion source. This is an ICT = 14 simulation.

The input data for this problem is shown in Table 16. Here 18 line segments are needed to simulate the electrodes. The ions injected (6mA) have a mass ratio (M/m_e) of 250,000, and about 2.05 mA make it into the beam. The results of this simulation are shown in Fig. 50.

The fine matrix covers the plasma region shown in Fig. 51. If any fine structure appears in the equipotentials on the mesh, the fine matrix ratio should be increased or the damping should be increased (BETA decreased) or both.

An emittance plot of the injected beam in the plasma at z = 6.0 is shown in Fig. 52. The complexity of the injection conditions are quite evident. At each injection point along the emitter, 29 particles are effectively injected (only 22 are actually needed because the program cannot tell the difference between a particle injected with azimuthal energy in the + or - θ direction). A total of 5353 particles are injected from the emitter. Needless to say, only a sampling of the particle trajectories (1 in 25) are actually plotted.

```
 100 600 181   61    0    4    0    8    7    0        241
   3   25    1    1   -1    1    0   16    0    0    1
   0.55E+00    40000.0     0.01000    0.10000 0.0000100     0.01800   250000.0   900.0000
   0.7000   0.0000   0.0000   0.0000   0.0000 0.01000              25.00    0.000
   6.000    9.000   17.000    0.000    8.000    0.000    0.000   18.000
  20.000    1.000    9.000    9.300    0.000    0.800
   30.000100    1   14   0.0000   0.1800   1.5000   0.3705      1.0
   0.0060    7    3    1    0    4    5    4.000    0.050    0
   9.500    9.000    8.000    2.000   10.000    5.000    0.300   10.000
SPH   0.1800   0.0000   0.3705   1.5000   6.1800   0.0000   6.0000            0.12500
PLA   0.3705   2.0000
CYL   0.0000   2.0000
   60.000100    1
CYL   0.0000   2.5000   6.2000   2.5000
PLA   6.2000   0.2000
CYL   6.4000   0.2000
TCN   9.0000   0.8000
TCN   9.5000   2.5000
PLA   9.5000   6.0000
    5     1.0    0
PLA  15.0000   6.0000  15.0000   2.0000
TCN  12.5000   1.1000
PLA  12.5000   0.9000
TCN  14.0000   1.0000
CYL  18.0000   1.0000
    4   0.0250    0
PLA   9.6000   6.0000   9.6000   2.4000
CYL  12.0000   2.4000
SPH  12.5000   2.9000                       12.0000   2.9000   0.5000
PLA  12.5000   6.0000
 PLASMA SPUTTER ION BEAM
    6
   0.000    7.000    9.000   12.000   14.000   18.000
   0.000    0.000    1.000    1.000    0.000    0.000
X
```

Table 16: Plasma sputter source input data

A couple of parameters are important here. With a fine matrix ratio of 8 to 1, BETA is 0.7 (the damping factor for the relaxation). If the matrix ratio were increased to 12 to 1, BETA could probably be increased to 1.0 but the execution time would increase significantly. Little would be gained from a finer mesh.

If the emittance plot in Fig. 52 becomes fuzzy or starts to break up, either the fine mesh should be increased or BETA reduced. The twisting shapes near the center of the plot are caused by particles passing near the axis of symmetry.

The emittance plot at z = 9.0 (I = 81) is shown in Fig. 53. Here the high angle particles have been stripped from the beam. The final beam emittance plot at z = 17.0 is shown in Fig. 54.
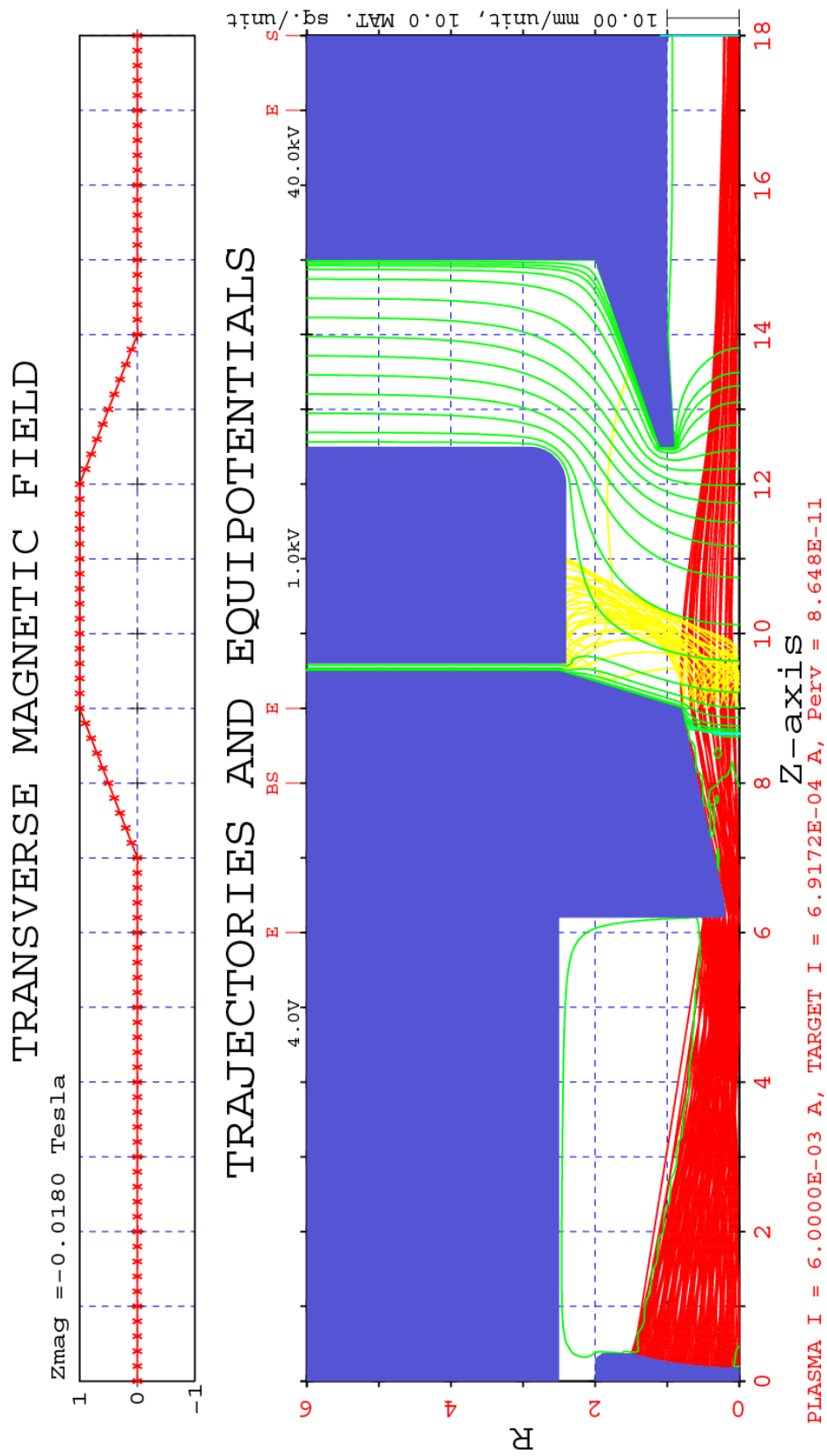
Figure 50: Sputter source negative ion beam extraction system with electron separator

FINE MATRIX
EQUIPOTENTIALS

1.0000 mm/DR, 8 Matrix sq./DZ

R

Z-axis
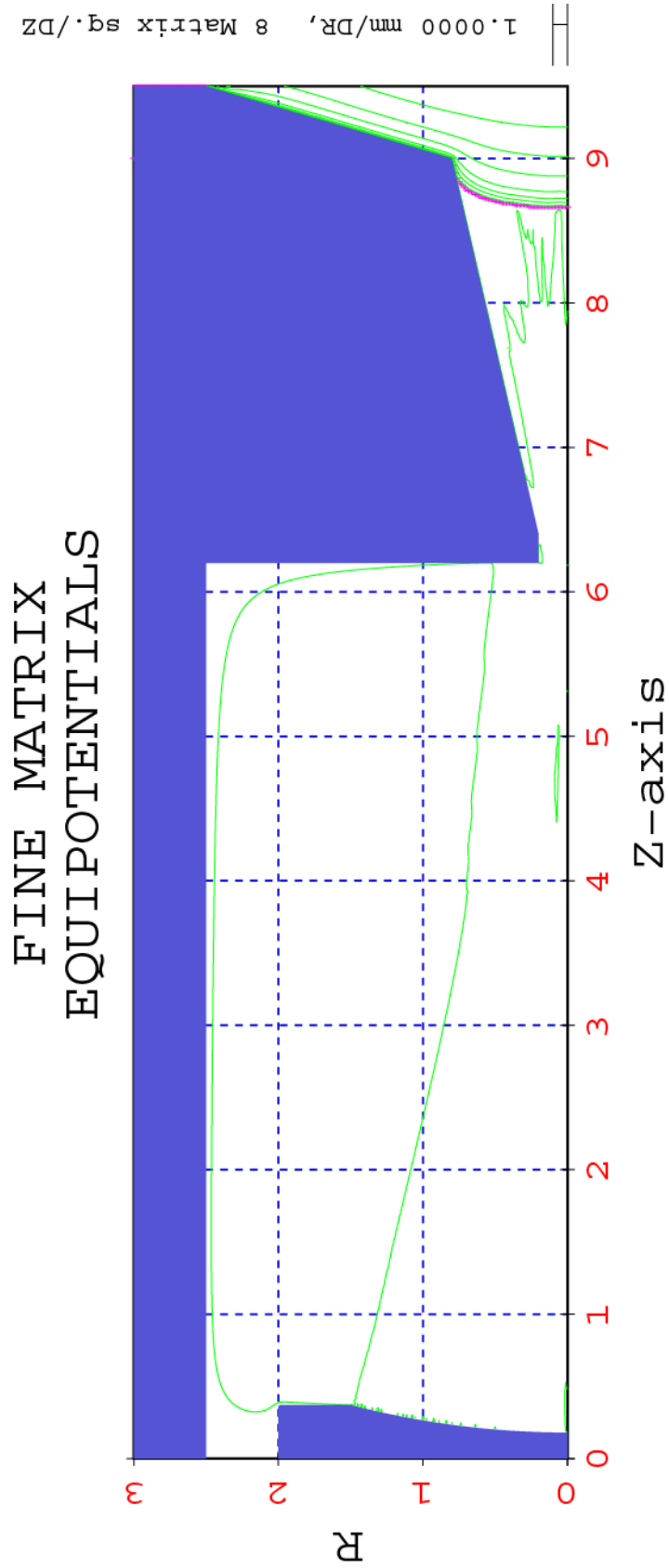
Figure 51: Fine matrix equipotentials for sputter source

EMITTANCE PLOT

RMS EMITTANCE =   5.2457E-02 pi*mm*mrad

Alpha
   −0.336179
Beta − mm/mrad
    0.027582
Gamma − mrad/mm
   40.352345

Prime Beam Curr. − A
    0.006000

R' (mrad)

R (mm)

No. of Rays = 5353, at Z =   6.00
BRIGHTNESS =   220.934
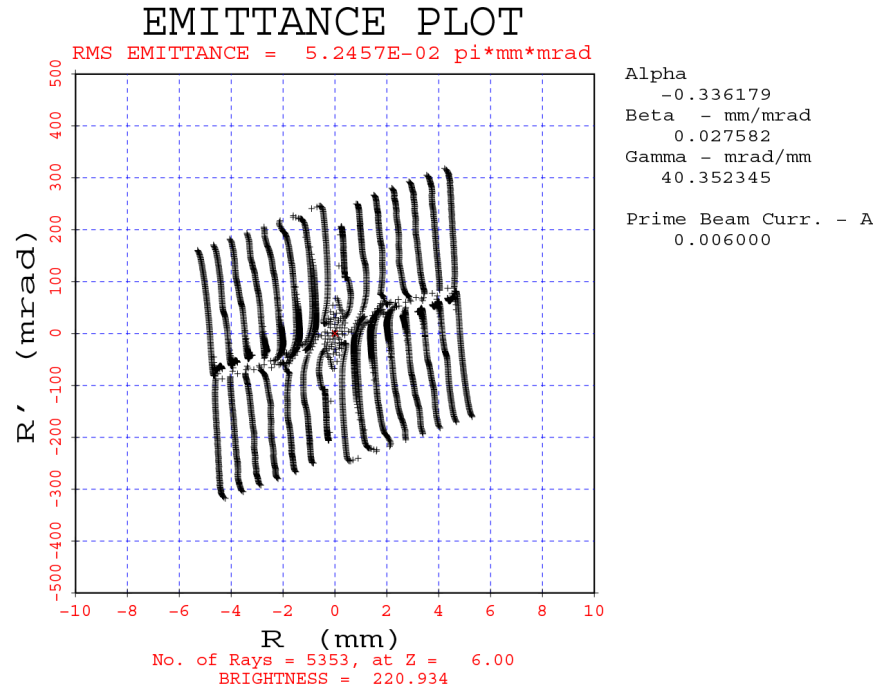
Figure 52: Emittance plot in source plasma before focus at Z = 6

EMITTANCE PLOT

RMS EMITTANCE =   1.9314E-02 pi*mm*mrad

Alpha
   −4.159364
Beta − mm/mrad
    0.190852
Gamma − mrad/mm
   95.887238

Prime Beam Curr. − A
   6.9193E−04

R' (mrad)

R (mm)

No. of Rays = 1663, at Z =   9.00
BRIGHTNESS =   187.937

Figure 53: Emittance plot after aperture at Z = 9 of sputter ion source

An important fact that effects the sputtered, drifting ions in the plasma, is that each angular distribution will focus in a plane at the center of curvature of the spherical emitter,

114

EMITTANCE PLOT

RMS EMITTANCE = 2.6055E-02 pi*mm*mrad

Alpha
    1.371224
Beta – mm/mrad
    0.080925
Gamma – mrad/mm
    35.591537

Prime Beam Curr. – A
    6.9193E-04

No. of Rays = 1663, at Z = 17.00
BRIGHTNESS = 103.273

Figure 54: EMittance plot in the beam drift region at Z = 17
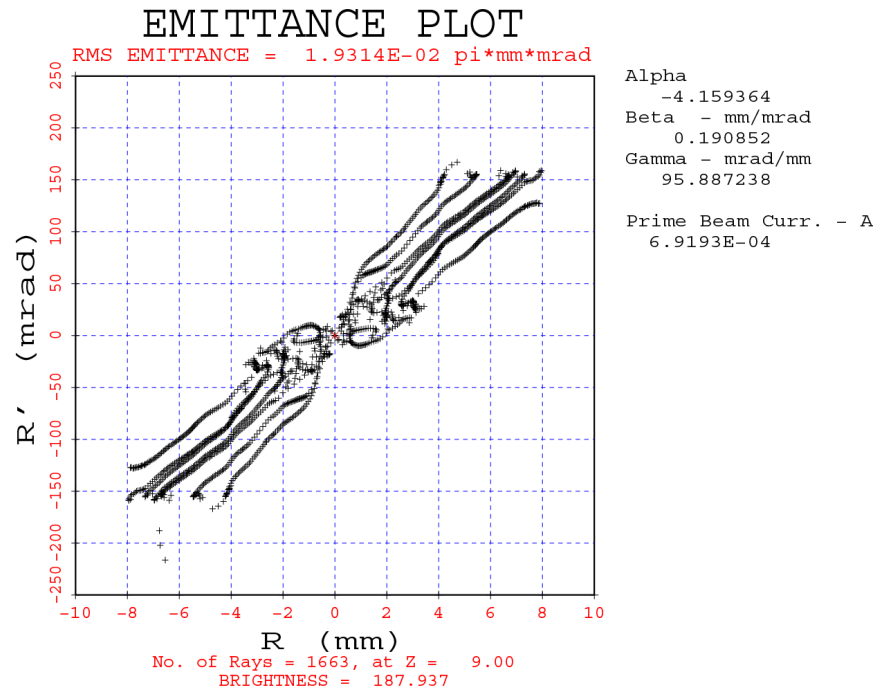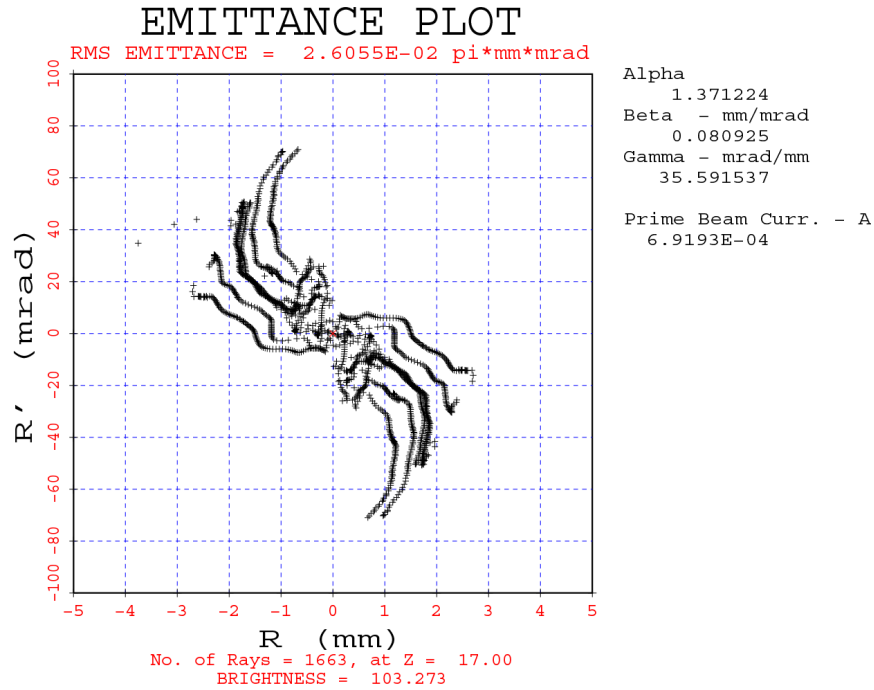
offset from the axis by a distance proportional to the injected angle. This means that an aperture placed at the center of curvature of the spherical surface will strip off all particles injected with an angle greater than some particular injection angle. The aperture will limit the flow of gas from the plasma source as well as reduce the angular spread in the particles. There is a possible downside to this in that the current density is extremely high at this crossover.

A second effect of the aperture may reduce the plasma density around the injected particles. All the plasma cannot be stripped of the negative ions or it would be nearly impossible to extract the ions due to their own space charge. Experimentally this can have a striking effect on the electrons extracted with the negative ions. The negative ions will drag positive ions along with them so that neutralization of the plasma continues to the extraction surface, but the electron density may be reduced so that relatively few electrons are extracted from the source. The PIR (positive to negative ion ratio) may be very high in the region around the negative ion source and relatively small after the aperture. It is now possible to guess at the plasma density and how it may vary in the z direction. If the one of the electrodes is part of the magnetic containment for the plasma it may contain the electrons and cause the plasma density to fall. All of these effects are not well understood.

A plot of the exit plane current density distribution for the above example is shown in Fig. 55.

EXIT PLANE CURRENT DENSITY
DISTRIBUTION

Figure 55: Exit plane current distribution

6.6.2   Primary Beam Sputter Ion Source

The second type of sputter sources uses a beam of ions (usually Cesium) impinging on a target consisting of the material desired as ions. Tables 17 and 18 show the input data files for the primary and secondary ion beams. The space-charge densities from the primary beam are used in the secondary (sputter) beam calculation to determine the secondary current densities.

The secondary input data was obtained by interactively modifying the primary beam. Note that each electrode potential must be reset remembering that the program always uses negative particles. Alternatively, the primary beam configuration can be regenerated with the configuration reversed so that both beams go to the right, this might be more useful if the secondary beam is to be extended.

Fig. 56 shows the primary beam of Cesium obtained by space charge limited emission from the ring ion emitter.

```
 211200 201 131    0    5    0    2    0    0    0    0    0    0    0    0    0    0    0    0
    3  16    0    0   -1    1    3    0    0    0    1    0    0    0    0    0    0    0  0 0.0
  500.0000     2000.0    0.00254    0.10000 0.0000100    0.00000   241896.0        0.500
    1.0000   0.0000      0.0    0.000    0.000 0.00010   0.0000    0.0000        0.0      0.0
   16.900    0.000    0.000    0.000    0.000    0.000    0.000    0.000    0.000   17.500
    4 0.00000    1    5 1.2344210.57442 6.5255815.86558 0.00000      0.00    0    0    0
    3 20.0000   0.0500
PLA   8.5000 13.0000   8.5000   1.2300
CYL 10.5700   1.2300                                                              0.25000
TCN 15.8700   6.5300                                                              0.12500
PLA 15.8700 13.0000
    3      1.0
TCN 20.0000   2.5000 17.0000   2.0000
PLA 17.0000   1.5000
SPH 17.5000   0.0000                          15.0    0.000      2.5
    3      0.0
CYL 20.0000   7.6500 17.0000   7.6500
PLA 17.0000   3.4100
CYL 20.0000   3.4100
    3      0.0
CYL   0.0000   2.0000   5.2500   2.0000
PLA   5.2500   2.5000
CYL   0.0000   2.5000
    4    -10.0
CYL   0.0000   4.0000   6.3000   4.0000
PLA   6.3000   2.5000
CYL   6.7500   2.5000
PLA   6.7500 13.0000
   INF = 2
X
```

Table 17: Input data for primary ion beam

```
 14 500 201 131    0    5    0    4    0    0    0    0    0    0    0    0    0    0    0   0
  3  12    0    1  -1    1    2    0    0    0    1    0    0    0    0    0    0    0   0 0.0
    0.1000     2000.0    0.00254    0.10000 0.0000100    0.00000   1.00E+05      0.000
  1.0000  0.0000       0.0    0.000    0.000 0.00010   0.0000 15.0000
  1.000  16.900    0.000    0.000    0.000    0.000    0.000    0.000
  3 0.00000    1    5 1.5000017.00000 0.0000017.50000 0.00000 0.00000    0    0    1
  3 20.0000   0.0500
TCN 20.0000   2.5000 17.0000   2.0000                                          0.2500
PLA 17.0000   1.5000
SPH 17.5000   0.0000                    15.0000   0.0000   2.5000             0.2500
  4  1.0000    0
PLA  8.5000 13.0000   8.5000   1.2300
CYL 10.5700   1.2300
TCN 15.8700   6.5300
PLA 15.8700 13.0000
  3  1.0000    0
CYL 20.0000   7.6500 17.0000   7.6500
PLA 17.0000   3.4100
CYL 20.0000   3.4100
  3  1.0000    0
CYL  0.0000   2.0000   5.2500   2.0000
PLA  5.2500   2.5000
CYL  0.0000   2.5000
  4 11.0000    0
CYL  0.0000   4.0000   6.3000   4.0000
PLA  6.3000   2.5000
CYL  6.7500   2.5000
PLA  6.7500 13.0000
 SECONDARY SPUTTERED IONS
X
```
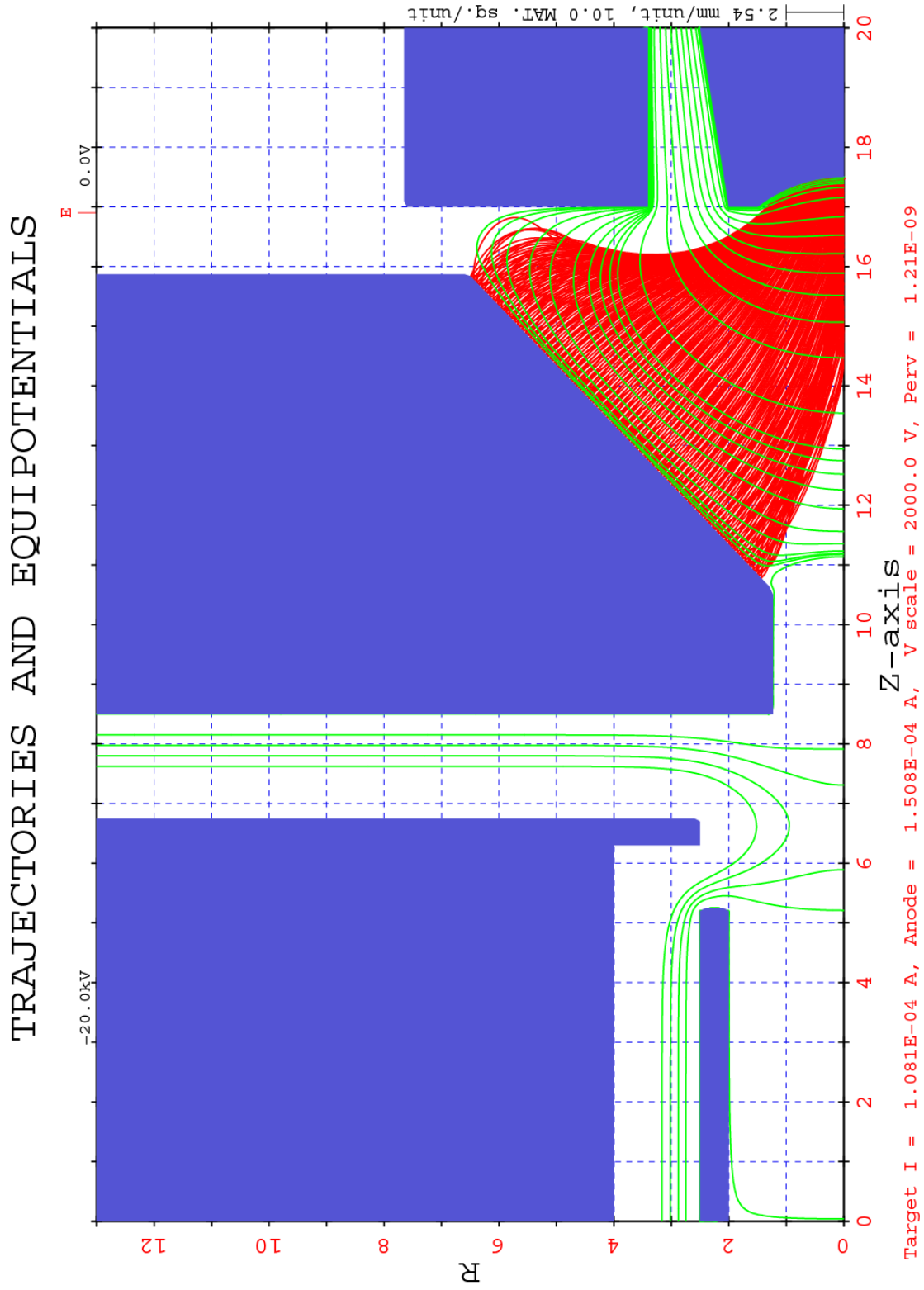
Table 18: Secondary beam input data

Figure 56: Primary beam for beam sputter ion source with Cesium ions impinging on the sputter target

6.6.3   Secondary Sputtered Ion Beam from Target

The secondary ion beam is shown in Fig. 57. The current distribution at the emitting surface is proportional the space-charge density of the Cesium at the surface. The distribution at each point along the secondary is a cosine distribution at the sputtered particles emission energy (typically around 25 Volts). This distribution is very important. The primary beam space-charge density matrix is saved and restored (with sign reversed) for the secondary run.

The emission of the primary beam current from the ion source is shown in Fig. 58. This current is computed with Child's law for space charge limited current. It could also be a forced or temperature limited emission current, if desired.

The secondary current distribution includes the angular spread required for the sputter emission. The actual emission current distribution is seen in the target current distribution from the primary beam target shown in Fig. 60. Note that the last cycle current distribution is for a flat plane at the axis of the target, while the average current follows the shape of the electrode.

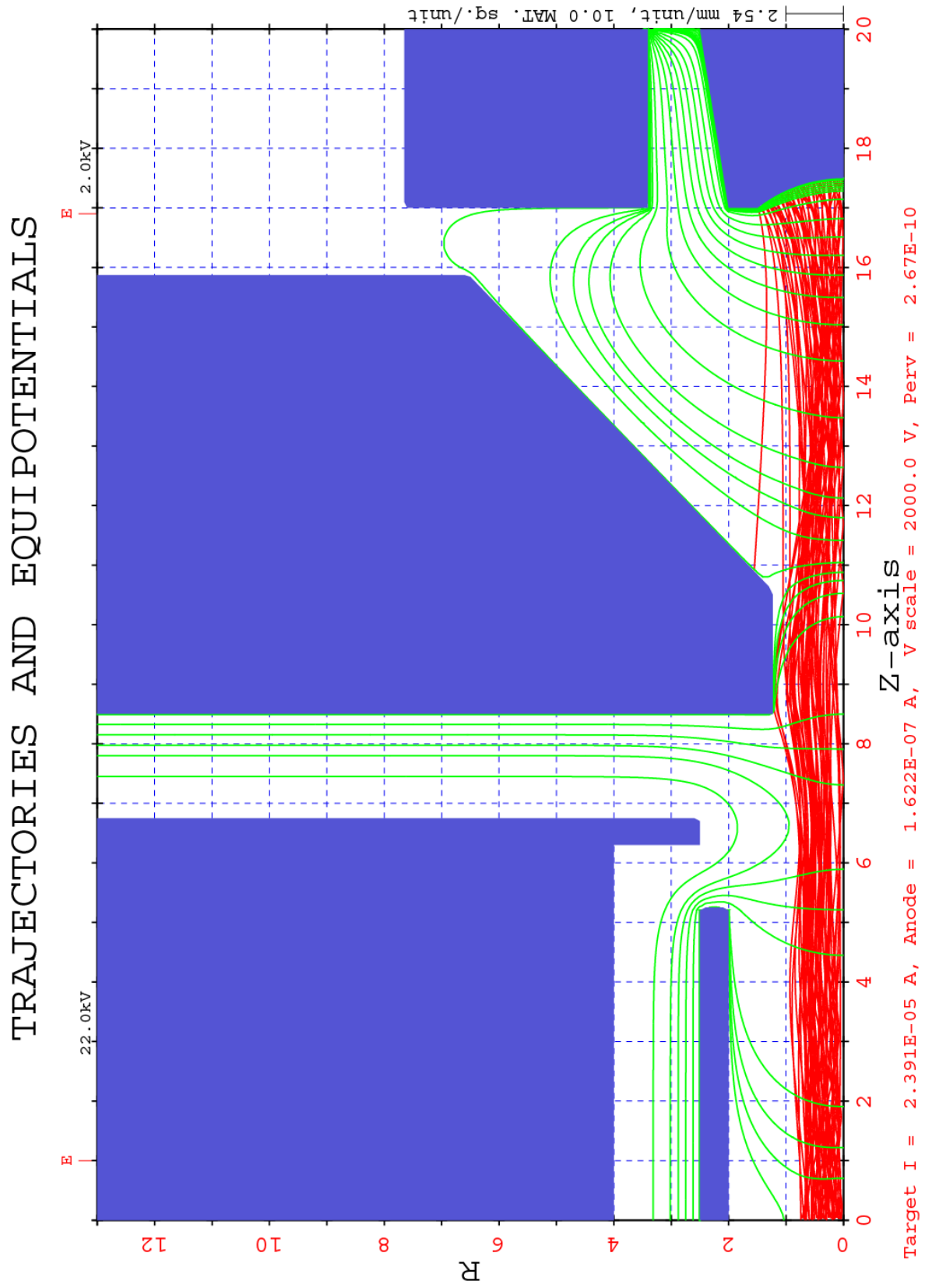The target current distribution for the secondary beam is shown in Fig. 61.

Figure 57: Secondary ion beam from the sputter electrode, with current distribution determined from the primary beam
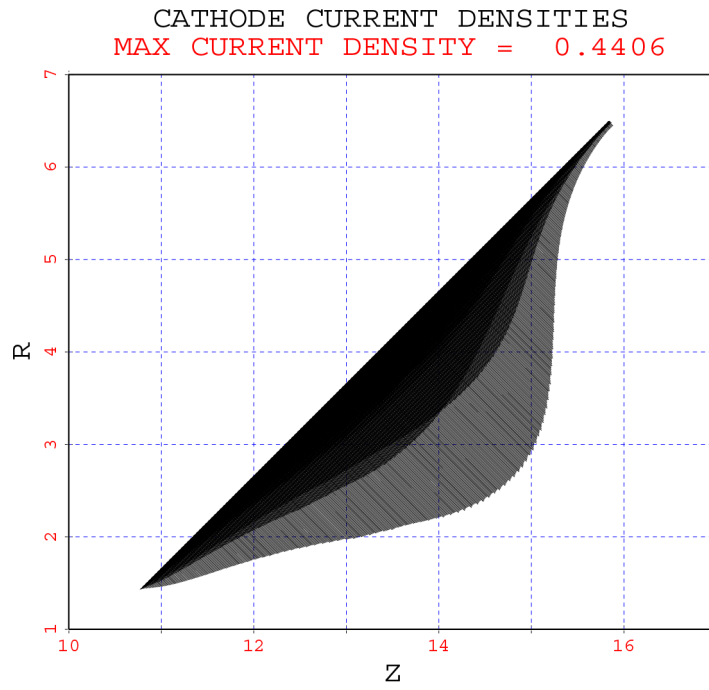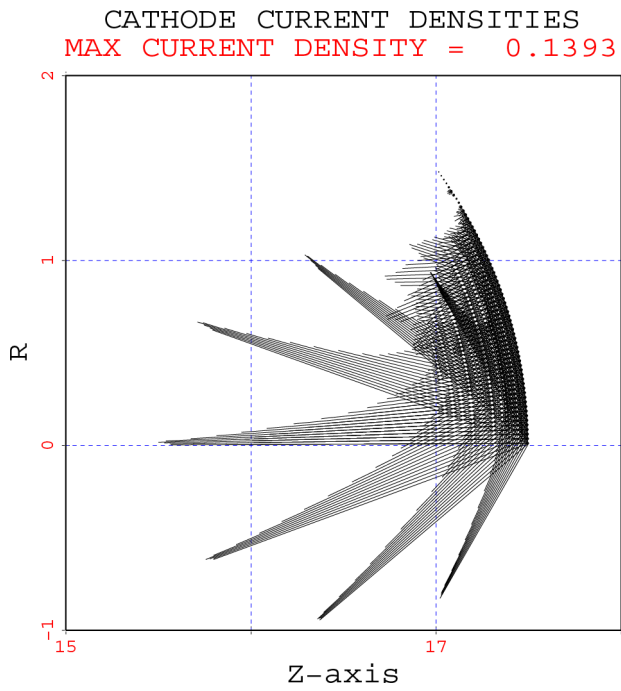
Figure 58: Distribution of emitted current of Cesium

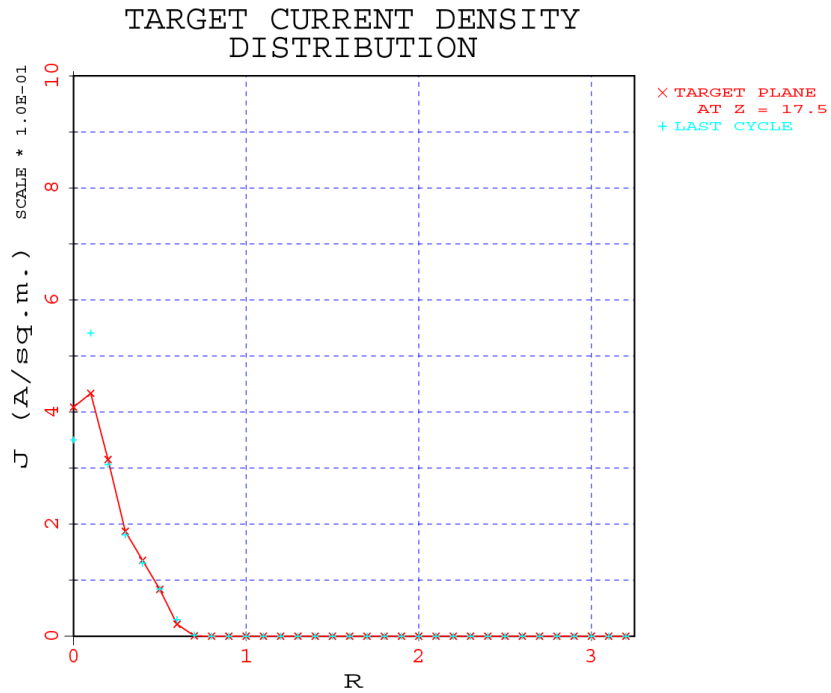Figure 59: Current distribution from secondary ion source

Figure 60: Current distribution along target electrode from primary beam of Cesium. This is also the current distribution ejected from the sputter electrode
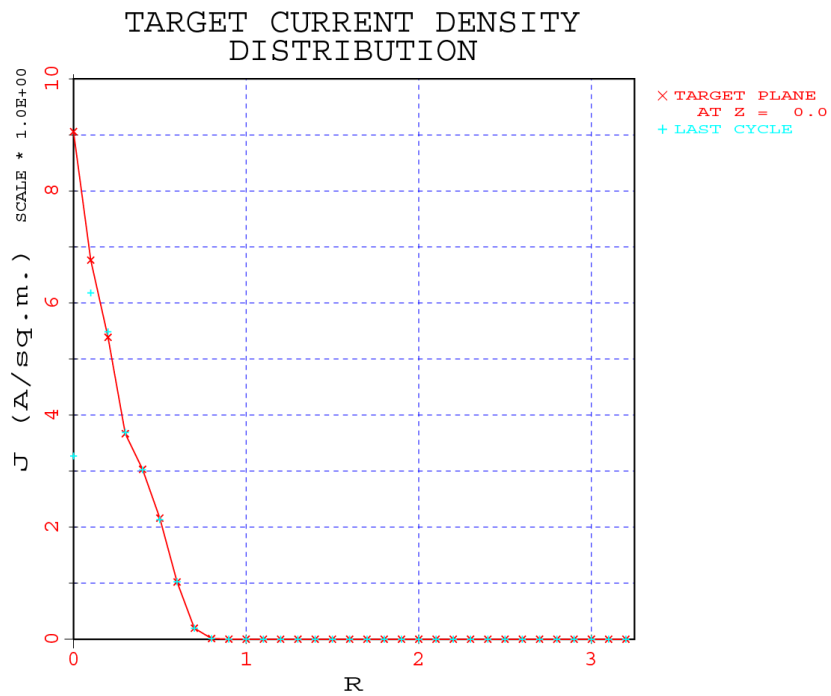

Figure 61: Exit plane current distribution for secondary beam

6.7   CRT Guns

Cathode Ray Guns present special problems. The electrons are usually emitted from a filament which is anything but axisymmetric or rectangular yet all the other components are symmetric. The electrons generated by the filament are extracted through a small hole in front of the filament, by yet a third electrode in front of the extraction plane. This electrode is generally held at around a kilovolt and also has a hole through which the electrons are extracted.

The swarm of electrons around the filament behave very much like the ions in a plasma and are probably neutralized by the ambient gas particles. PBGUNS models this phenomena by treating the swarm as a plasma. So although we are simulating an electron beam, the source is a plasma ion (or in this case electron) source. A simple CRT gun data set is shown in Table 19.

```
 99 800 201 101   0   2   0  16   0   0
  6   6   0   1  -1   1   0   0   0   0   1
    0.5500    2000.0    0.00100    0.10000 0.0000100    0.00000     1.000     4.000
  0.7000  0.0000      0.0    0.000    0.0000.000000  0.0000  0.0000
    2.500  10.000  19.000    0.000    0.000    0.010    0.000    0.000    0.000  20.000
    5 0.00250   1  11   0.0000  1.2000  1.0000  1.2000 1.00000     0.00   0   0
  0.00200    4   3   1   0   1   1  15.000    0.050   0  20.000  20.000
    2.200   1.400   0.800   1.000    0.000    0.000    0.000    0.000
PLA  1.2000   0.0000  1.2000  1.0000                                  0.06250
CYL  1.7000   1.0000
PLA  1.7000   0.5000
CYL  2.0000   0.5000
PLA  2.0000 10.0000
    3    1.00   0
PLA  6.0000 10.0000  6.0000  1.0000
CYL  7.0000   1.0000
PLA  7.0000 10.0000
  POSITIVE ION BEAM
X
```

Table 19: Simple CRT gun

In this case it should be noted that the electron beam temperature is now TPI, (Temperature of Positive Ions) and the ion temperature becomes TE (Temperature of Electrons) as the function of the ions and electrons is now reversed. In this case TE (the actual ion temp) is 0.8 eV, while the TPI is 1.0 eV.

The result of this plasma source electron beam calculation is shown in Fig. 62. A beam crossover is seen just after extraction of the beam. Most of the extracted current passes through the extractor aperture with the 2 mm hole in it. The crossover looking back from the exit plane would appear very close the extraction aperture. The current distribution at the exit plane is shown in Fig. 63.
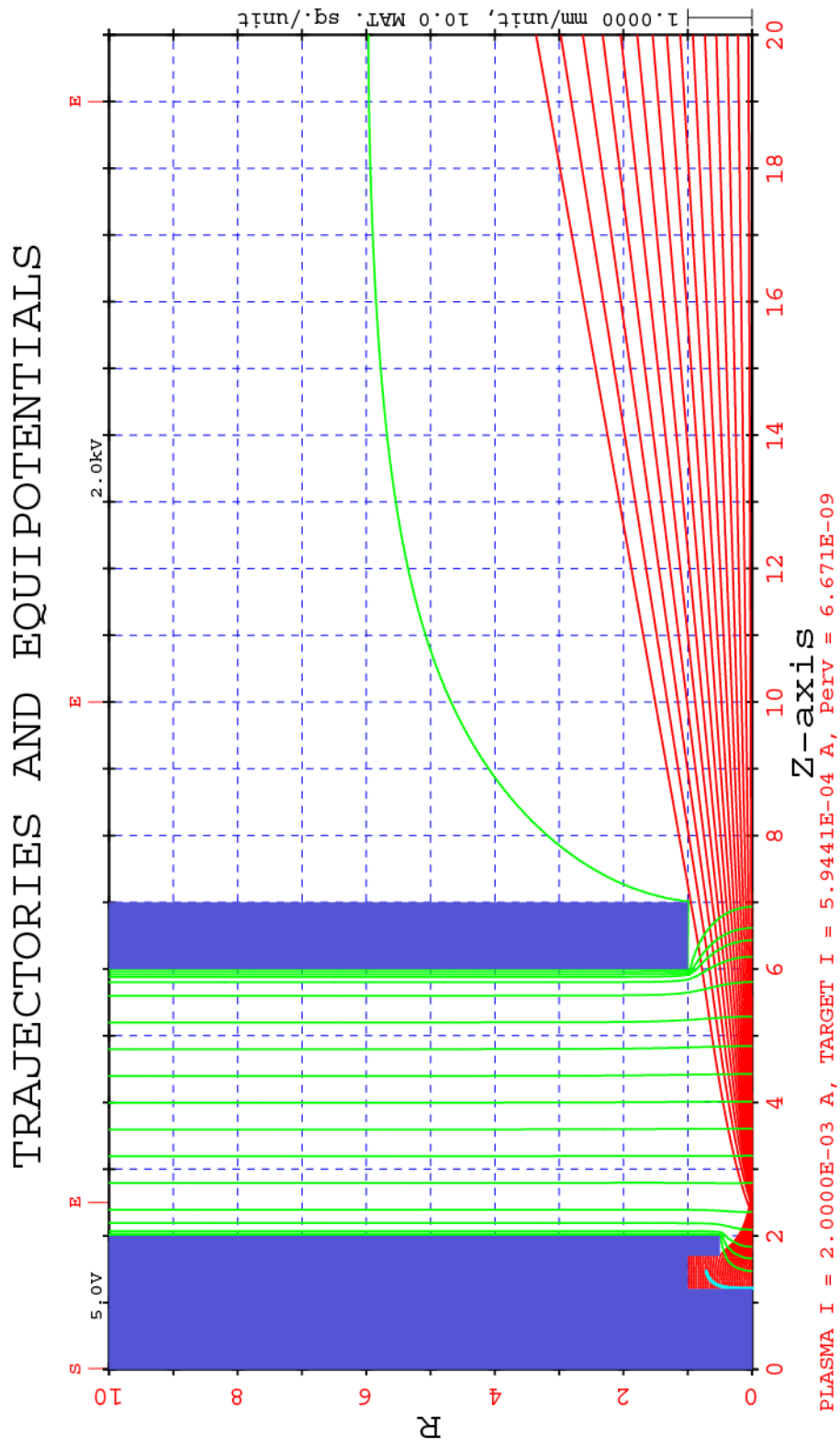
Figure 62: Cathode Ray Tube election beam extraction from an electron plasma

EXIT PLANE CURRENT DENSITY DISTRIBUTION

Figure 63: Current density distribution at exit plane of CRT gun

The details of the fine matrix which covers the plasma region are displayed in Fig. 64. Here the plasma surface (marked by the small +'s) is deep behind the 1.0 mm diameter extraction aperture, causes the actual crossover of the electron beam about 1 mm in front of the extractor plate.

The Emittance plot at the crossover is shown in Fig. 65, and the plot near the end in Fig. 66 where a nearly uniformly diverging beam is evident.

All of this is interesting but is probably not the way this gun really works. The following plots were run using a Maxwellian distribution in the plasma with an electron temperature of 1 eV using the input data given in Table 20. The first effect is to raise the current about 10 percent, this is a result of the angular spread where higher current carrying particles from greater radii now are making it out of the plasma cup. The beam is shown in Fig. 67. The

beam crossover is changed significantly as most of the particles no longer cross the axis at one spot. Indeed many do not cross the axis at all.

The fine matrix equipotentials and plasma surface, in Fig. 68, are somewhat changed from those shown in Fig. 64.

The emittance plot for the particles near the crossover point, shown in Fig. 69, are now quite complex. There are five different angles in the particle distribution with three (four) particles injected in up, down and skew directions at each point. The end result shown in Fig. 70 is a somewhat more realistic emittance shape.

The current distribution at the exit plane is shown in Fig. 71.

The injected current distribution is shown in Fig. 72. Here the line length represents the current density while the slope shows the direction at injection. Note that skew energy is included.

This still needs considerable study, but work many years ago on a similar problem suggested that the results can be quite good when compared to experimental devices.

```
 99 800 201 101    0    2    0   16    0    0
   3  46    0    1   -1    1    0    0    0    0    1
     0.5500     2000.0    0.00100    0.10000 0.0000100    0.00000      1.000      4.000
   0.7000   0.0000      0.0    0.000    0.0000.000000  0.0000   0.0000
   2.500   10.000   19.000    0.000    0.000    0.010    0.000    0.000    0.000   20.000
     5 0.00250    1   15  0.0000   1.2000   1.0000   1.2000 1.00000     0.00    0    0
 0.00200    4    3    1    0    1    1   15.000    0.050    0   20.000   20.000
   2.200    1.400    1.000    1.000    0.000    0.000    0.000    0.000
PLA   1.2000   0.0000   1.2000   1.0000                                0.06250
CYL   1.7000   1.0000
PLA   1.7000   0.5000
CYL   2.0000   0.5000
PLA   2.0000 10.0000
   3     1.00    0
PLA   6.0000 10.0000   6.0000   1.0000
CYL   7.0000   1.0000
PLA   7.0000 10.0000
  POSITIVE ION BEAM
X
```

Table 20: Input data for 1 eV Maxwellian distribution in the plasma of simple CRT gun
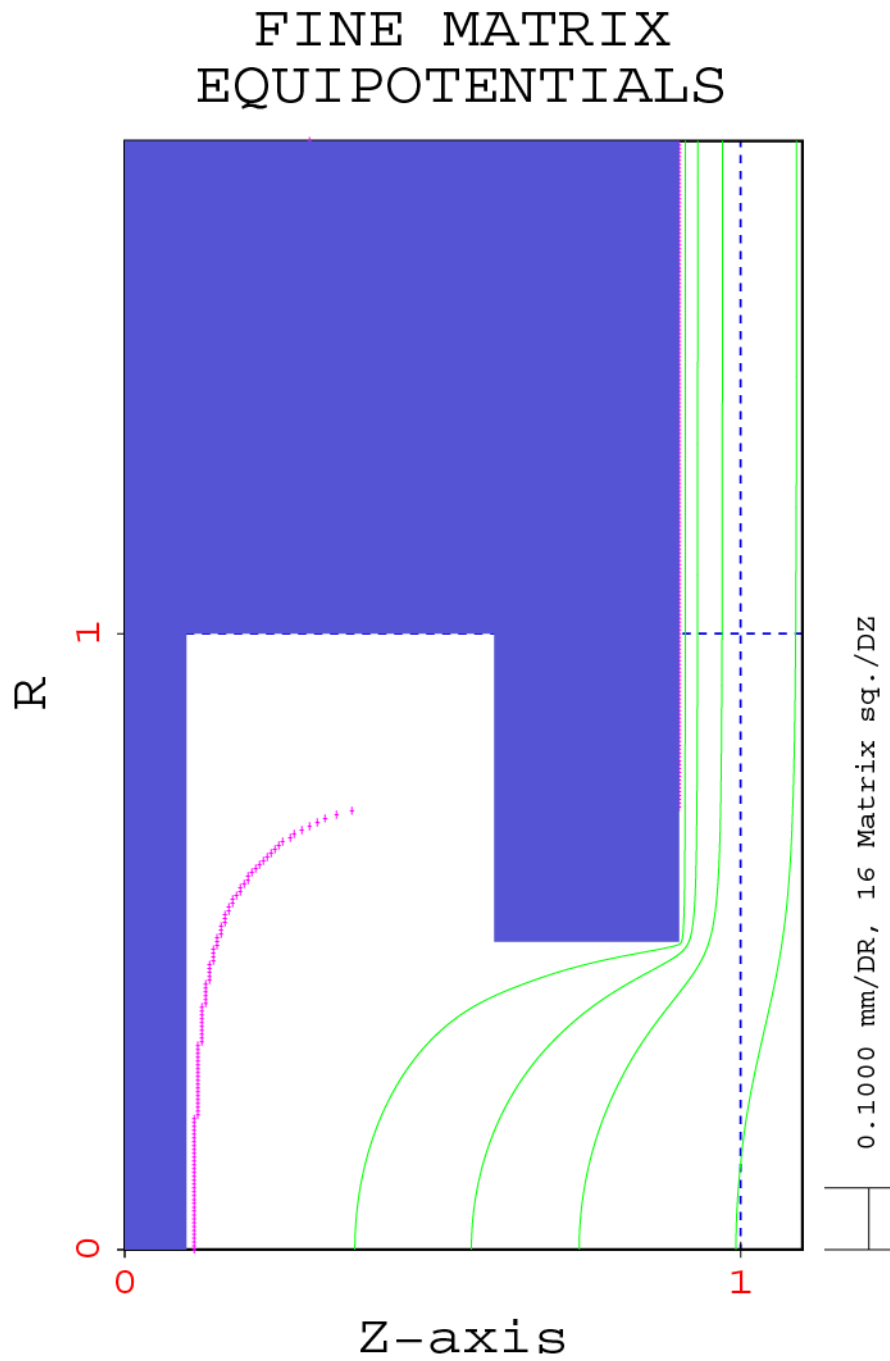
Figure 64: Equipotentials and Plasma surface (+'s) on fine matrix that covers the plasma region
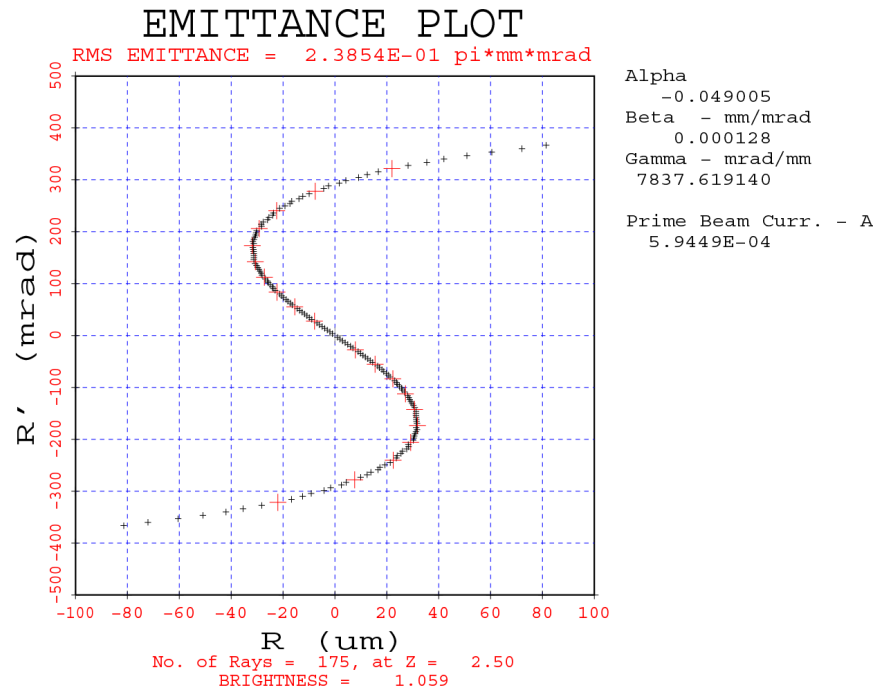
EMITTANCE PLOT

RMS EMITTANCE = 2.3854E-01 pi*mm*mrad

Alpha
  −0.049005
Beta − mm/mrad
   0.000128
Gamma − mrad/mm
 7837.619140

Prime Beam Curr. − A
  5.9449E−04

R′ (mrad)

R (um)

No. of Rays = 175, at Z =   2.50
BRIGHTNESS =   1.059

Figure 65: Emittance plot at beam crossover, z = 2.5

EMITTANCE PLOT

RMS EMITTANCE = 3.4255E-01 pi*mm*mrad

Alpha
  −64.704025
Beta − mm/mrad
   1.096107
Gamma − mrad/mm
 3820.438960

Prime Beam Curr. − A
  5.9449E−04

R′ (mrad)

R (mm)

No. of Rays = 175, at Z = 19.00
BRIGHTNESS =   0.513
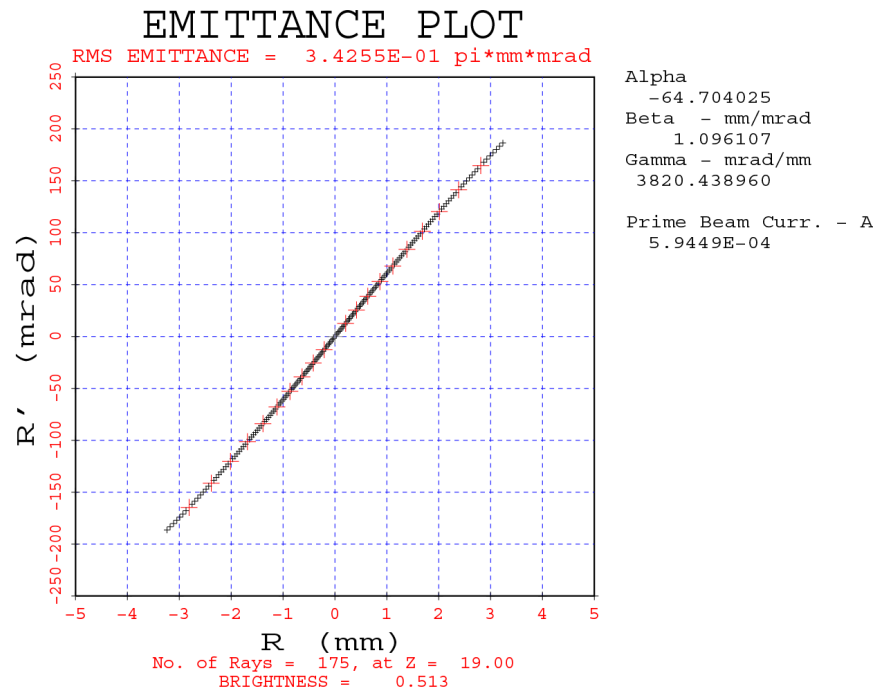
Figure 66: Emittance plot near exit of CRT electron gun

TRAJECTORIES AND EQUIPOTENTIALS
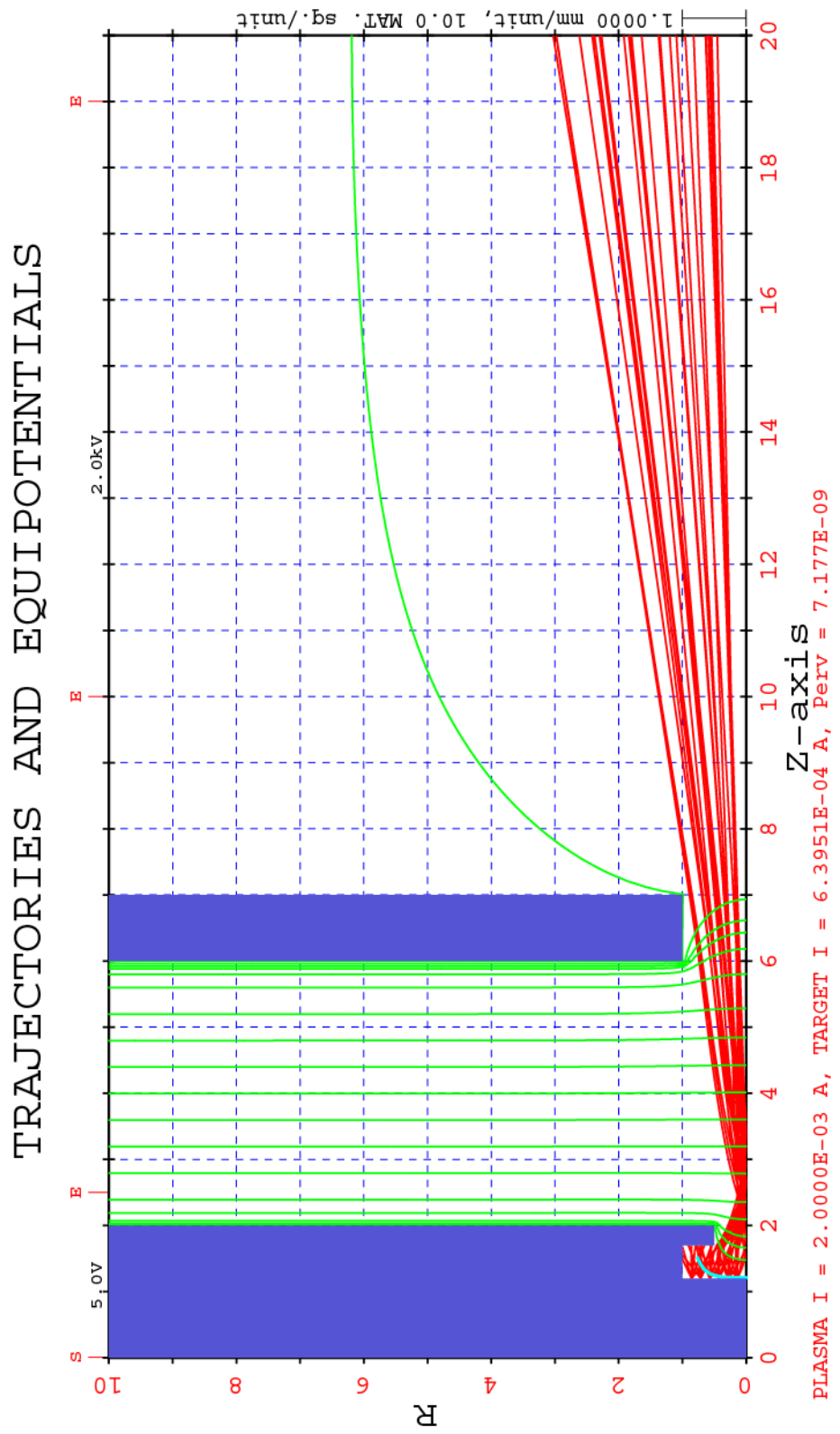
Figure 67: CRT gun with 1.0 eV Maxwellian thermal distribution
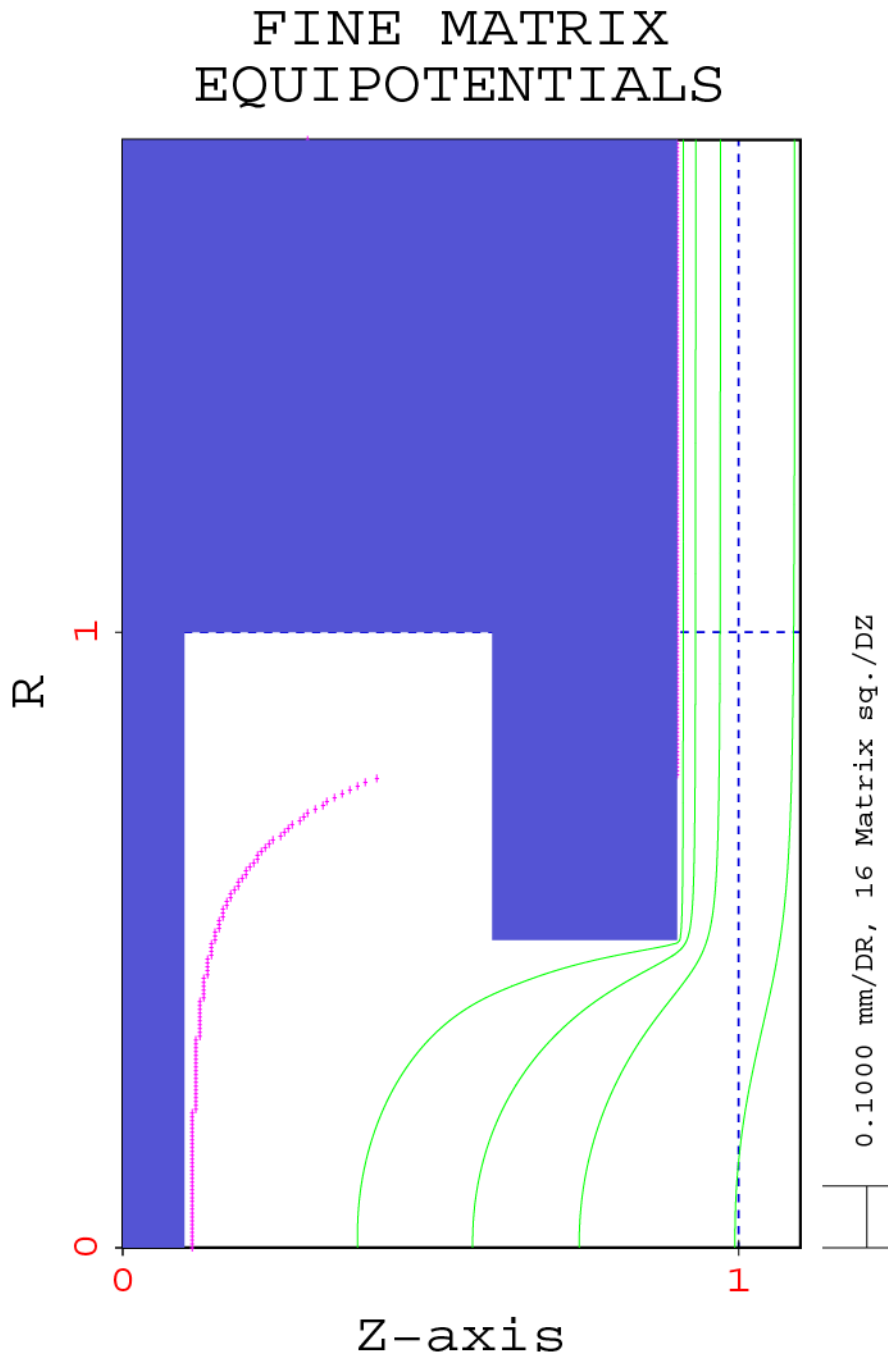
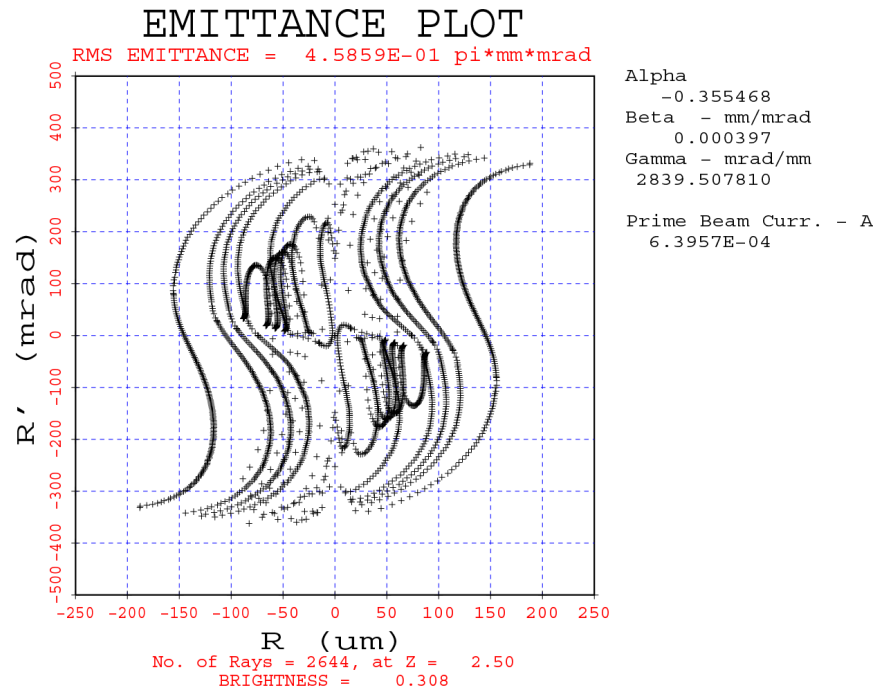Figure 68: Fine matrix equipotentials over the plasma with Maxwellian injection

Figure 69: Emittance plot near crossover point for thermal spread beam
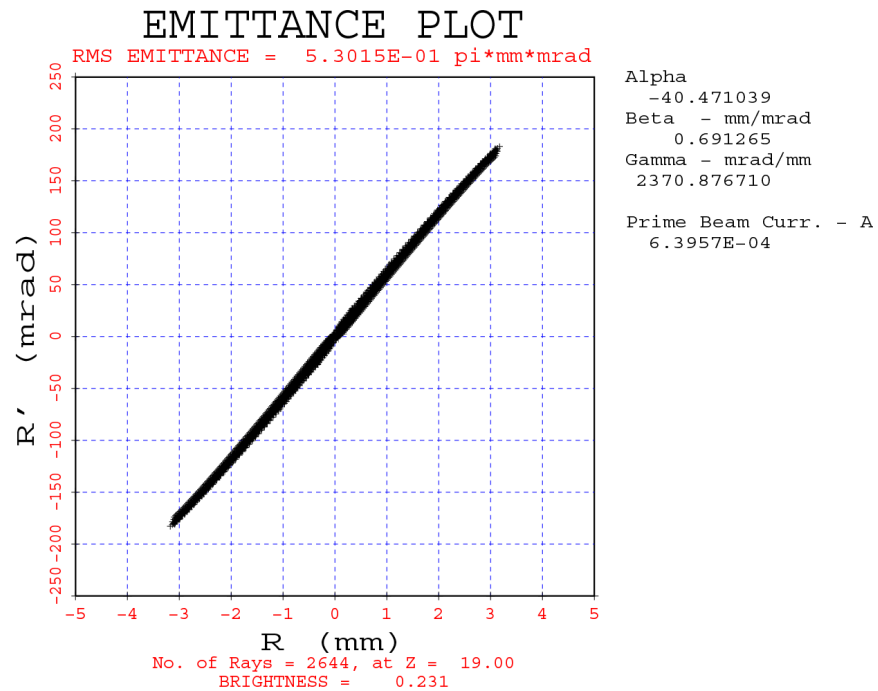

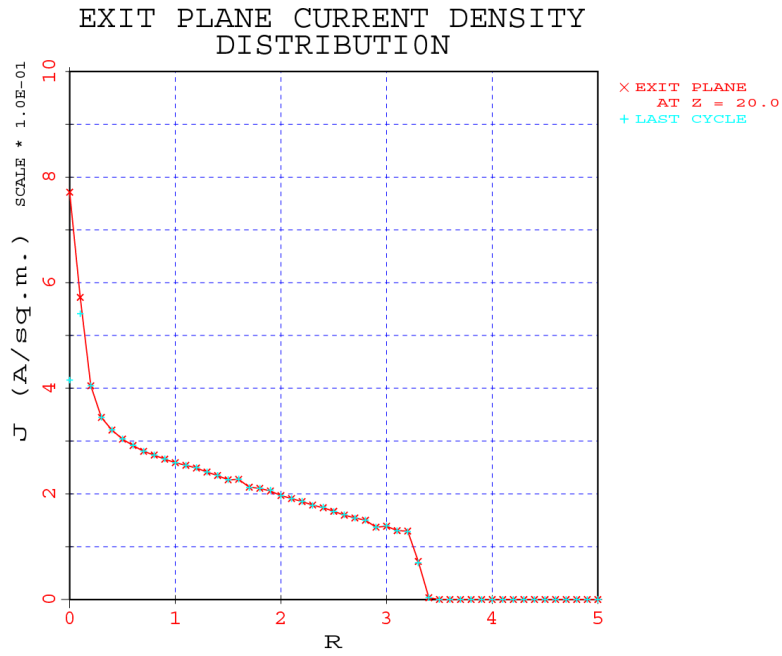Figure 70: Emittance plot near exit plane including Maxwellian distribution in the plamsa

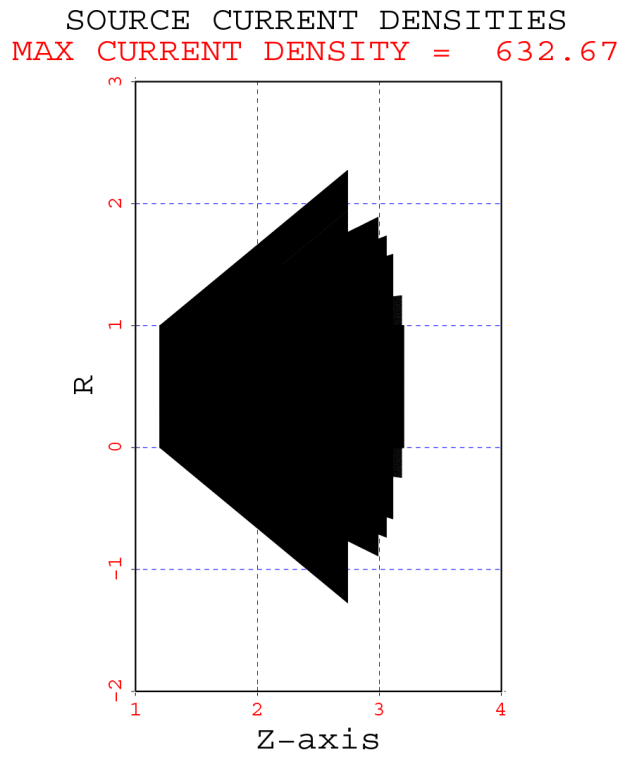Figure 71: Exit plane current distribution with thermal spread in the plasma

Figure 72: Current distribution at injection plane

6.8 Ion Beam Extraction From a Plasma

6.8.1 Negative Ion Beam Extraction From a Plasma

The input data for a negative beam extraction system is shown in Table 21. Here a negative ion beam is being extracted with 25 percent stripping (25 percent of the negative ions lose their charge in the extraction region) of the extracted ions. No angular distribution of particles is employed on this initial run.

```
100 700 121   51    0    2    0   16    0    0    0    0    0    0    0    0    0    0    0
  6  12    1    1   -1    1    0    0    0    0    1    0    0    0    0    0    0    0    0
  0.30E+00     35000.0    0.00100    0.10000 0.0000600    0.00000    2000.0    10.0000
  1.0000 30.0000  0.0000   0.0000   7.5000 0.01000                              0.00
  10.000  11.900   0.000    0.000    0.000    0.000   0.000   0.000   0.000  12.000
  6 0.00005    1   11 0.00000 0.35000 1.69690 0.35000 1.00000 0.00000    0    0
  0.12200    3    3    1    0    1    2   20.000   0.100    0
  0.800    0.500  10.000    2.000    8.000    2.000   0.250   1.200     0.      0.
PLA  0.3500   0.0000   0.3500   1.7000                              0.06250
CYL  0.5000   1.7000
PLA  0.5000   1.5000
CYL  0.6000   1.5000
TCN  0.7000   1.6000
PLA  0.7000   5.0000
   5      1.0    0
PLA  5.0000   5.0000   5.0000   1.7000
SPH  5.2000   1.5000                   5.2000   1.7000   0.2000
CYL  6.1000   1.5000
TCN  6.5500   2.5000
CYL 12.0000   2.5000
 NIB IF = 16,   10 EV ELECTRONS,   10 EV IONS SPACING = 0.0625  BETA = 1.0
X
```

Table 21: Input data for negative ion beam extraction simulation.

The negative ion beam extraction is shown in Fig. 73. The equipotentials in Fig. 73 are on the regular voltage mesh, and are not indicative of the equipotentials in the fine mesh region (as seen later in Fig. 80, which includes the effects of the background plasma).

There is a 16 to 1 fine matrix ratio, which is a somewhat larger ratio than is used typically for electron beams. The program determines the plasma surface automatically, an initial value is specified (0.500) to give the program an initial starting point. The end of the fine mesh region is set at 0.800. The extraction and scaling voltage is 35 kV with an injected ion current of 0.122 A.

The electron temperature in the plasma is 10.0 eV, the ion drift energy is 10 eV and

negative ion temperature is 4 eV (used for thermal distributions below), the background positive ion temperature is 2 eV and the positive to negative ion ratio is 8.

The neutralization region starts at z = 7.5 and is fixed at this point, the best compromise for a negative ion beam since traps are seldom used for negative ion beams.

Fig. 74 shows the same run, but with a Maxwellian beam distribution. The beam is seen to be somewhat larger than the non-thermal beam. The effect on the exit plane current distribution for negative ion beams with and without thermal spread (Maxwellian) is shown in Figs. 75 and 76, where the current is spread more uniformly over the beam by taking account of the angular distribution. The emittance plots of the two negative ion beams, with and without a thermal spread, are shown in Figs. 77 and 78, respectively.
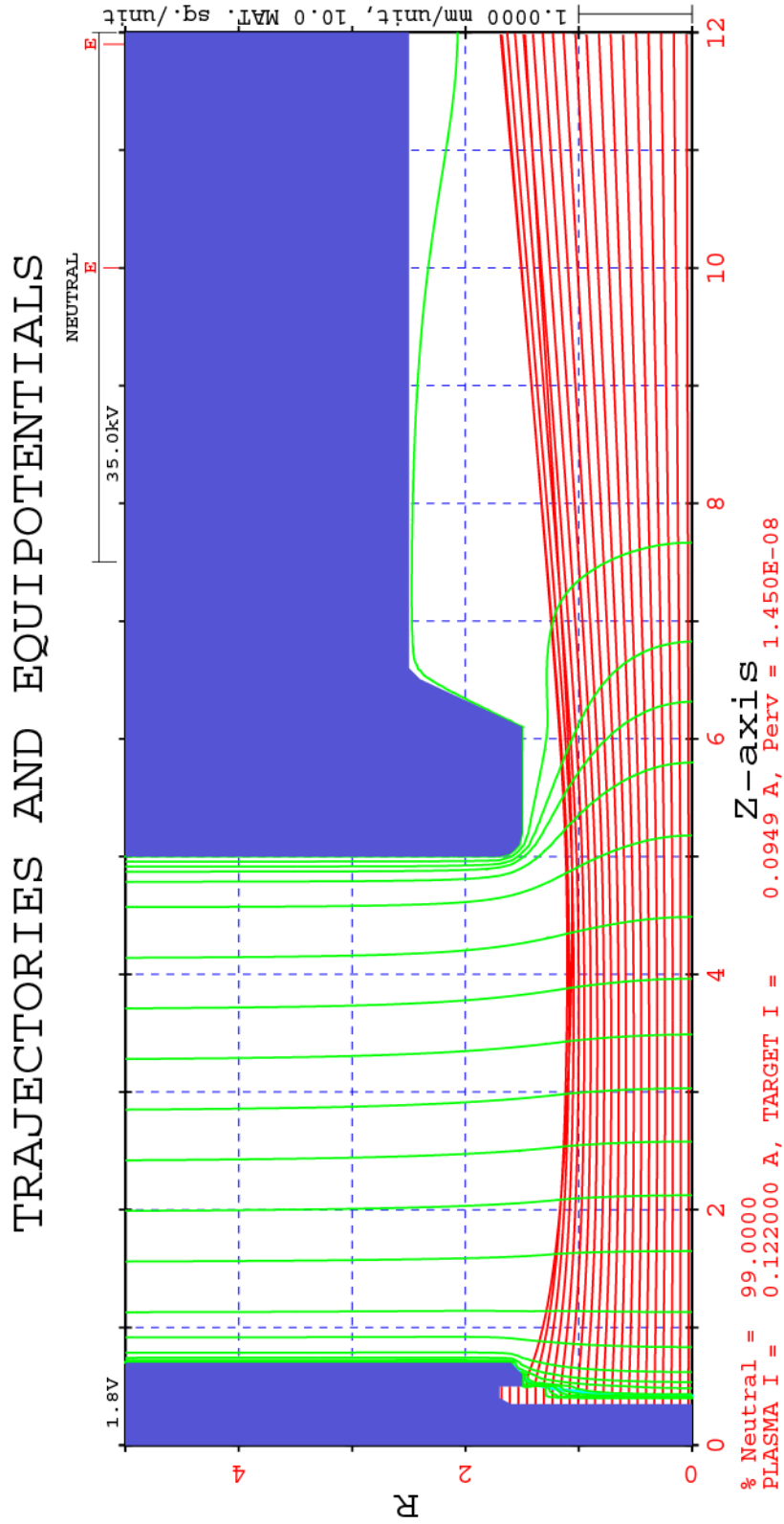
Figure 73: Negative ion beam extraction system
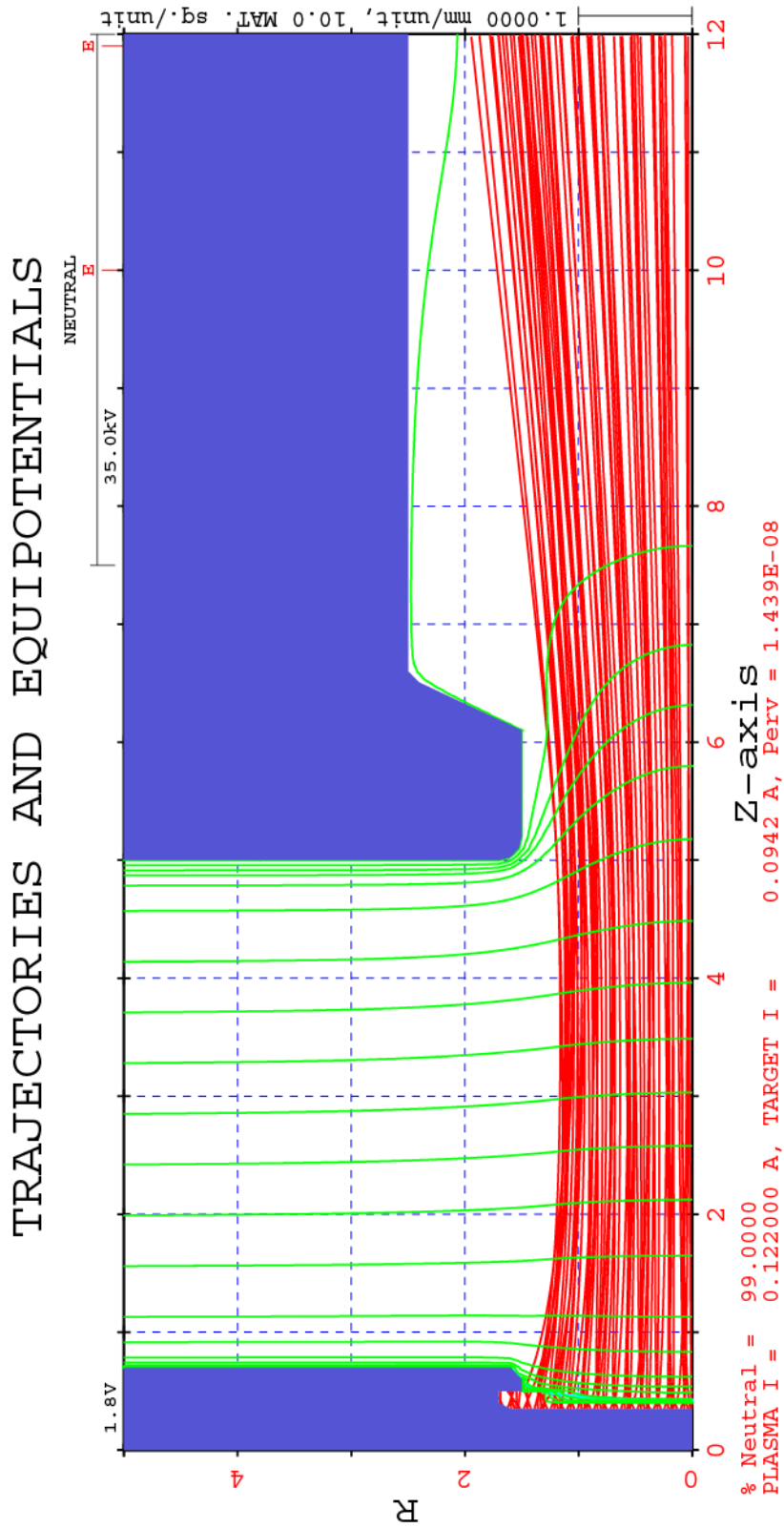
Figure 74: Negative ion beam with uniform Maxwellian current distribution
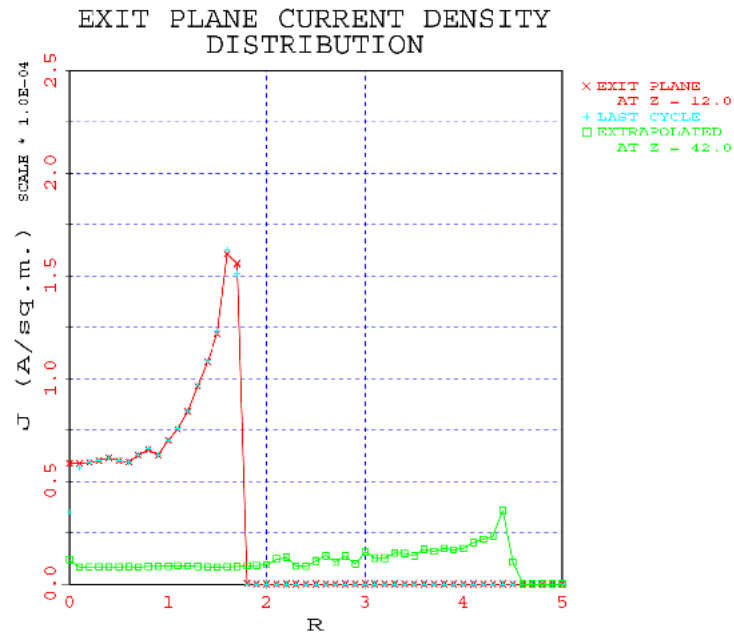
Figure 75: Exit plane current density plots for negative ion beams for zero temperature ions
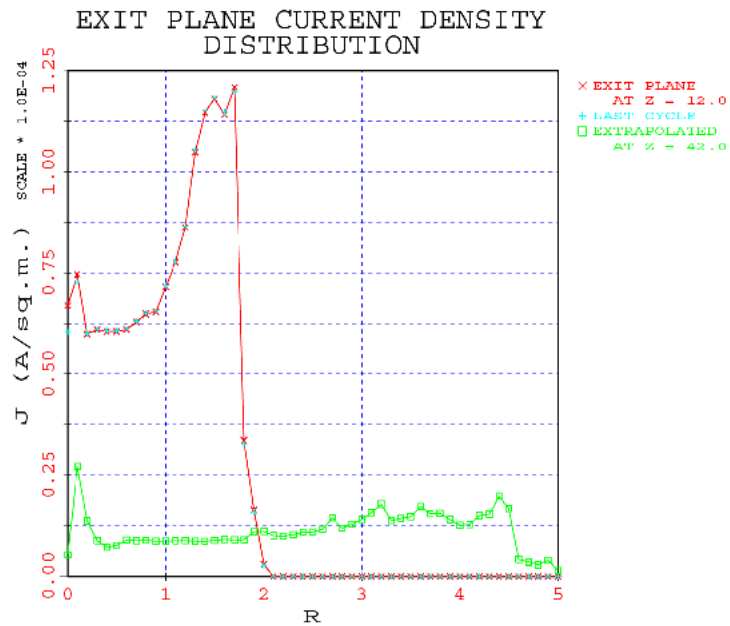
Figure 76: Exit plane current density plots for negative ion beams with thermal spread

Figure 77: Emittance plot at exit plane for the case of an ion source with a zero temperature

Figure 78: Emittance plot at exit plane for the case of an ion source with a 2 eV Maxwellian temperature distribution

6.8.2   Positive Ion Beam Extraction From a Plasma

A run was made with similar data to that for the negative ion case discussed above, with positive ions and no stripping. Here it was necessary to make the plasma much deeper for the case of positive ions. The input data for this extraction system is shown in Table 22. The run for the positive beam case is shown in Fig. 79.
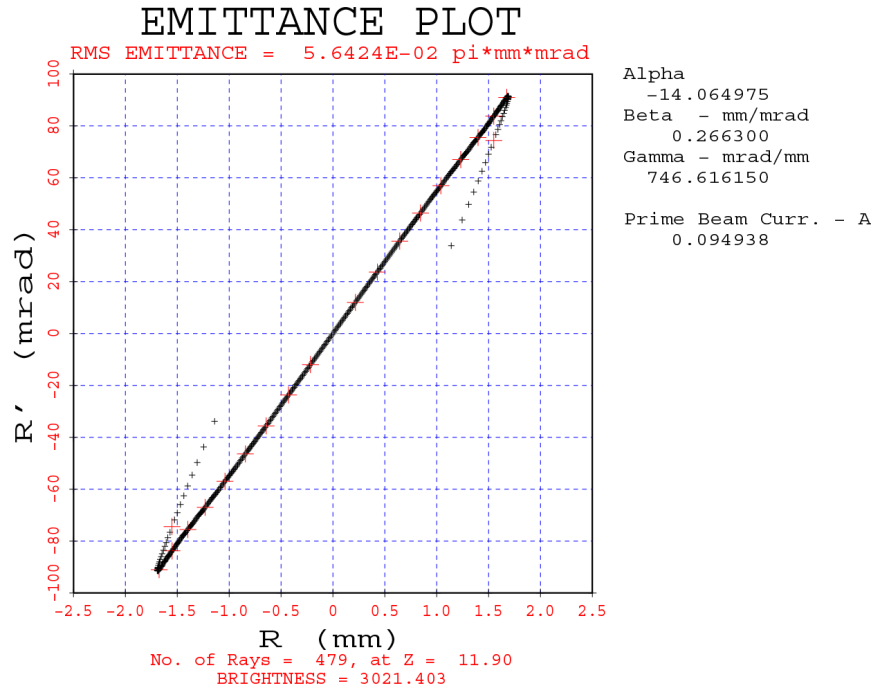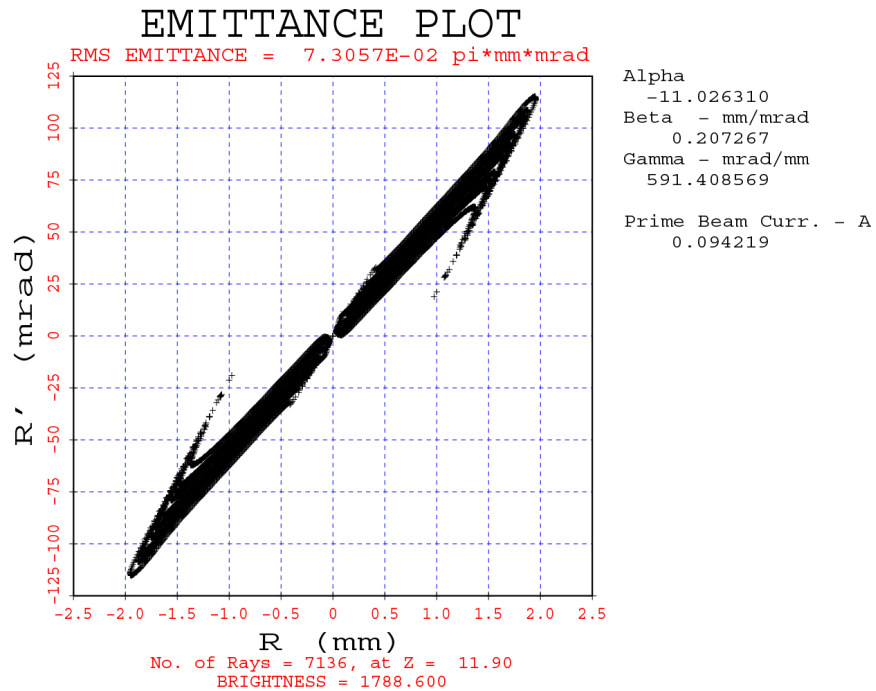
```
100 900   81   41    0    3    0   10    6    0    0    0    0    0    0    0    0    0    0    0
   3  16    0    1   -1    1    0    0    0    0    2    0    0    0    0    0    0    0    0 0.0
    0.3000    35000.0    0.00100    0.12500 0.0000600    8.00000  1840.000    10.000
  1.0000  0.0000      0.0    0.000    9.000 0.01000   0.0000   0.0000    1.00
  4.000   8.000    9.750    0.000    0.000    0.000    0.000    0.000    0.000  10.000
  6 0.00005    1   12      0.0    0.20    1.7    0.20    1.0
 0.16100    0    3    1    0    1    2  10.000    0.100    0    0.000    0.000
  0.750    0.400  10.000    2.000    8.000    0.000    0.000    2.000
  1840.    3640.
 0.9500   0.0500
 10.000   10.000
PLA   0.2000   0.0000   0.2000   1.7000                                    0.1000
CYL   0.4000   1.7000
PLA   0.4000   1.5000
CYL   0.5100   1.5000
TCN   0.7000   1.6900
PLA   0.7000   5.0000
    5      1.0
PLA   5.0000   5.0000   5.0000   1.7000
SPH   5.2000   1.5000                  5.2000   1.7000   0.2000
CYL   6.3000   1.5000
SPH   6.5000   1.7000                  6.3000   1.7000   0.2000
PLA   6.5000   5.0000
    4   0.9429
PLA   7.6000   5.0000   7.6000   1.7000
CYL   8.6000   1.7000
PLA   8.6000   2.7000
CYL 10.0000   2.7000
 POSITIVE ION BEAM   IF = 16,   10 EV ELECTRONS,   10 EV IONS BETA = 1.0
    7
    0.000    0.800    3.000    5.000    6.000    9.000   10.000   0.0000
    0.200    0.200    0.000    0.000    1.000    1.000    0.000   0.0000
X
```

Table 22: Input data for positive ion beam extraction simulation
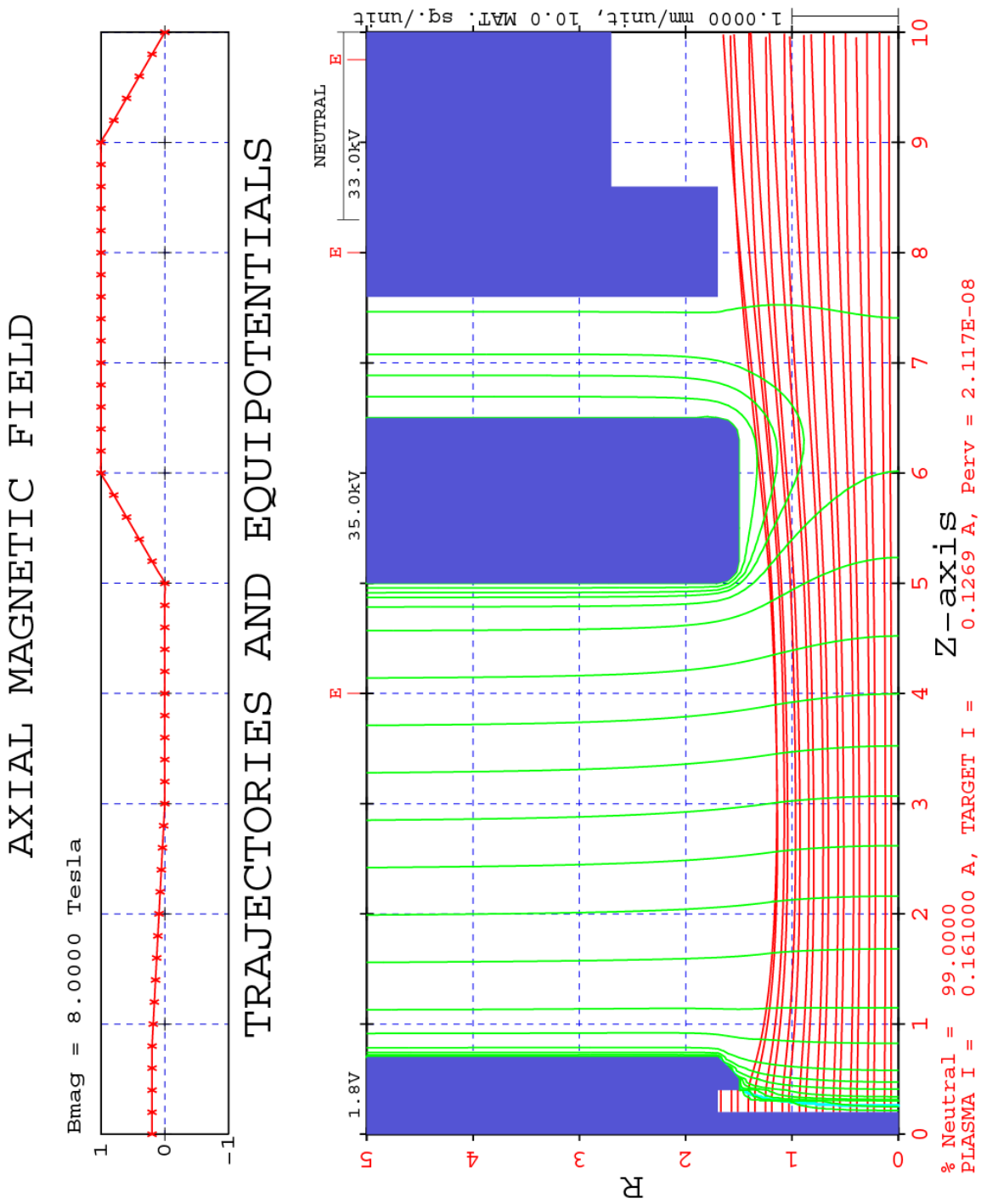
Figure 79: Positive ion beam extraction system with magnetic lens

6.8.3   Negative and Positive Ion Beam Extraction Comparison

The fine matrix equipotentials for both negative and positive ions are presented in Fig. 80. The effect of using positive ions and no stripping on the plasma surface is quite striking. The magnetic field shown was added merely to show the capability and has no effect in the extraction region.

The effect of taking the background electrons, positive ions and stripping into account has a striking effect on the formation of the plasma surface for negative ions extracted from a plasma. All the effects seem to move the plasma surface forward and cause the beam to become more divergent, which is the general effect that has been reported. Unfortunately we do not have experimental data to compare the effects of the different parameters on the results.

Figure 80: Fine matrix equipotentials for negative ion beam, NIB with Maxwell Distribution, and Positive ion beam

6.8.4   Cyclotron Resonance (ECR) Source

Ion sources with very low ion energies (1.0 eV), such as ECR (Electron Cyclotron Resonance) sources, present special problems. The ions have such a low energy that 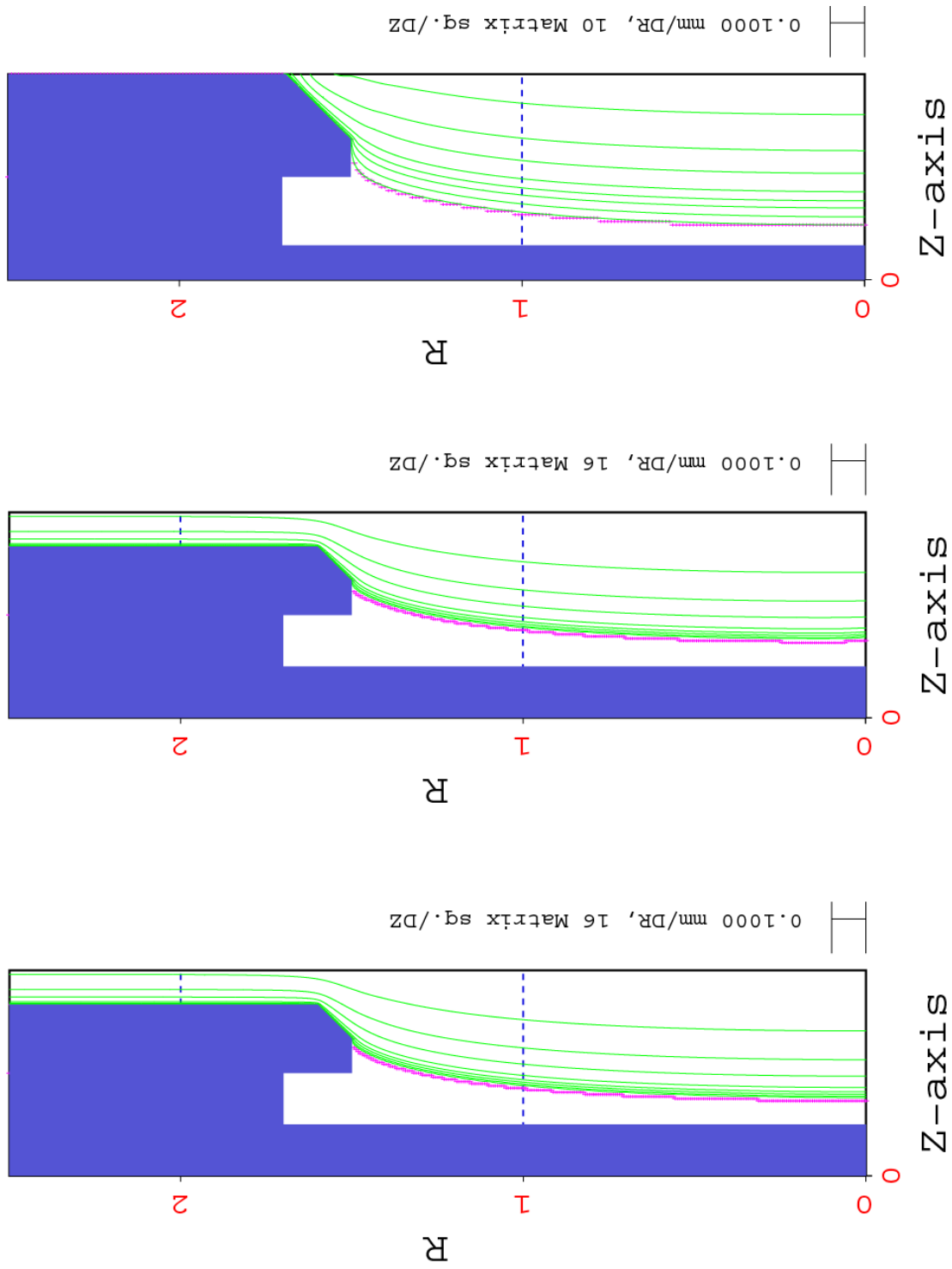they are easily deflected by any electrode near them. If this deflection is across the aperture (or worse yet, backward) this can cause instabilities to develop in the plasma or at it's surface.

It may be necessary to increase the energy of the ions and the fineness of the mesh (fine mesh for sure, regular mesh possibly), and decrease the damping factor, BETA. Any time the ion energy gets close to 1.0 eV, a fine mesh 16 to 20 times finer than the regular mesh is recommended.

The better the focusing and shape of the plasma surface, the lower the initial energy may be, however, to stabilize the problem the initial energy may need to be increased.

6.8.5   Emittance Plots for Multi Ion Beams

The emittance calculations and plots have been modified for multiple ion mass beams. The plots now sort the particles into the primary (first) beam and all other masses that are injected. On the screen the first mass is plotted using the white +'s as before, all the remaining masses are plotted using red x's.

Note that if there are no magnetic fields the plot will be nearly all red as the secondary beams will over write the primary beam. In a black and white printer plot the red usually plots as near black and the white is printed as black. If the plot is not totally black you can sometimes distinguish the +'s from the x's.

Without a magnetic field all the masses will follow essentially the same paths.

For those running ECR sources in particular, note that there is always a small effect in the ion source from the magnetic field. A tenth of a Tesla produces a small but significant effect, while a half a Tesla will produce very significant effects for hydrogen beams. Higher fields produce stronger effects, and will cause lower masses to diverge in the beam more than higher masses.

The cause of the effect is a term in the radial acceleration which causes the beam to rotate as it crosses magnetic flux lines. As the beam exits the magnetic field this azimuthal motion is transformed into an outward radial motion. There is a fringe benefit in that the particles will not cross the axis due to the skew motion.

The magnetic field in the source will always cause the beam to diverge more than it would without the magnetic field. The effect should be more visible near the outer edge of the beam.

An ion beam with two masses and an applied magnetic field is shown in Fig. 81. The

separation of the two masses is not obvious in this plot. The separation of the particles is obvious in the emittance plot shown in Fig. 82. The +'s represent the primary beam and the x's the second particle mass. The primary beam is seen to be bigger than the secondary ions because of the mass differences.

Run the data file in Table 23 (below) to see the effect.

```
 99 800 201  61   0   3   0  16   6   0   0   0   0   0   0   0   0   0   0   0
  2  16   0   1  -1   1   0   0   0   0   2   0   0   0   0   0   0   0   0 0.0
    0.3000   60000.0    0.00254   0.10000 0.0000600    0.50000  1840.000    10.000
  0.6000 30.0000      0.0   0.000   9.0000.050000  0.0000  0.0000    0.00
  8.000  10.000  19.900   0.000   0.000   0.000   0.000   0.000   0.000 20.000
  7 0.00005   1  11 0.00000 0.50000 1.70000 0.50000 1.00000    0.00   0   0
 0.09500   0   3   1   0   1   2  10.000   0.100   0   0.000   0.000
  1.000   0.700  10.000   2.000   8.000   0.000   0.000   0.000
  1840.   3672.
  0.9500  0.0500
  10.000  10.000
PLA   0.5000   0.0000   0.5000  1.7000                              0.0625
CYL   0.5500  1.7000
PLA   0.5500  1.5000
CYL   0.6000  1.5000
TCN   1.0000  3.4000
CYL   3.7000  3.4000
PLA   3.7000  6.0000
  3     1.0   0
PLA   6.8000  6.0000  6.8000  2.0000
CYL   8.3000  2.0000
PLA   8.3000  6.0000
  4  0.9167   0
PLA   9.0000  6.0000  9.0000  2.0000
CYL 10.0000  2.0000
PLA 10.0000  2.9900
TCN 20.0000  3.0000
  IF = 16,  10 EV ELECTRONS,  10 EV IONS SPACING = 0.0625  BETA = 1.0
  4
  0.000   1.000   6.000  20.000
  1.000   1.000   0.000   0.000
X
```

Table 23: ECR ion source with two masses and a strong (0.5 Tesla) magnetic field in the ion source region

AXIAL MAGNETIC FIELD

Bmag = 0.5000 Tesla

TRAJECTORIES AND EQUIPOTENTIALS

2.54 mm/unit, 10.0 MAT. sq./unit

NEUTRAL

55.0kV

60.0kV

3.0V

Z-axis

% Neutral =   95.0000
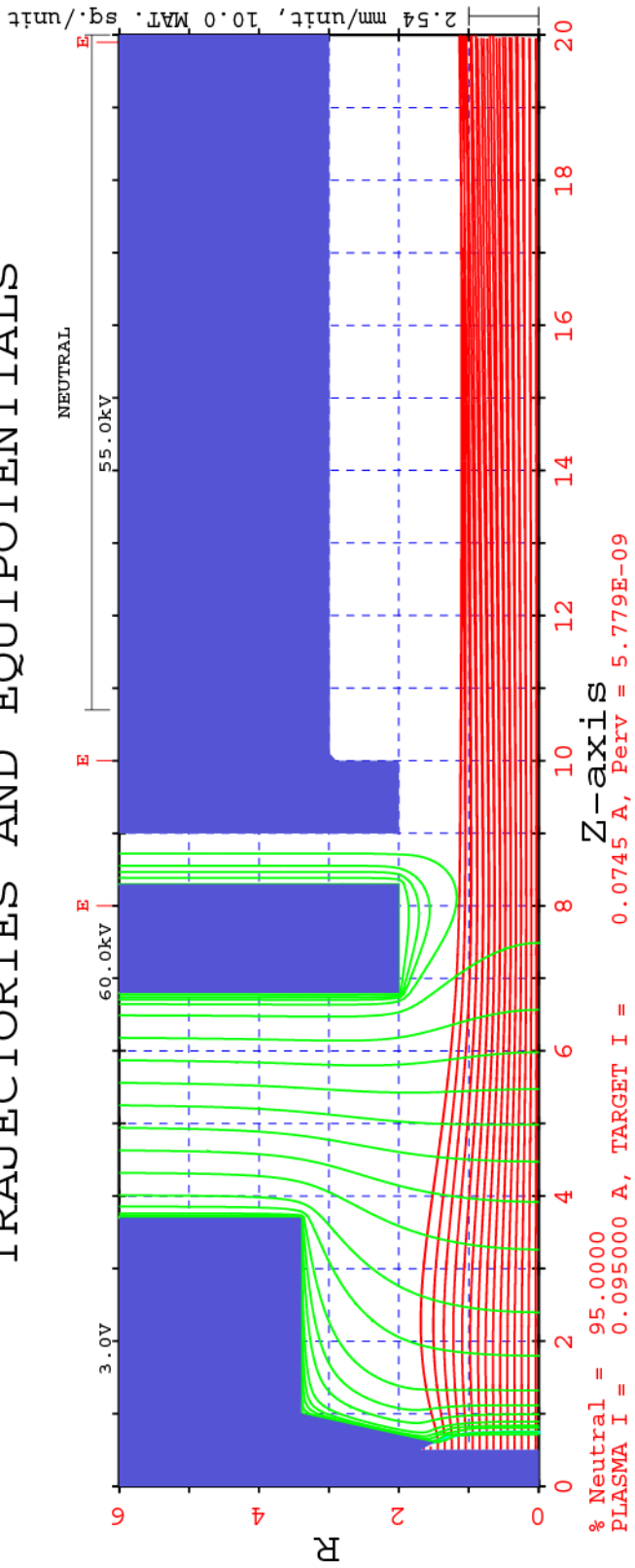PLASMA I =   0.095000 A,   TARGET I =   0.0745 A, Perv = 5.779E-09
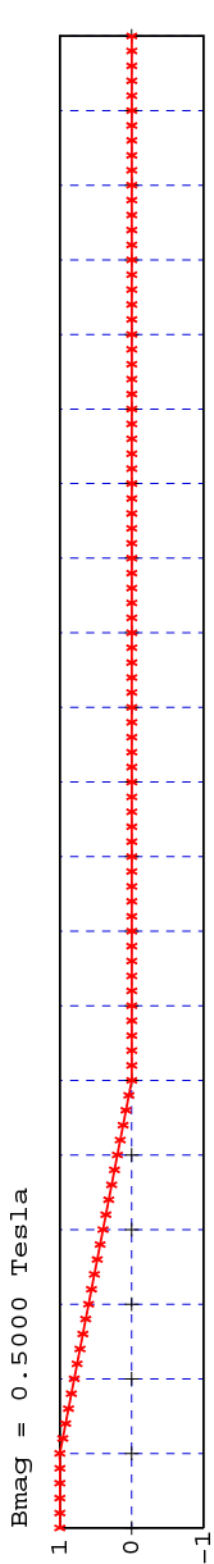
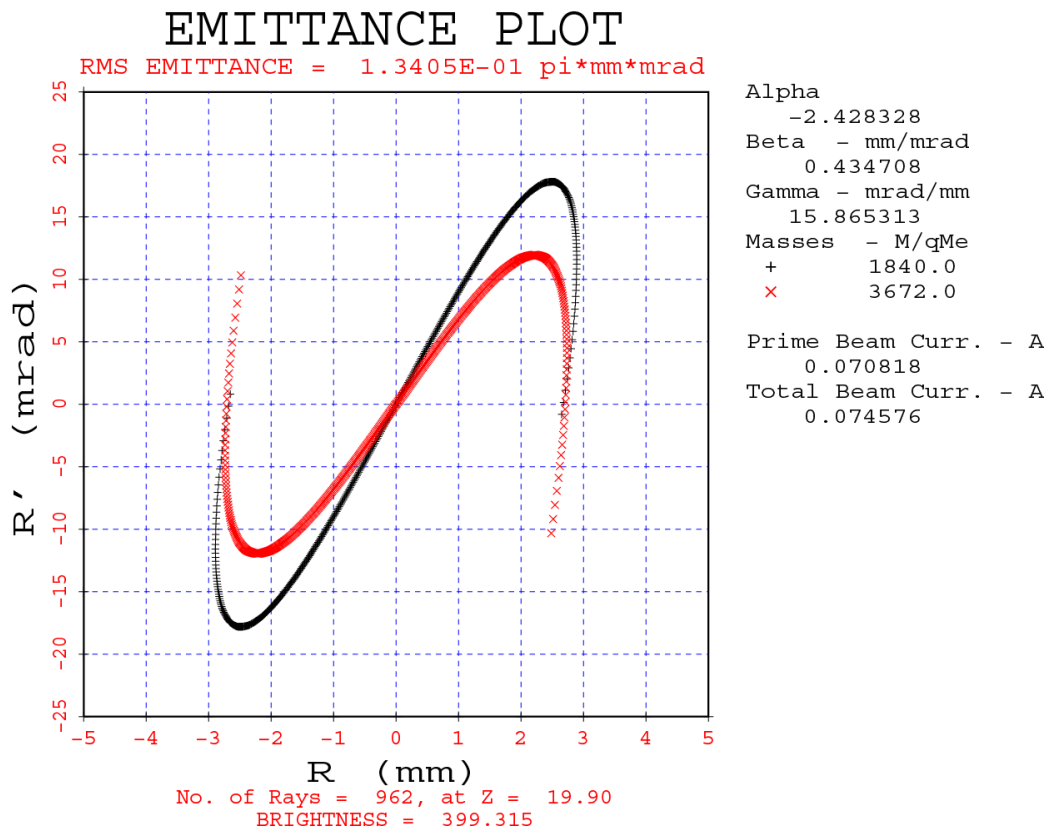Figure 81: ECR source ion beam with two masses and rather high magnetic field

Figure 82: Emittance plot for two ion mass beam with magnetic field on plasma source

6.9 Injected Beams in a Drift Space and Neutralization

6.9.1 Injected Beam Through a Lens

It is now possible to inject a simple beam into a drift, lens, accel, or decel region. Table 24 is the input data for a simple lens using an injected beam. An ion beam with a uniform current distribution is injected at the left edge using a breakpoint method, and the particles are traced through the lens. This is a simple problem generated interactively in about an hour on the computer. Note that there are electron traps at both ends of the lens to keep the ion beam neutralized as it enters and leaves the lens.

Fig. 83 shows the trajectories and equipotentials for the above data set and Fig. 84 is the emittance plot near the exit plane.

```
  99 800 721 201    0   5   0   4   0   0   0   0   0   0   0   0   0   0   0   0
   3  11   0   1  -1   1   0   0   0   0   1   0   0   0   0   0   0   0   0 0.0
 0.0000000    55000.0    0.00100    0.20000 0.0000010    0.00000    1836.0  0.52E+05
  1.0000  0.0000     0.1  30.000 100.000 0.01000  0.0000  0.0000
 10.000  80.000 -110.00 140.000   0.000   0.000   0.000   0.000   0.000 144.000
   3 1.03640   0  18 0.00000 0.00000 4.00000 0.00000 0.00000    0.00   2   0   0
  0.000   4.000
  1.000   1.000
  0.000   0.000
PLA 30.5000 40.0000 30.5000  7.0000
CYL 40.0000  7.0000
PLA 40.0000 40.0000
   4     0.0
PLA 48.0000 40.0000 48.0000 21.8000
TCN 62.5000 16.8000
TCN 77.0000 21.8000
PLA 77.0000 40.0000
   3  1.0364
PLA 85.0000 40.0000 85.0000  7.0000
CYL 94.5000  7.0000
PLA 94.5000 40.0000
  4   0.9455
CYL  0.0000 20.0000 15.0000 20.0000
PLA 15.0000  7.0000
CYL 28.0000  7.0000
PLA 28.0000 40.0000
  4   0.9455
PLA 97.0000 40.0000 97.0000  7.0000
CYL110.0000  7.0000
PLA110.0000 20.0000
CYL144.0000 20.0000
LENS injected beam
X
```

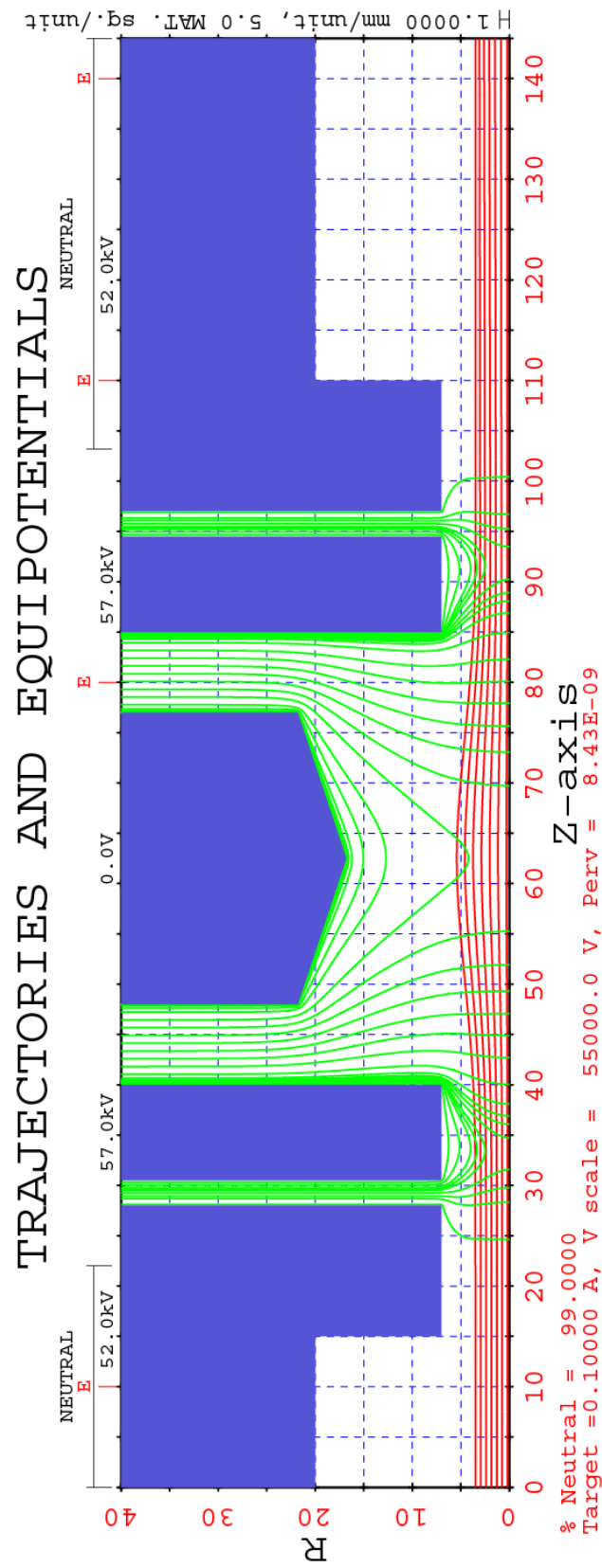Table 24: Lens simulation using injected beam

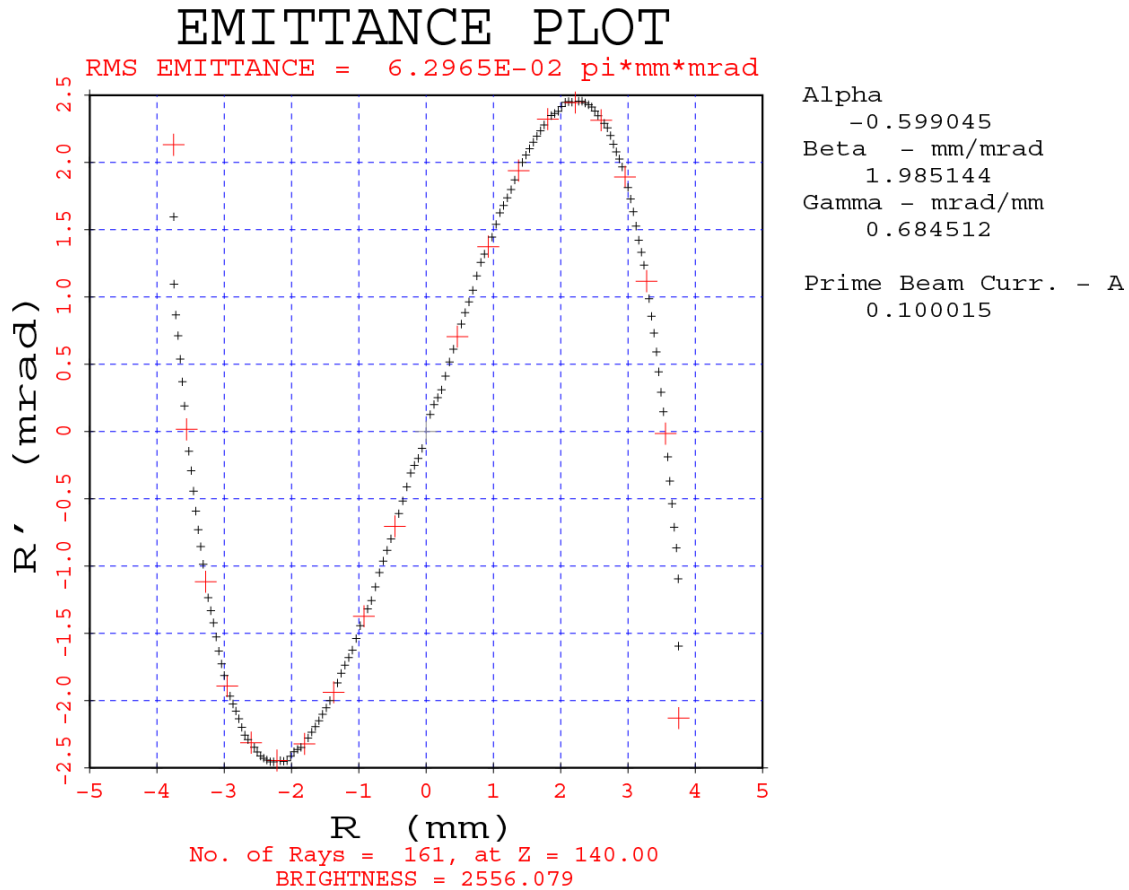Figure 83: Simple Einzel lens test for injected ion beam

EMITTANCE PLOT

RMS EMITTANCE = 6.2965E-02 pi*mm*mrad

Alpha
    -0.599045
Beta   - mm/mrad
    1.985144
Gamma - mrad/mm
    0.684512

Prime Beam Curr. - A
    0.100015

No. of Rays = 161, at Z = 140.00
BRIGHTNESS = 2556.079

Figure 84: Emittance plot near exit plane for injected ion beam

6.9.2 Low Energy Ion Beam Neutralization

The following variation on the neutralization problem was discovered by John Keller (K2 Keller Consulting) while trying to obtain an extremely low energy beam at a target. The input data for this problem is given in Table 25. Fig. 85 shows his excellent design for a low energy beam at the target using the normal beam neutralization routine that just looks at the axis while determining the neutralization point and then neutralizing the entire beam radially. It is seen that there is a problem around the 2.0 unit radius. There is a region to the left of the axial neutralization point that should also be neutralized.

Fig. 86 is the same simulation with the neutralization point determined for each radial matrix position. The last equipotential now pretty well defines the neutralization region. The potentials are now much more uniform in the neutralized region. Note that there has been a significant change in the trajectories near the outer edge. This variable neutralization point is invoked by making ZITC a negative number in Table 25.

```
 99 400 121   519999   3   0   8   0   0                      0   0   0   0   0   0
  3   8   0   0  -1   1   0   0   0   0   1   2   0   0   0   0   0   0   0 0.0
 0.0000000    10000.0    0.02540    0.10000 0.0000020    0.00000 20196.000   3000.000
  1.0000   0.0000   0.0327   0.000   10.00 0.00010   0.000   0.0000
  10.640  11.900   0.000  0.0000   0.000   0.000   0.000   0.000   0.000 12.0000
   2   0.3000   0  18 0.00000 0.00000 1.20000 0.00000 1.00000   0.00   2   0   0
    0.000   1.200
    1.000   1.000
    0.000   0.000
CYL   0.0000   1.8000   2.0000   1.8000
PLA   2.0000   5.0000
   4   1.4000
PLA   3.0062   5.0000   3.0062   1.9989
TCN   3.6032   1.9963
TCN   4.0000   2.0000
TCN   4.0062   5.0000
   3   0.0400
PLA   6.0000   5.0000   6.0000   4.0000
TCN   8.0000   3.0000
CYL 12.0000   3.0000
   INJECTED ION BEAM
 0.00003 0.00010 0.00020 0.03400 0.03500 0.03600 0.03700 0.03800 0.03900 0.04000
 0.05000 0.10000 0.15000 0.20000 0.25000 0.30000 0.35000 0.40000 0.45000 0.50000
 0.55000 0.60000 0.65000 0.70000 0.75000 0.80000 0.85000 0.90000 0.95000 0.96000
 0.97000 0.98000 0.99000 0.99990 1.01000 1.02000 1.03000 1.04000 1.05000 1.10000
X
```

Table 25: Input data for following neutralization plots

This example is most significant for extremely low energy beams, 400 eV in this case. Higher energy (multi-kVolt) beams would in general be much less effected. However a very high current beam could produce similar effects at somewhat higher voltages.

Additional equipotentials at and slightly below 400 volts were added to show the effect more clearly in Fig. 85.
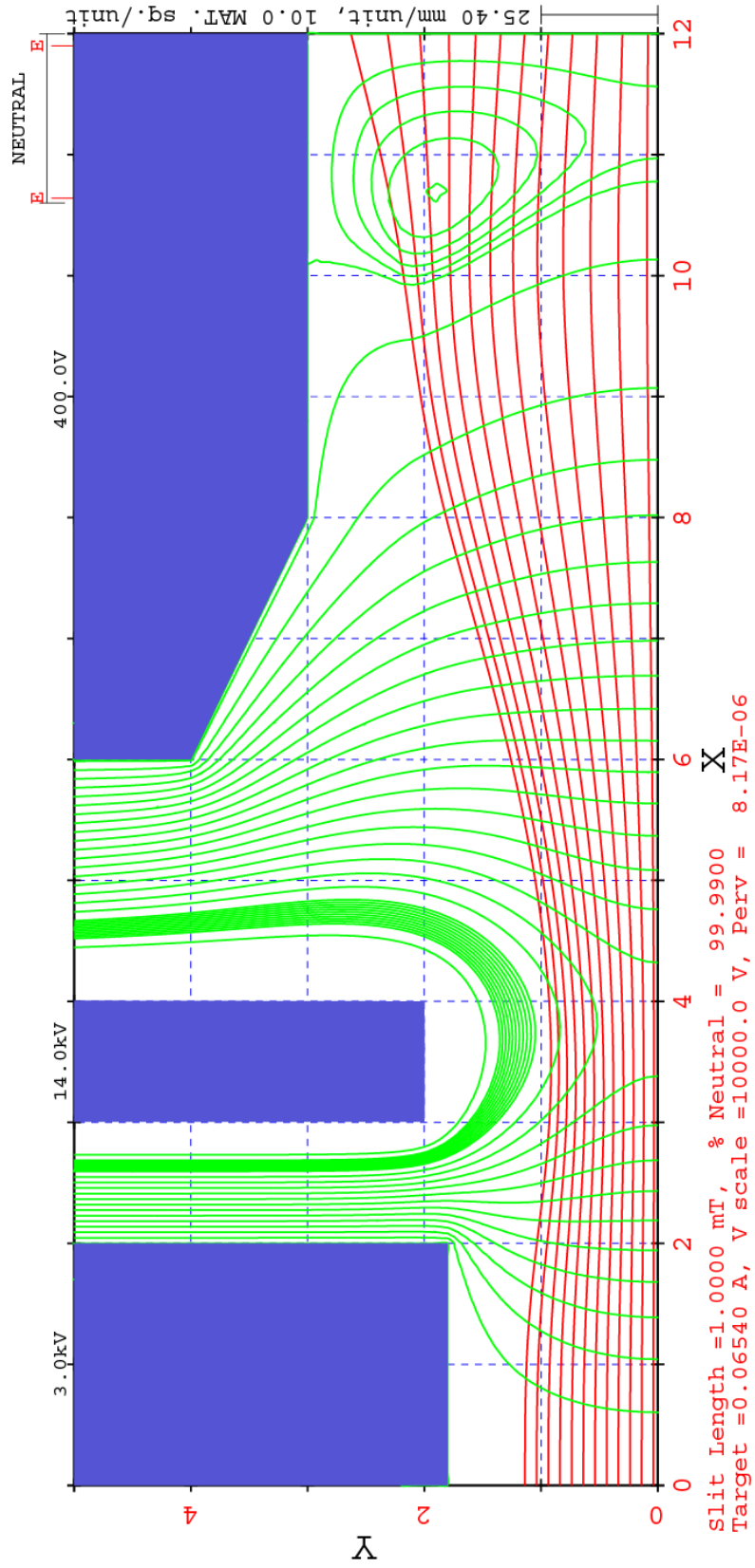
Figure 85: Faraday cup with neutralization point determined on the axis
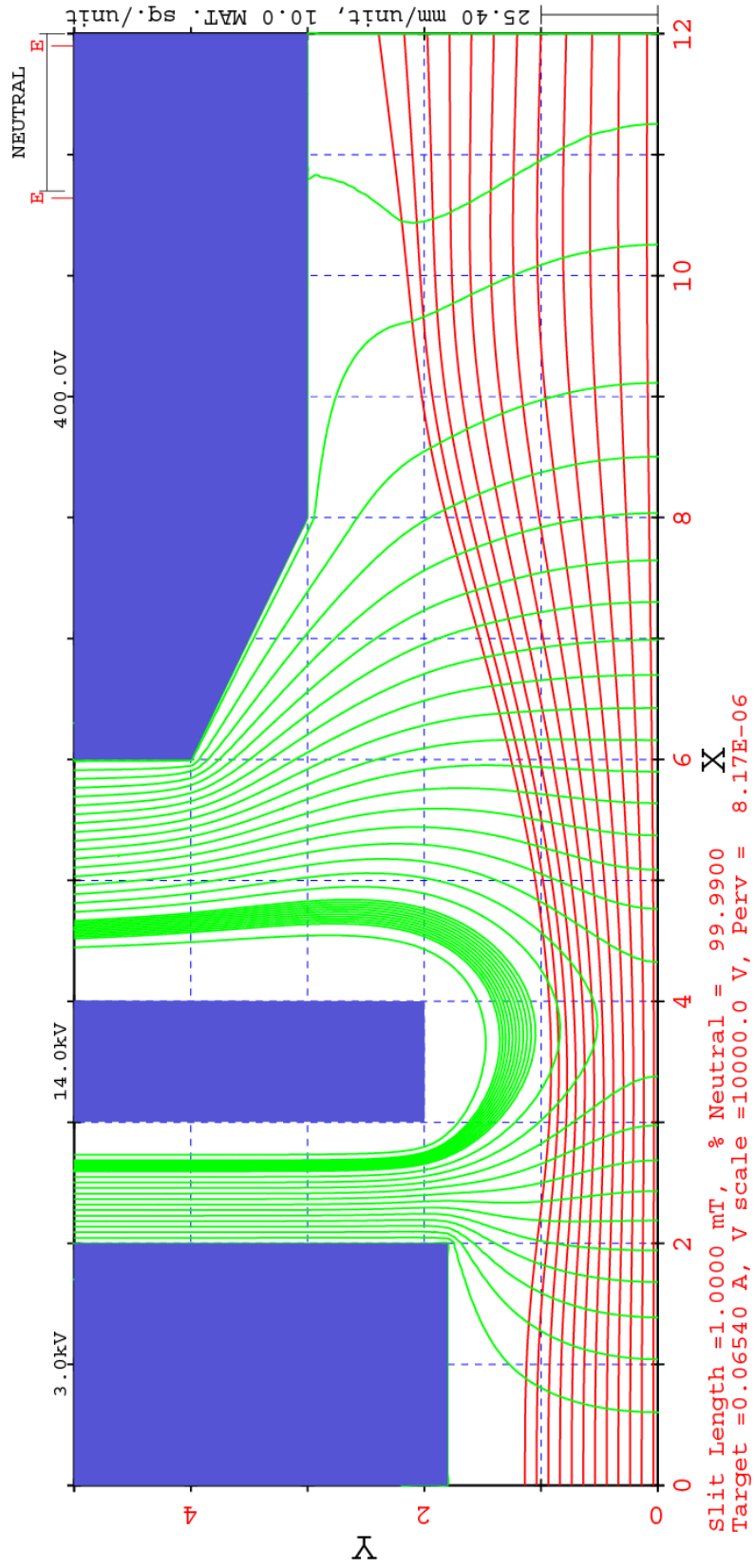
TRAJECTORIES AND EQUIPOTENTIALS

Figure 86: Faraday cup with neutralization point determined at each radial point

7 Appendix A: Trouble-Shooting PBGUNS

If **PBGUNS** is run interactively it should be almost impossible to enter data incorrectly. It is therefore suggested that one does not make up a new data set manually. Should the program get locked up and does not respond to the keyboard or mouse, type <CTRL-ALT-DELETE> (Control-Alt-Delete keys, simultaneously), click on 'Task Manager', and then select the 'PBGUNS - Particle Beam GUN Simulation' or 'pbgh.exe' line and click on 'End Task'.

Many diagnostics have been built into the program, and where possible, **PBGUNS** will try to fix badly formatted input data so that it can run. However, most of these diagnostics were added as problems were encountered, and obviously not every potential problem has been identified. Again, many problems can be avoided if the data is generated interactively. Some errors are recognized, however cannot be fixed by the program. These will be noted in both the on-screen printout and the PBGI.LOG file. Unfortunately, there are problems that cannot be easily recognized by the program. One earlier problem has been addressed with a check on circles (SPH's) and their endpoints. The program has been extensively tested, however there are an enormous number of possible combinations of the input parameters, and not every conceivable combination has been tested.

Some problems can be fixed while the program is running, either using a number supplied by the user or one determined by the program. There are several circumstances where the program will ask if a value it has determined is acceptable or if the user wants to supply an alternative one. Note that after the simulation has resumed running, following a parameter change by the input data routines, that parameter is **NOT** automatically changed in the interactive data set.

Some of the diagnostics are self explanatory, and will be printed both on the screen and in the PBGI.LOG file (usually, but not always, at the end of the file). The program checks the input data as much as possible as it is read. Should the program terminate with no diagnostic, the input data file should be the first thing examined, especially the input data associated with circles defining electrodes and the number of line segments (NK) for each electrode. If only the matrix parameters are printed in the PBGI.LOG file, then one of the first five lines is likely formatted incorrectly.

The most likely place for a problem is in the initial set up of the configuration. In the case of an error that the program recognizes, a diagnostic is printed and should point to the problem. The easiest diagnostic for the user to add is to set the printer control parameter IDG, the tenth integer number on the first line of the data. Setting IDG=1 results in the printing of most of the data used to set up the problem before execution and lists the major

subroutines as they are called.

One of the typical errors is that the end point of a line segment does not agree with the beginning point of the next section, this is easily found and will be marked by the program. (This error cannot happen at all if the data is generated interactively.) It is also possible that in the case of circles, the end points may not be sufficiently close to the circle, this too will usually be noted by the program.

Another common error occurs when the end points of the emission region are not accurate enough. In this case the program will usually generate too many trajectories, or run off the matrix and produce a diagnostic to the effect. The easiest way to find this error is to set IDG=1, as this will print out the trajectory starting points, and the exact value needed can be obtained from the printed output. If the starting point of the emission region can not be found, usually small variations can be made in RSTRT and ZSTRT until the emission set up starts. The exact endpoints can more easily be set by using the interactive graphical modification routines.

If the beam is saved in one run and restarted in the next section of beam line, the next section of beam line must be started from scratch. The restoration of previous data will overwrite/delete the new beam starting conditions. Once the new run has been initialized, it can then be restarted if the beam remains the same, i.e., a NEW saved beam must be started from scratch, not a restart.

Execution time diagnostics are somewhat trickier. The relaxation process can runaway and get into a condition from which it can not recover. This will usually manifest itself with wide variations in current and/or beam fluctuations. The usual cure for the instability is to either reduce BETA to less than 1.0 or to decrease KMM so that fewer passes are made through the matrix relaxation (on the other hand, sometimes increasing these same parameters will cure the problem). Experience seems to be the best teacher. The program will now recognize some of these problems, and either fix them or tell you about them. Remember you can change many parameters interactively while the program is running.

Extensive damping has been added to the electron beam calculations. It should be remembered that the initial current distribution on a thermionic cathode will most likely be quite inaccurate because there is no space-charge present and the relaxation is nowhere near convergence. Typically 5 to 6 cycles are required to correct the distribution with an additional 5 to 10 cycles to stabilize the results. Magnetron Injection Guns typically require 40 to 200 (or more) heavily damped cycles to converge.

If the program is stable, but converging slowly, one may want to increase KMM, the number of relaxation passes through the matrix, (and/or BETA, if BETA < 1.0) to speed up convergence. This can be done interactively.

Instabilities in the ion beam plasma are usually cured by making the plasma matrix finer (i.e., making INF larger) or decreasing BETA. Remember that low electron temperature and negative ion beam source plasmas usually require finer meshes. Both of these cause a sharper transition region between the plasma and the acceleration region. High temperature (>10 eV) electrons will usually be more stable and 1 eV electrons will generally require a 16:1 mesh (fine to regular) to be stable.

8   Appendix B: Theoretical Development of PBGUNS

The method employed in the analysis developed here is basically the same as that of other analysis [1][2][3]; the advantages lie in the fundamental techniques used. Added to these programs are liberal amounts of techniques developed by others [4][5]. The development of an elementary, iterative solution procedure for the difference equations outlined below permits the realization of a relatively compact program. This in turn permits large matrices and ultimately greater accuracy for the computations.

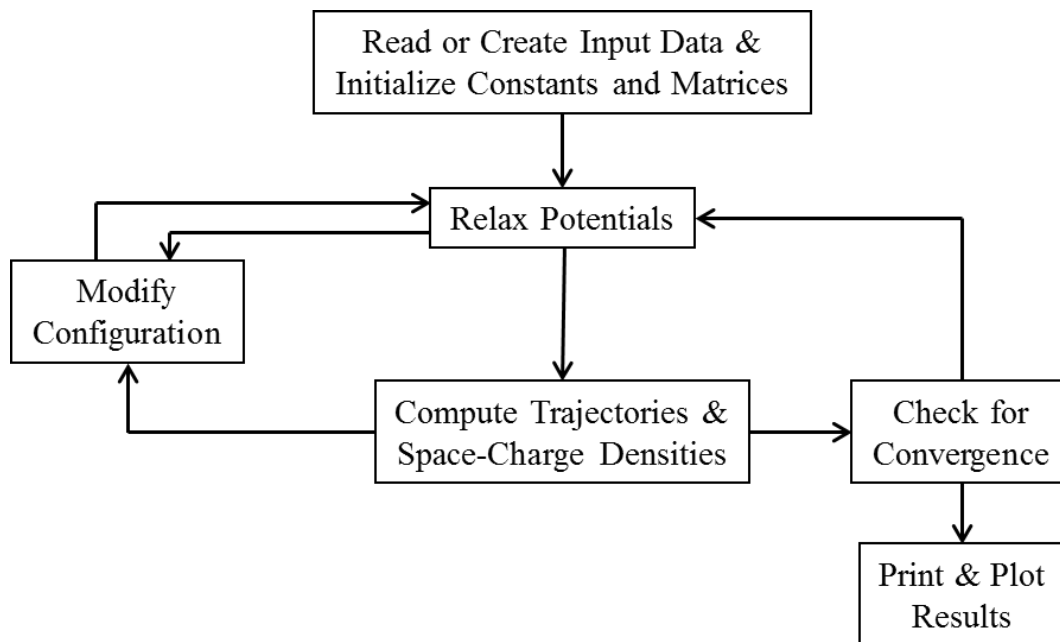The general flow chart for the **PBGUNS** program is shown in Fig. 87.

Figure 87: Basic flow chart for PBGUNS.

The main divisions are seen to be:

1. The reading of data and setting of initial conditions (or restoring of earlier data).

2. The relaxation of the potentials.

3. The calculation of the trajectories.

4. Possible entry to interactive routines.

5. A test for convergence or end of run, with result of either a return to relaxation or result output.

6. The printing, plotting and saving of results.

The trajectories are computed by solving either the relativistic Lagrangian

$$L = eV - e(\mathbf{A} \cdot \mathbf{v}) - m_0 c^2 \left(1 - \frac{v^2}{c^2}\right)^{1/2} \tag{6}$$

where e is the electronic charge, V the potential, $\mathbf{A}$ the magnetic vector potential, $\mathbf{v}$ the vector velocity, m_0 the rest mass, and c the velocity of light, all expressed in MKS (SI) units; or the non-relativistic Lorentz force equation

$$\mathbf{F} = -e(\mathbf{E} + \mathbf{v} \times \mathbf{B}) \tag{7}$$

where $\mathbf{F}$ is the force vector on the particle, $\mathbf{E}$ the vector electric field, and B the magnetic field vector; in axisymmetric cylindrical or rectangular (2-D) coordinates.

The solution of the voltage matrix is accomplished by the most elementary of relaxation techniques, i.e., the iterative solution of Poisson's equation,

$$\nabla^2 V = -\frac{\rho}{\varepsilon_0} \tag{8}$$

where ρ is the space charge density and ε_0 is the permittivity of free space, expressed in difference form, at each point within the electrode configuration.

8.1 Trajectory Computations

Expanding the relativistic Lagrangian with the Lagrange equation,

$$\frac{d}{dt}\left(\frac{\partial L}{\partial q}\right) - \frac{\partial L}{\partial q} = 0 \tag{9}$$

where q takes on the values r, θ and z in cylindrical coordinates. The equations obtained are

$$\frac{d}{dt}\left(-eA_r + \frac{m_0 \dot{r}}{\sqrt{1-\beta^2}}\right) - e\frac{\partial V}{\partial r} + e\left(\mathbf{v} \cdot \frac{\partial \mathbf{A}}{\partial r}\right) + e\dot{\theta}A_\theta - \frac{m_0 \dot{\theta}^2 r}{\sqrt{1-\beta^2}} = 0, \tag{10}$$

$$\frac{d}{dt}\left(-eA_z + \frac{m_0 \dot{z}}{\sqrt{1-\beta^2}}\right) - e\frac{\partial V}{\partial z} + e\left(\mathbf{v} \cdot \frac{\partial \mathbf{A}}{\partial z}\right) = 0, \tag{11}$$

where $\beta = v/c$. Assuming axial symmetry, derivatives of scalars with respect to θ can be set to zero:

$$\frac{d}{dt}\left(-eA_\theta r + \frac{m_0 r^2 \dot\theta}{\sqrt{1-\beta^2}} - e\frac{\partial V}{\partial\theta} + e\frac{\partial}{\partial\theta}(\mathbf{v}\cdot\mathbf{A})\right) = 0. \tag{12}$$

And then after a great deal of manipulation, if one defines

$$\alpha = A_\theta - \frac{r_0}{r}A_{\theta_0}, \tag{13}$$

$$\eta = e/m_0 \tag{14}$$

$$\sigma = c^2 + \eta^2\alpha^2, \tag{15}$$

$$\delta = \sqrt{1-\beta^2}, \tag{16}$$

$$\lambda = \eta^2\alpha(c^2 - \dot z^2 - \dot r^2)\frac{(\partial A_\theta/\partial z)\,\dot z + [(r_0/r^2)A_{\theta_0} + (\partial A_\theta/\partial r)]\,\dot r}{\delta^2\sigma^2}, \tag{17}$$

and notes that then the axisymmetric relativistic trajectory equations become

$$\ddot r\left(\frac{1+\dot r^2/\delta^2\sigma}{\delta}\right) = \dot r\frac{\lambda}{\delta} - \ddot z\frac{\dot r\dot z}{\delta^3\sigma} + \eta\frac{\partial V}{\partial r} + \eta\dot z B_\theta + \eta^2\delta\alpha\left(\frac{r_0 A_{\theta_0}}{r^2} + \frac{\partial A_\theta}{\partial r}\right), \tag{18}$$

$$\ddot z\left(\frac{1+\dot r^2/\delta^2\sigma}{\delta}\right) = \dot z\frac{\lambda}{\delta} - \ddot r\frac{\dot r\dot z}{\delta^3\sigma} + \eta\frac{\partial V}{\partial z} + \eta\dot z B_\theta + \eta^2\delta\alpha\frac{\partial A_\theta}{\partial z}. \tag{19}$$

B_θ, the induced circumferential magnetic flux density, can be defined as

$$B_\theta = \frac{\mu_0}{r}\int_0^r r J_z dr \tag{20}$$

where J_z is the axial component of the current density, and A_θ is defined by

$$A_\theta = \frac{1}{r}\int_0^r r B_z(r)dr \tag{21}$$

where $B_z(r)$ is the axial applied magnetic field density. If B_z a slowly varying function of r and the beam is near the axis this can be approximated by

$$A_\theta \approx \frac{r B_z(0)}{2} \tag{22}$$

With this approximation it is only necessary to have the magnetic field values on the

axis. The derivatives are readily computed by

$$\frac{\partial A_\theta}{\partial r} = \frac{B_z(z_k)}{2} = \frac{1}{2}\left[B_i\left(1 - \frac{h_z}{\Delta z}\right) + B_{i+1}\frac{h_z}{\Delta z}\right], \tag{23}$$

$$\frac{\partial A_\theta}{\partial z} = \left[\frac{B_{i+1} - B_{i-1}}{2\Delta z} + \frac{(B_{i+1} - 2B_i + B_{i-1})h_z}{(\Delta z)^2}\right]\frac{r_k}{2} \tag{24}$$

where the magnetic field is assumed known at points along the V matrix axis and h_z is distance between column i and the z_k coordinate of the trajectory.

Similarly the relativistic Lagrangian can be solved in rectangular $(x\text{–}y)$ coordinates with an applied z directed magnetic field, yielding the following equations:

$$\ddot{x} = \left(C - \frac{BF}{D}\right)\bigg/\left(A - \frac{B^2}{D}\right), \tag{25}$$

$$\ddot{y} = \left(F - \frac{BC}{A}\right)\bigg/\left(D - \frac{B^2}{A}\right) \tag{26}$$

where

$$A = 1 - \frac{\dot{y}^2}{c^2}, \tag{27}$$

$$B = \frac{\dot{x}\dot{y}}{c^2}, \tag{28}$$

$$C = (1 - \beta^2)\left(-\eta\frac{\partial V}{\partial x} + \eta\dot{y}B_z\right), \tag{29}$$

$$D = 1 - \frac{\dot{x}^2}{c^2}, \tag{30}$$

$$F = (1 - \beta^2)\left(-\eta\frac{\partial V}{\partial y} + \eta\dot{x}B_z\right). \tag{31}$$

Equations (25) and (26) are highly nonlinear and are solved by iteratively feeding results of the calculation back into them until a self consistent solution is obtained. These are the equations for a 2-D beam with (or without) an applied magnetic field perpendicular to the simulation. B_z is the self induced magnetic field of the beam plus any applied magnetic field. The self induced beam magnetic field is automatically calculated, and the applied field which may vary in x must be supplied by the user.

Alternatively the Lorentz force equation [Eq. (7)] can be expanded into three axisym-

metric, cylindrical, scalar equations:

$$\ddot{z} = -\eta(E_z - r\dot{\theta}B_r), \tag{32}$$

$$\ddot{r} - r\dot{\theta}^2 = -\eta r(E_r - r\dot{\theta}B_z), \tag{33}$$

$$\frac{d}{dt}(r\dot{\theta}^2) = \eta r(\dot{r}B_z - \dot{z}B_r) \tag{34}$$

To get these equations in a form suitable for the computer simulation the applied magnetic fields are expressed in terms of the magnetic vector potential

$$\mathbf{B} = \nabla \times \mathbf{A}. \tag{35}$$

Expanded in axisymmetric coordinates this becomes

$$B_z = \left(\frac{1}{r}\right)\frac{\partial(rA_\theta)}{\partial r},$$
$$B_r = -\frac{\partial A_\theta}{\partial z}. \tag{36}$$

Substituting these expressions into Eq. (34) gives, with some rearranging,

$$\frac{d}{dt}(r^2\dot{\theta}) = \eta\frac{d}{dt}(rA_\theta) \tag{37}$$

which can be integrated to give

$$\dot{\theta} = \frac{\eta}{r}A_\theta - \eta\frac{r_0}{r^2}A_{\theta_0}, \tag{38}$$

where r_0 is the initial radius of the particle and $A_{\theta_0} = A_\theta(r_0)$ the initial flux linking the trajectory. Equation (38) is Busch's theorem expressed in terms of the magnetic vector potential. Substituting into Eqs. (33) and (32) yields the following expressions for the radial and axial acceleration:

$$\ddot{r} = -\eta\left[E_r + \eta\left(\frac{r_0}{r}A_{\theta_0} - A_\theta\right)\left(\frac{\partial A_\theta}{\partial r} + \frac{r_0}{r^2}A_{\theta_0}\right)\right], \tag{39}$$

$$\ddot{z} = -\eta\left[E_z + \eta\left(\frac{r_0}{r}A_{\theta_0} - A_\theta\right)\frac{\partial A_\theta}{\partial z}\right]. \tag{40}$$

A_θ and its derivatives can be expressed as above. Setting d^2r/dt^2 equal to a_r, d^2z/dt^2 equal

to a_z, these equations become, in difference form

$$z_{k+1} = 2z_k - z_{k-1} - \eta(\Delta t)^2 a_z, \tag{41}$$

$$r_{k-1} = 2r_k - r_{k-1} - \eta(\Delta t)^2 a_r,$$

where Δt is the time increment between consecutive points $k-1$, k, and $k+1$.

Alternatively, Eq. (34) can be solved with skew particles (finite values of azimuthal energy) by assuming

$$\dot{\theta} = \frac{\eta}{r} A_\theta - \eta \frac{r_0}{r^2} A_{\theta_0} + \frac{r_0^2}{r^2} \dot{\theta}_0 \tag{42}$$

where an additional term is added for the initial azimuthal velocity of the particles.

Substituting Eq. (42) into Eqs. (33) and (32) and using

$$r_0 v_{\theta_0} = r_0^2 \dot{\theta}_0 \tag{43}$$

we obtain modified a version of the trajectory equations including this initial skew velocity,

$$\ddot{r} = -\eta \left[E_r + \eta \left(\frac{r_0}{r} A_{\theta_0} - \frac{r_0 v_{\theta_0}}{r\eta} - A_\theta \right) \left(\frac{\partial A_\theta}{\partial r} + \frac{r_0}{r^2} A_{\theta_0} - \frac{r_0 v_{\theta_0}}{\eta r^2} \right) \right], \tag{44}$$

$$\ddot{z} = -\eta \left[E_0 + \eta \left(\frac{r_0}{r} A_{\theta_0} - \frac{r_0 v_{\theta_0}}{r\eta} - A_\theta \right) \frac{\partial A_\theta}{\partial z} \right]. \tag{45}$$

If there is no magnetic field present these two equations become (as Chan, et al. derived) simply

$$\ddot{r} = -\eta \left[E_r + \frac{r_0^2 v_{\theta_0}^2}{\eta^2 r^3} \right], \tag{46}$$

$$\ddot{z} = -\eta E_z. \tag{47}$$

In PBGUNS v_{θ_0} is determined by

$$v_{\theta_0} = \sqrt{2\eta(E_0 \tan^2(\Theta))} \tag{48}$$

where E_0 is the initial energy of the ion and Θ is the angle between this particle and the first beam that is injected (and which must *not* have any skew energy). The skew energy printed out in the log file is given by the product $E_0 \tan^2(\Theta)$.

For rectangular (2-D) configurations only a magnetic field in the z-direction can exist

and the Lorentz force equation can be expressed in terms of its components as

$$\ddot{x} = -\eta(E_x + \dot{y}B_z), \tag{49}$$

$$\ddot{y} = -\eta(E_y - \dot{x}B_z), \tag{50}$$

$$\ddot{z} = -\eta E_z. \tag{51}$$

If there are no variations in the z-direction, $E_z = 0$ and Eq. (51) can be dropped. Expanding Eqs. (49) and (50) in difference form yields

$$\frac{x_{k+1} - 2x_k + x_{k-1}}{(\Delta t)^2} = -\eta\left(E_x + \frac{y_{k+1} - y_{k-1}}{2\Delta z}B_z\right), \tag{52}$$

$$\frac{y_{k+1} - 2y_k + y_{k-1}}{(\Delta t)^2} = -\eta\left(E_y - \frac{x_{k+1} - x_{k-1}}{2\Delta z}B_z\right). \tag{53}$$

When these are solved for x_{k+1} and y_{k+1}, the following equations are obtained for a trajectory time increment Δt:

$$x_{k+1} = \frac{1}{\left(1 + \frac{w^2}{4}\right)}\left[2x_k - \left(1 - \frac{w^2}{4}\right)x_{k-1} + w(y_k - y_{k-1}) - \eta\left(E_x + \frac{w}{2}E_y\right)(\Delta t)^2\right], \tag{54}$$

$$y_{k+1} = \frac{1}{\left(1 + \frac{w^2}{4}\right)}\left[2y_k - \left(1 - \frac{w^2}{4}\right)y_{k-1} - \eta\left(E_y - \frac{w}{2}E_x\right)(\Delta t)^2\right], \tag{55}$$

where $w = \eta B_z \Delta t$.

The electric fields $E_r(E_y)$ and $E_z(E_x)$ can be represented in difference form using voltages from the V matrix. Including second order terms the fields become

$$E_r = -\frac{\partial V}{\partial r} \approx -\frac{V_{i,j+1} - V_{i,j-1}}{2\Delta r} - \frac{V_{i,j+1} - 2V_{i,j} + V_{i,j-1}}{(\Delta r)^2}h_r, \tag{56}$$

$$E_z = -\frac{\partial V}{\partial z} \approx -\frac{V_{i+1,j} - V_{i+1,j}}{2\Delta z} - \frac{V_{i+1,j} - 2V_{i,j} + V_{i-1,j}}{(\Delta z)^2}h_z \tag{57}$$

where h_r and h_z are the normalized distances between row j and r_k and column i and z_k respectively.

8.2   Voltage Relaxation

The solution of the voltage matrix is obtained by elementary relaxation techniques, i.e., the iterative solution of Poisson's equation,

$$\nabla^2 V = -\frac{\rho}{\varepsilon_0} \tag{58}$$

expressed in difference form. For this program it is expanded in axisymmetric, cylindrical coordinates (r, θ, z). Setting derivatives with respect θ equal to zero:

$$\frac{1}{r}\frac{\partial}{\partial r}\left(r\frac{\partial V}{\partial r}\right) + \frac{\partial^2 V}{\partial z^2} = -\frac{\rho}{\varepsilon_0} \tag{59}$$

Using the differences defined in Fig. 88 and expressing this equation in second order difference form and solving for $V_{i,j}$ we obtain

$$V_{i,j} = \frac{1}{4}(V_{i,j+1} + V_{i,j-1} + V_{i+1,j} + V_{i-1,j}) + \frac{\Delta r}{8r}(V_{i,j+1} - V_{i,j-1}) + \rho_{i,j} \tag{60}$$

here

$$\rho_{i,j} = \frac{(\Delta r)^2 \rho}{4\varepsilon_0} \tag{61}$$

and similarly on the axis

$$V_{i,j} = \frac{1}{6}(4V_{i,j+1} + V_{i+1,j} + V_{i-1,j}) + \frac{2}{3}\rho_{i,j} \tag{62}$$

Here, i, j indexes the column, row of the voltage matrix, V, which overlays the problem grid (mesh). For two-dimensional problems this equation becomes

$$V_{i,j} = \frac{V_{i+1,j} + V_{i-1,j} + V_{i,j-1} + V_{i,j+1}}{4} - \rho_{i,j} \,. \tag{63}$$

The above calculations are straightforward as long as the space-charge densities are not a direct function of the voltages, i.e., the space-charge is a function of the ion velocity which in turn is a function of the voltage. This error is averaged out over a few major cycles through the program. The potential at each point within the electrode configuration can be determined by iteratively solving Eqs. (60) and (62), or Eq. (63) for rectangular configurations. This solution can usually be reached quite rapidly using various over and under relaxation techniques. However, if one now wishes to solve this problem for positive ions in a plasma with the space-charge density a function of both the ion and electron
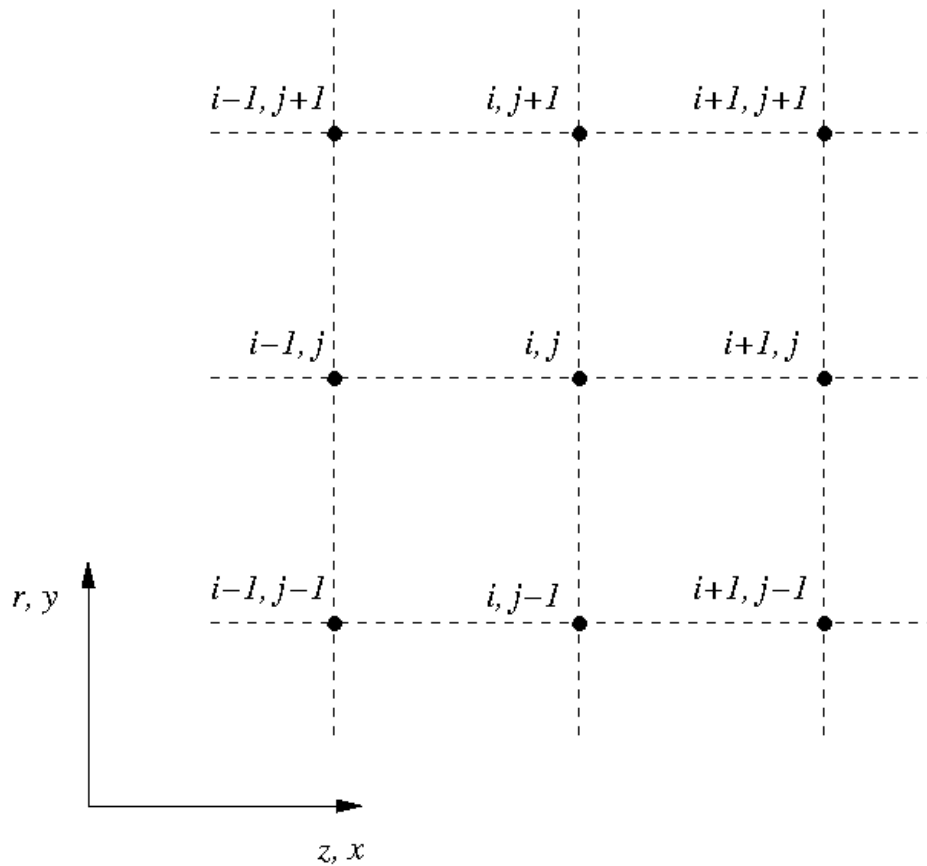
Figure 88: Voltage matrix layout with axis of symmetry - $z, x = 0$

densities, the problem is much more complex. If the electrons are assumed to be in a Boltzman distribution,

$$\rho_e = \rho_{e0} \exp\left(\frac{-eV}{kT_e}\right), \tag{64}$$

$$\rho = \rho_i + \rho_e, \tag{65}$$

where ρ_{e0} and T_e are the electron space-charge density (numerically equal to the ion space-charge density at the injection plane) and temperature in the plasma, then becomes a sensitive function of the voltage, due to the exponential, and the solution of Eq. (59) becomes much more complex.

Similarly, for negative ions, both the positive ions and electrons can be represented by

Boltzman functions

$$\rho_e = \rho_{e0} \exp\left[\frac{-e(V_{1,1} - V_{i,j})}{kT_e}\right], \tag{66}$$

$$\rho_{\mathrm{p}i} = \rho_{\mathrm{p}i0} \exp\left(\frac{-eV}{kT_{\mathrm{p}i}}\right), \tag{67}$$

then giving

$$\rho = \rho_{\mathrm{n}i} + \rho_e - \rho_{\mathrm{p}i}, \tag{68}$$

$\rho_{\mathrm{p}i}$ being the positive ion space charge density, $\rho_{\mathrm{n}i}$ the negative ion space charge density, $T_{\mathrm{p}i}$ the positive ion temperature and the sign of the exponent for the electron distribution has been modified and reversed to account for the voltage reversal for negative ions. At the ion emission surface the electron density exponent is reversed again to decrease the number of electrons as they are swept away by the accelerating voltage. The total space-charge density at the entrance plane [Eq. (66)] is set to zero.

Since Eq. (61) is now a highly nonlinear function of the voltage it is necessary to find a suitable solution for $V_{i,j}$. The technique used here is to solve the right hand side of the equation with voltages available from the matrix to determine a new value for $V_{i,j}$ on the left side. This new value is averaged with the previous value and the calculation is repeated once. The final value is further damped by the under relaxation parameter β (BETA)

$$VF_{i,j} = (VN_{i,j}^n - VF_{i,j})\beta + VF_{i,j} \tag{69}$$

where $VF_{i,j}$ on the left is the final value on the fine (plasma) mesh and on the right is the initial value at that point, and VN^n is the last value computed above. β is a number less than or equal to 1. For negative ions this calculation is only carried out once for stability reasons.

For positive ions, with electron temperatures of 10 eV or more and initial ion energies of 10 eV or more, the above calculation is quite stable, and β can usually be started at 1.0. As these energies are reduced to 1-5 eV, the calculation becomes less stable and it may become necessary to start β at smaller values. However it has also been found that making the plasma matrix finer will also help stabilize the results. The larger β, the faster the program will converge. The amount of plasma that the ions must travel through before it reaches the plasma surface will also effect the stability of the results, the thinner the plasma the more stable the result. Fortunately, the lower these energies, the more uniform the plasmas seem to become and the need to go deep in the plasma is reduced. In general, the initial value of β should not be reduced from 1.0 until there is a known problem.

For negative ions, higher electron and (negative) ion energies tend to be more stable. For sputter ion sources (kV level ions) the program is very stable. For intense ion sources the positive ion density must be quite high and the calculation becomes less stable. Also, for low positive ion temperatures the calculation becomes less stable. Where 4 to 1 fine mesh ratios may work with positive ion extraction, 16 to 1 ratios may be needed for negative ion beams.

In the accelerating column, only the primary ion beam is taken into account in the space charge. Any electrons or ions resulting from ionization of the background gas are ignored. All electrons would be swept out by the accelerating field at any reasonable gas pressure and at the low pressures assumed here (a few millitorr), the secondary ions are also assumed negligible. In the case of negative ions this may not be true. Los Alamos calculates that as much as 25 per cent of the negative ions may be stripped of their electrons in the acceleration region. This effect is simulated by increasing the space charge density by 33 per cent ($1.33 \times 0.75 = 1.0$) at and behind the plasma surface, and linearly reduced to normal as the beam is accelerated. Experience suggests this is more important for negative ion beam extraction than for positive ion extraction. More on this below.

In the drift space after acceleration, the space-charge density will almost certainly be neutralized by electrons for a positive ion beam and by positive ions for a negative ion beam. The simplest way of handling this effect is to reduce the space charge density by a multiplying factor (typically 0.01 to 0.05). This seems to produce results nearly as good as (and a lot easier) than a calculation of the neutralization as arrived at by the Holmes' method[7] which assumes a background electron density in the well, formed by the beam, that produces a current to the wall that equals the ion generation rate in the beam. This calculation is in the program, however is extremely difficult to use and is not recommended under most circumstances (in fact, it is currently disabled).

A solution with these equations is obtained by iteratively passing back and forth through the voltage matrix. The forward and reverse calculation significantly speeds the propagation of corrections in all directions.

Most of the points within the simulation region are solved using the difference equations above. In the early cycles of a problem, two additional relaxations can be added to speed up the solution. The overall mesh can be relaxed using only the odd numbered matrix points, and a region that might otherwise be slow to converge can be relaxed before the main relaxation begins. The coarse mesh propagates corrections much faster in all directions, and the regions that would ordinarily be slow to converge can be significantly accelerated.

Near electrodes, within one matrix increment of the surface, the voltages are computed from a quadratic fit to the voltages at the electrode and the first two points in front of

167

the electrodes that are relaxed. The point just in front of the electrode, and one or two points inside the electrode, are set using the quadratic equation for the potentials. This creates smooth equipotentials so that it is possible to compute particle trajectories and current densities even in the immediate vicinity of the electrodes. In particular, potentials immediately in front of the cathode are computed with good accuracy (a few percent of theory), permitting the use of Child's Law (with the Langmuir-Blodgett, corrections for curvature of the cathode[8][9]) employing potentials two matrix increments off the cathode. Many of the codes described in the literature use potentials far from the cathode to compute current densities, which can sharply mask variations in current density especially near the edge of the cathode. Results shown in Section 6.3 show how effective this technique is.

8.3   Space–Charge Densities

The space-charge densities are stored at the matrix points on both sides of each trajectory as it is computed, the total space charge at a matrix point being the sum from all particles passing within one matrix increment. We will consider the calculation for one trajectory. The space-charge density terms must be calculated with great care or erroneous values can be obtained. Equation (61) can be expressed in terms of the current density and velocity by

$$\rho_{i,j} = \frac{(\Delta r)^2 J}{4 v \varepsilon_0} \tag{70}$$

where $\rho = J/v$. The details of the development of this calculation are given in **Reference**[2], and only the results will be presented here. The final result in an axisymmetric simulation for a particle crossing a matrix row at an angle (Θ) to the row of greater than 45 degrees is

$$\rho_{i,j} = \rho_{i,j} + \frac{J_0 \Delta t (1 - R_z)(\Delta r)^2 r_0}{4 \varepsilon_0 \Delta s \, r \text{SIN}\Theta}, \tag{71}$$

$$\rho_{i+1,j} = \rho_{i+1,j} + \frac{J_0 \Delta t R_z (\Delta r)^2 r_0}{4 \varepsilon_0 \Delta s \, r \text{SIN}\Theta}, \tag{72}$$

where J_0 is the current density computed at the cathode, R_z is the normalized (to Δz) distance from the z-coordinate to the vertical line through i, r_0 is the radius of the particle at the cathode, r is the radius of the particle, SINΘ is the maximum of sin(Θ) or cos(Θ) and

$$\Delta s = \sqrt{(r_{l,k+1} - r_{l,k})^2 + (z_{l,k+1} - z_{l,k})^2} \tag{73}$$

Similarly for the crossing of a vertical line

$$\rho_{i,j} \;=\; \rho_{i,j} + \frac{J_0 \Delta t (1 - R_r)(\Delta r)^2 r_0}{4\varepsilon_0 \Delta s\, r \text{SIN}\Theta}, \tag{74}$$

$$\rho_{i,j+1} \;=\; \rho_{i,j+1} + \frac{J_0 \Delta t R_r (\Delta r)^2 r_0}{4\varepsilon_0 \Delta s\, r \text{SIN}\Theta}, \tag{75}$$

where R_r is the normalized distance from the r-coordinate to the line through j.

The above relations hold at any point except those on the axis ($j = 1$) in an axisymmetric configuration. Here the space charge is doubled on the axis to account for the particles that (by symmetry) will be approaching from the opposite side of the axis. The center trajectory space charge is not doubled because it has no reflection.

8.4   Current Emission Calculations

Space charge limited calculations are made with Child's Law as modified by Langmuir-Blodgett for curved cathodes[8][9], where r is the distance from the cathode (2*DRF*ZSCALE) to the point where V is computed.

$$J = \frac{4\varepsilon_0}{9}\sqrt{\frac{2e}{m}}\,\frac{V^{3/2}}{r^2} \tag{76}$$

These currents are corrected in cylindrical configurations so that

$$J_{\text{cyl}} = \frac{4\varepsilon_0}{9}\sqrt{\frac{2e}{m}}\,\frac{V^{3/2}}{r^2 \beta^2} \tag{77}$$

where

$$\beta = u - 0.4u^2 + 0.0917u^3 - 0.001424u^4 + 0.00168u^5 \tag{78}$$

where $u = \log(r/r_c)$ and r_c is the cathode radius from the symmetry axis or the cylinder radius in 2-D simulations. In spherical coordinates the equation becomes

$$J_{\text{sph}} = \frac{4\varepsilon_0}{9}\sqrt{\frac{2e}{m}}\,\frac{V^{3/2}}{r^2 \alpha^2} \tag{79}$$

where

$$\alpha = u - 0.3u^2 + 0.075u^3 - 0.001432u^4 + 0.00216u^5 \tag{80}$$

and again $u = \log(r/r_c)$ and r_c is the spherical radius of the cathode.

For field emission the Fowler-Nordheim equation is used.

$$J = \left(1.54 \times 10^{-6}\right) \frac{E^2}{W} \exp\left[9.52\sqrt{W} + (6.36 \times 10^9)W^{1.57}/E\right] \tag{81}$$

where W is the work function value in eV, and E is the electric field in Volts/m at the emission surface.

References

[1] J. E. Boers, "Digital Computer Simulation of Charged Particle Beams and Electrostatic Lenses," Journal of Vacuum Science and Technology. Vol 10, Nov/Dec. 1973, pp 1120-1123.

[2] J. E. Boers, "Computer Simulation of Space-charge Flows," RADC-TR-68-175, The University of Michigan, Ann Arbor, Mich. April 1968.

[3] J. E. Boers, "Proceedings of the 11th Symposium on Electron, Ion, and Laser Beam Technology," edited by R. F. M. Thornley (San Francisco Press, San Francisco, 1971), p. 167.

[4] C. N. Dorney, Proc. IEEE (letters). Vol. 57, May 1969, pp. 856-858.

[5] Special appreciation to (then Captain) C. M. Rogers of the Air Force Weapons Laboratory, Albuquerque, 1971.

[6] C.F. Chan, W.S. Cooper, J.W. Kwan, and W.F. Steele, "Dynamics of Skew Beams and the Projectional emittance," Nuclear Instruments and Methods in Physics Research Section A306 (1991) pp112-122.

[7] A.J.T. Holmes, "Theoretical and experimental study of space charge in intense ion beams," Physics Review A, 19, Jan. 1979, pp. 389-407.

[8] I. Langmuir, K. Blodgett, "Currents Limited by Space Charge Between Coaxial Cylinders," Physics Review A, 22, Oct. 1923, p. 347.

[9] I. Langmuir, K. Blodgett, "Currents Limited by Space Charge Between Concentric Spheres," Physics Review A, 24, July 1924, p. 49.